MICROCOPY RESOLUTION TEST CHART

NATIONAL BUREAU OF STANDARDS-1963-A

AD-A161 730

DNA-TR-84-12

AIRBLAST SIMULATOR STUDIES

R.E. Duff
L. Kennedy
K. Lie
S-CUBED
Division of Maxwell Laboratories, Inc.
P. O. Box 1620
La Jolla, CA 92038-1620

1 February 1984

Technical Report

CONTRACT No. DNA 001-83-C-0095

Approved for public release;
distribution is unlimited.

DTIC FILE COPY

DTIC
ELECTE
S D
NOV 1 4 1985

B

Prepared for
Director
DEFENSE NUCLEAR AGENCY
Washington, DC 20305-1000

85 09 24 042

REPORT DOCUMENTATION PAGE

1a REPORT SECURITY CLASSIFICATION	1b RESTRICTIVE MARKINGS
UNCLASSIFIED	

2a SECURITY CLASSIFICATION AUTHORITY	3 DISTRIBUTION/AVAILABILITY OF REPORT
	Approved for public release;
2b DECLASSIFICATION/DOWNGRADING SCHEDULE	distribution is unlimited.
N/A since Unclassified	

4 PERFORMING ORGANIZATION REPORT NUMBER(S)	5 MONITORING ORGANIZATION REPORT NUMBER(S)
SSS-R-84-6495	DNA-TR-84-12

6a NAME OF PERFORMING ORGANIZATION	6b OFFICE SYMBOL (If applicable)	7a NAME OF MONITORING ORGANIZATION
S-CUBED, A Division of Maxwell Laboratories, Inc.		Director Defense Nuclear Agency

6c. ADDRESS (City, State, and ZIP Code)	7b ADDRESS (City, State, and ZIP Code)
P.O. Box 1620 La Jolla, CA 92038-1620	Washington, DC 20305-1000

8a NAME OF FUNDING SPONSORING ORGANIZATION	8b OFFICE SYMBOL (If applicable)	9 PROCUREMENT INSTRUMENT IDENTIFICATION NUMBER
		DNA 001-83-C-0095

8c ADDRESS (City, State, and ZIP Code)	10 SOURCE OF FUNDING NUMBERS			
	PROGRAM ELEMENT NO	PROJECT NO	TASK NO	WORK UNIT ACCESSION NO
	62715H	G55AMXG	R	DH006664

11 TITLE (Include Security Classification)

AIRBLAST SIMULATOR STUDIES

12 PERSONAL AUTHOR(S)
R. E. Duff, L. Kennedy, K. Lie

13a TYPE OF REPORT	13b TIME COVERED	14 DATE OF REPORT (Year, Month, Day)	15 PAGE COUNT
Technical Report	FROM 830101 TO 831231	840201	132

16 SUPPLEMENTARY NOTATION
This work was sponsored by the Defense Nuclear Agency under RDT&E RMSS
Code B345083466 G55AMXGR00001 H2590D.

17	COSATI CODES		18 SUBJECT TERMS (Continue on reverse if necessary and identify by block number)		
FIELD	GROUP	SUB-GROUP	Blast Simulator	Shock Tube	DASACON
14	2		Gas Detonation Driver	Flow Blockage	
20	11				

19 ABSTRACT (Continue on reverse if necessary and identify by block number)

The effects of flow blockage in a blast simulator were investigated and means sought to mitigate those effects. Flow characteristics were studied by two-dimensional hydrodynamic calculations for flared and vented test chambers as compared with straight tubes at similar blockage. Several conditions up to 30 psi blast overpressure and 30% blockage were investigated. It was shown that the diffraction phase of blast interaction was best reproduced in a straight tube in spite of blockage. Flared and vented designs seemed to reproduce desired conditions better in the drag phase. In general, blockage effects did not seem as dramatic as suggested by the flow choking concept. Driver options potentially useful in the reactivation of DASACON were investigated. Gas detonation and combustion systems seemed capable of producing conditions covering the entire range of Army blast simulation interest. DASACON with a gas detonation driver could be useful in Hardened Mobile Launcher or some Army applications, but it would not satisfy the requirements for a large blast simulation facility.

20 DISTRIBUTION/AVAILABILITY OF ABSTRACT	21 ABSTRACT SECURITY CLASSIFICATION
☐ UNCLASSIFIED/UNLIMITED ☒ SAME AS RPT ☐ DTIC USERS	UNCLASSIFIED

22a NAME OF RESPONSIBLE INDIVIDUAL	22b TELEPHONE (Include Area Code)	22c OFFICE SYMBOL
Betty L. Fox	202-325-7042	DNA/STTI

DD FORM 1473, 84 MAR

83 APR edition may be used until exhausted
All other editions are obsolete.

SECURITY CLASSIFICATION OF THIS PAGE

TABLE OF CONTENTS

TABLE OF CONTENTS (Continued)

QUALITY INSPECTED 3

2

LIST OF ILLUSTRATIONS

LIST OF ILLUSTRATIONS (continued)

4

LIST OF ILLUSTRATIONS (continued)

LIST OF ILLUSTRATIONS (continued)

LIST OF ILLUSTRATIONS (continued)

LIST OF ILLUSTRATIONS (continued)

LIST OF TABLES

SECTION 1
INTRODUCTION

The Defense Nuclear Agency has long recognized the importance of blast simulation experiments to assure the survivability of military equipment and facilities on the nuclear battlefield. As a result, an ongoing series of high explosive tests is conducted, and simulation facilities have been provided at a number of military installations or are being planned for the future. The work to be described in the following sections provides a summary of research done during 1983 in support of airblast simulator development. The objectives of the study are:

- To study the potential utility of a flared test section to reduce the influence of flow blockage and to increase the capability of a particular airblast simulator.

- If this concept is attractive, to consider the potential utility of a flare in the context of a possible DASACON reactivation.

- To investigate alternate driver options for DASACON.

- To consider the rarefaction wave eliminator problem in the DASACON context.

- To make a limited investigation of distributed charge fuel air explosive configurations for blast simulator applications.

During the course of this study, increased interest in the Hardened Mobile Launcher (HML) led to a broadening of the areas of potential interest for DASACON and flared test section geometry from general purpose simulation activities supporting primarily Army requirements to include the HML applications of DNA/BMO interest. We believe that interesting, useful contributions have been made in both areas.

11

The following sections will discuss each of the subjects outlined above in some detail, but brief conclusions can be stated now. An extensive series of calculations has demonstrated that for 10 and 30 psi overpressure and 10 and 30 % blockage the flared test section degrades the blast simulator performance in the diffraction phase and improves it during the drag phase of a blast wave. Incidentally, all calculations were done for a square wave of infinite duration. It appears that the influence of flow blockage is less severe than might have been expected for strong shock waves in that flow choking in the transient hydrodynamic processes does not lead to dramatic modifications of the flow field during a time equivalent to 13 shockwave transits across the test object. Certainly flow parameters are modified by blockage, but they are also modified by "real world" factors influencing a tactical situation like surface roughness, local reflections, weather conditions, etc.

A flare could be used in DASACON, but it is unlikely that this would qualitatively increase the ability of that facility to meet all of the requirements of either the Army or HML applications. Section 2.4 lists a number of specific conclusions relative to the importance of blockage and the utility of the flare.

A limited study was also made of perforations in the vicinity of the test chamber as an alternative to a flare to limit the influence of flow blockage. Some attractive results were obtained, but perforations by themselves do not appear to provide an acceptable solution to the blockage problem.

The influence of a modest heated region of air in front of the test object which might be generated by a thermal radiation source has been investigated and found to make relatively minor modification to the otherwise obtained blast forces with or without a flare present.

As originally developed, the DASACON facility was driven by detonating solid high explosives. For a variety of reasons, this driver system was less than satisfactory. A number of calculations have been done which show that gas detonation and/or combustion drivers provide excellent high pressure, high yield equivalent flows. A continuous combustion system has been described which would develop low pressure, high yield simulations. The detonation driver appears particularly attractive in the HML context.

The rarefaction wave eliminator does not appear to be a major feature of DASACON because the tube is relatively long beyond the test chamber. A number of calculations suggest that an active RWE is preferable to a passive one, but perfect flow matching was difficult to obtain. A passive-active RWE system is disclosed in this work.

A small calculational study of a distributed FAE charge was made to investigate potential utility of such a system. The configuration investigated was comparable to that used in the short DABS high explosive system. No particularly interesting or attractive results were obtained.

SECTION 2
FLARED TEST SECTION STUDIES

2.1 BACKGROUND

It has long been recognized that any object placed in a blast simulator will obstruct the cross sectional area of the simulator and modify the late-time flow field developed in it. The problem can be alternatively understood in terms of waves reflected from the object travelling to the walls of the simulator, reflecting there and returning to the object, thus generating a flow field different from what would be obtained in a free field environment. A number of calculations of the quantitative influence of blockage in a particular configuration have been made primarily by Ethridge and co-workers at BRL (U. S. Army Ballistic Research Laboratory) (References 1 and 2). Supplementary work was done by Duff et al (Reference 3). The supplementary calculations looked at the possibility of flaring the test section area of a blast simulator so as to preserve the flow area of the facility and thereby minimize choking which would otherwise occur at a constriction which would act somewhat as a nozzle throat. The calculations to be described below extend this earlier work and investigate more of the relevant variables.

The fundamental idea in the flared concept is the following. In a quasi-one-dimensional, steady flow, the hydrodynamic variables are functions of area. It is well known that subsonic flow conditions approach sonic values as the flow contracts. This effect is shown in Figures 2.1 and 2.2 which show the way flow Mach number and dynamic pressure change with channel area. This is in the context of a blast simulator and the area changes are induced by blockage. If a flare is installed such that the area at the test chamber with the test object in place is the same as the area in front of the test chamber, to first approximation blockage effects would be eliminated. Calculations to be described below investigate the influence of wave strength obstacle shape, flow blockage, and flare shape on the forces and moments which are developed in a blast simulator.

14
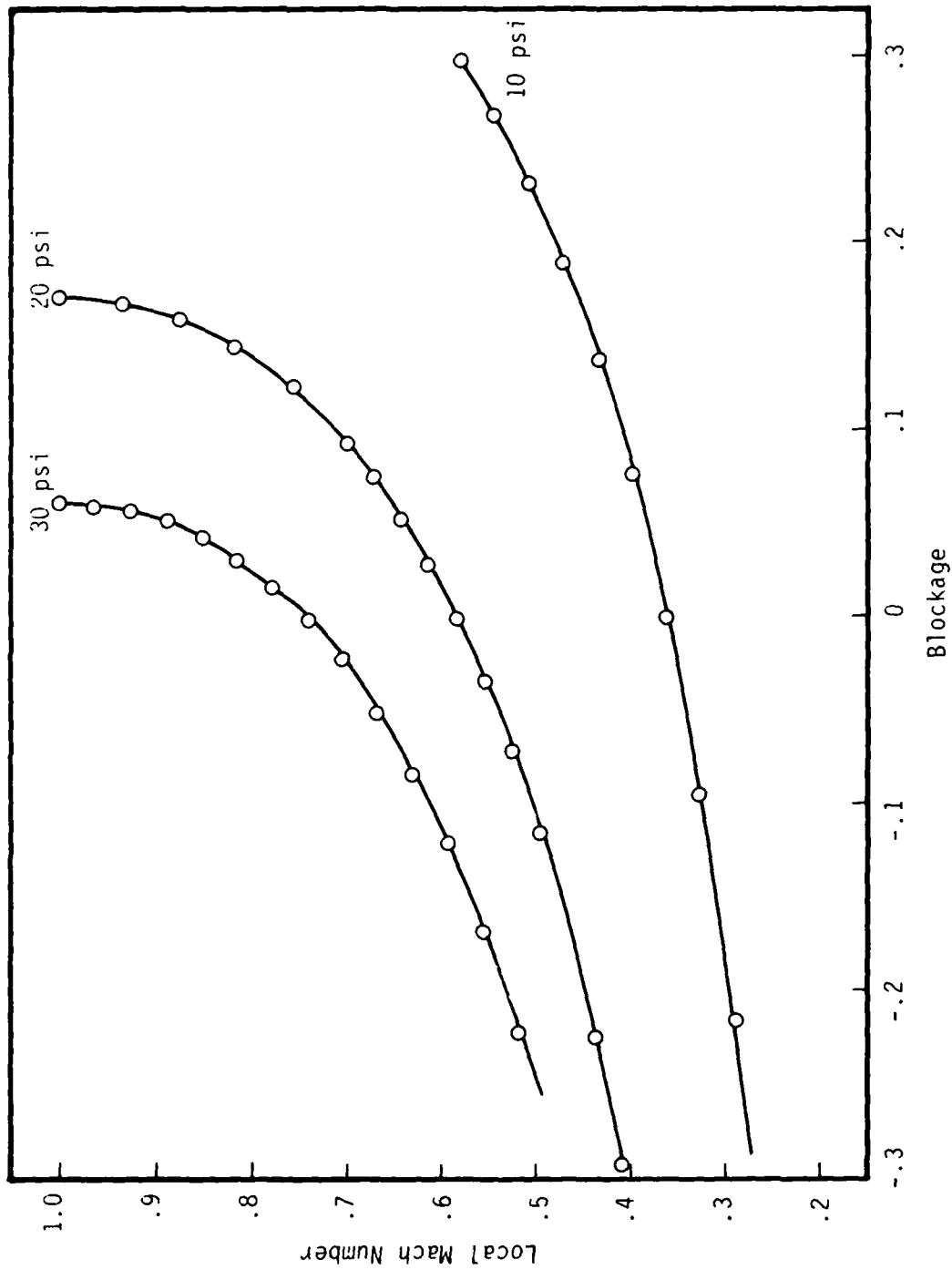
Figure 2.1. Influence of flow blockage on flow or local Mach number. Each curve represents a given blast strength defined in terms of the shock wave overpressure. The calculations assumed steady nozzle flow starting at the Mach number for a blockage of 0. The working fluid was air with $\gamma = 1.4$.
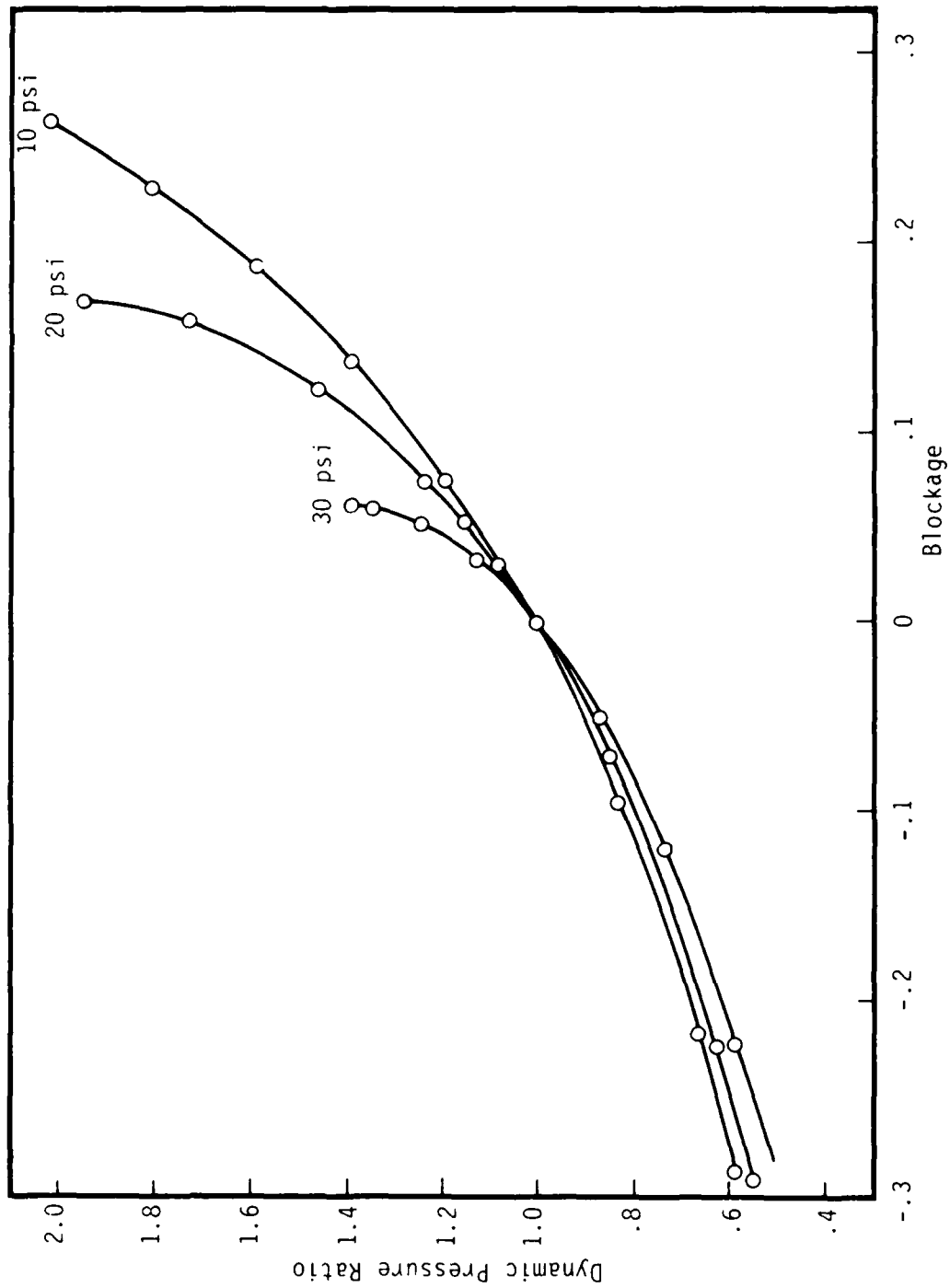
Figure 2.2. Influence of flow blockage on dynamic pressure ratio. For each shock strength the reference dynamic pressure is the value behind the shock.

2.2 CALCULATIONS

All of the calculations done in this study were accomplished
using the HULL code, using a flow configuration identical to that used
at BRL (Reference 1). Figure 2.3 shows this axisymmetric configura-
tion. It is an area mockup for a 2-1/2 ton army truck carrying a
communications shelter. Most of the calculations have investigated
the flow conditions at a nominal 30% blockage at 10 and 30 psi blast
overpressure conditions. Long-duration, flat-topped waves were
assumed in order to maximize blockage effects. Earlier BRL work
(Reference 2) has shown that blockage is much less important for
short-duration flows. Straight, flared and free-field (2% blockage)
cases have been investigated. (The 2% blockage case actually included
a small flare also. This had no significant influence on the results.)
The shapes studied were the block, triangle, and "truck" shape shown
in Figure 2.3. More extensive data edits were obtained than those
reported in the earlier BRL studies. These include forces, moments,
moment arms, pressure and flow velocity contours, and plots of
pressure at indicated stations as functions of time. Finally, this
suite of calculations was extended to include the influence of the
thermal radiation source on flow conditions in a blast simulator. An
alternative approach to the moderation of blockage influence, namely
the provision of a perforated wall, has also been investigated in a
limited set of calculations.

2.3 RESULTS

Many two-dimensional hydrodynamic calculations have been made.
A tremendous volume of numerical results was obtained. As in many
comparable problems a major difficulty is extracting the essence from
this mass of data and deriving the proper conclusions from the work.
In this case, the decision was made to concentrate on graphical output
in the form of forces acting over the objects involved, moments, moment
arms, as well as pressure and velocity contours and pressure as a
function of time at individual points on various objects. We believe
that these representations are adequate for present purposes. As men-
tioned above, the axisymmetric calculations were done which can be

17
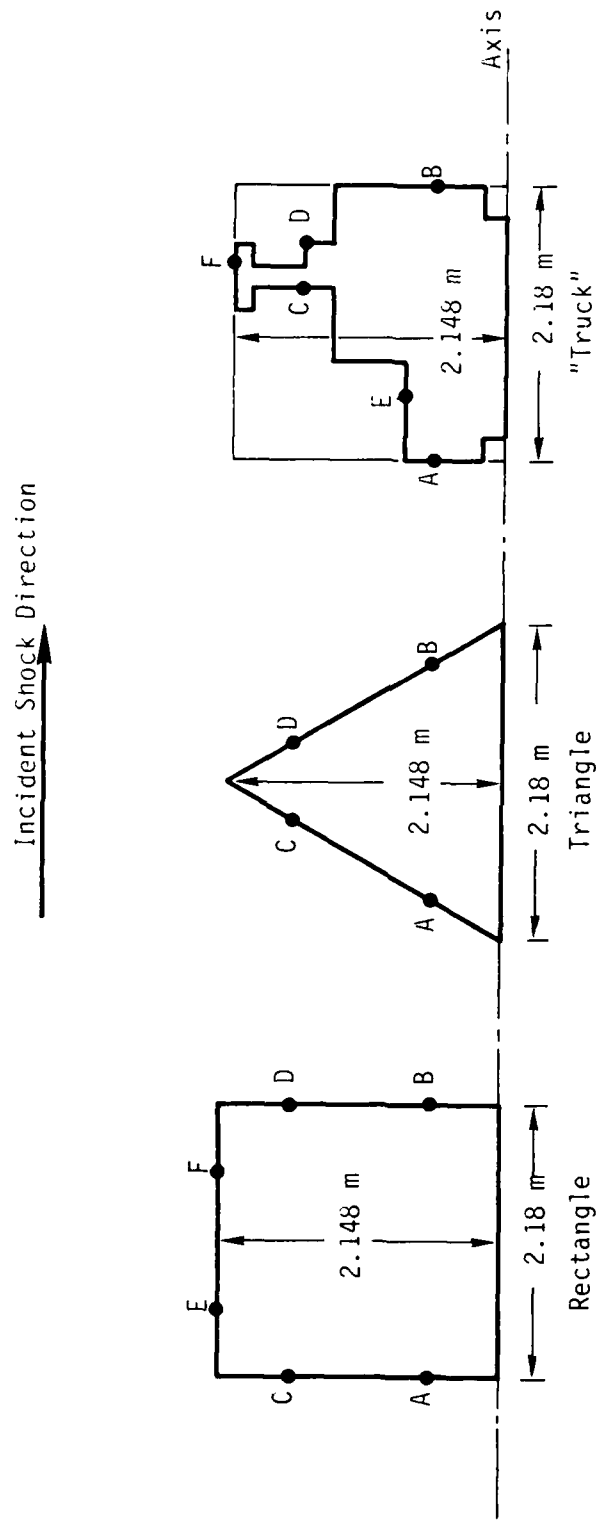
Figure 2.3 Block shape and dimensions used in calculations of flow interactions. The letters on each object indicate the locations of stations at which pressure is monitored as a function of time.

visualized as cylindrical objects located on the axis of cylindrical
flow tubes. For the purposes of data analysis the results have been
interpreted as the flow around a semicircular object in a blast simula-
tor of semicircular cross section. This means that the rectangular
object shown in Figure 2.3 can be considered as half of a cylindrical
disk mounted end on in the blast simulator. The major forces acting
on the object are the net axial force, which is the difference between
the force on the front and back faces, and the vertical force tending
to hold the object to the floor of the blast simulator. This latter
force is derived from the radially inward force calculated in the
axisymmetric representation by simple trigonometric resolution of the
radially inward force over the cylindrical surface keeping only the
vertical component. The following paragraphs and figures will be
concerned with the net force and the top force. These are the area
integrals of the axial and trigonometrically adjusted radial force
components. Impulses will also be presented and these are the simple
integrals of the net force and top force as a function of time.
Moment arms for both the net force and the top force were also calcu-
lated. They differ little for the various conditions considered and
contribute little insight to simulator performance. No further
mention of moment arms will be made in this report. Additional
insight into the flow phenomena can be gained from contours of axial
velocity and pressure in the vicinity of the objects. Finally,
pressure as a function of time at several stations around the object
will be presented. Figure 2.3 shows the location of these stations on
the front, back, and top surface of the object.

In most of the following discussion, 50 ms of calculation will
be summarized for 30 psi overpressure shocks. This time represents
approximately 13 shock transit times across the object. In general,
results from a reference calculation will be compared with data from
a straight tube, a flared tube or a vented tube. A straight tube is,
as the name implies, a simple cylindrical tube with an object on axis
the area of which is 30% of the tube area. The flare geometry is
shown in Figure 2.4. The flow area upstream and downstream of the
object is identical to that in the straight walled region of the flare.

19
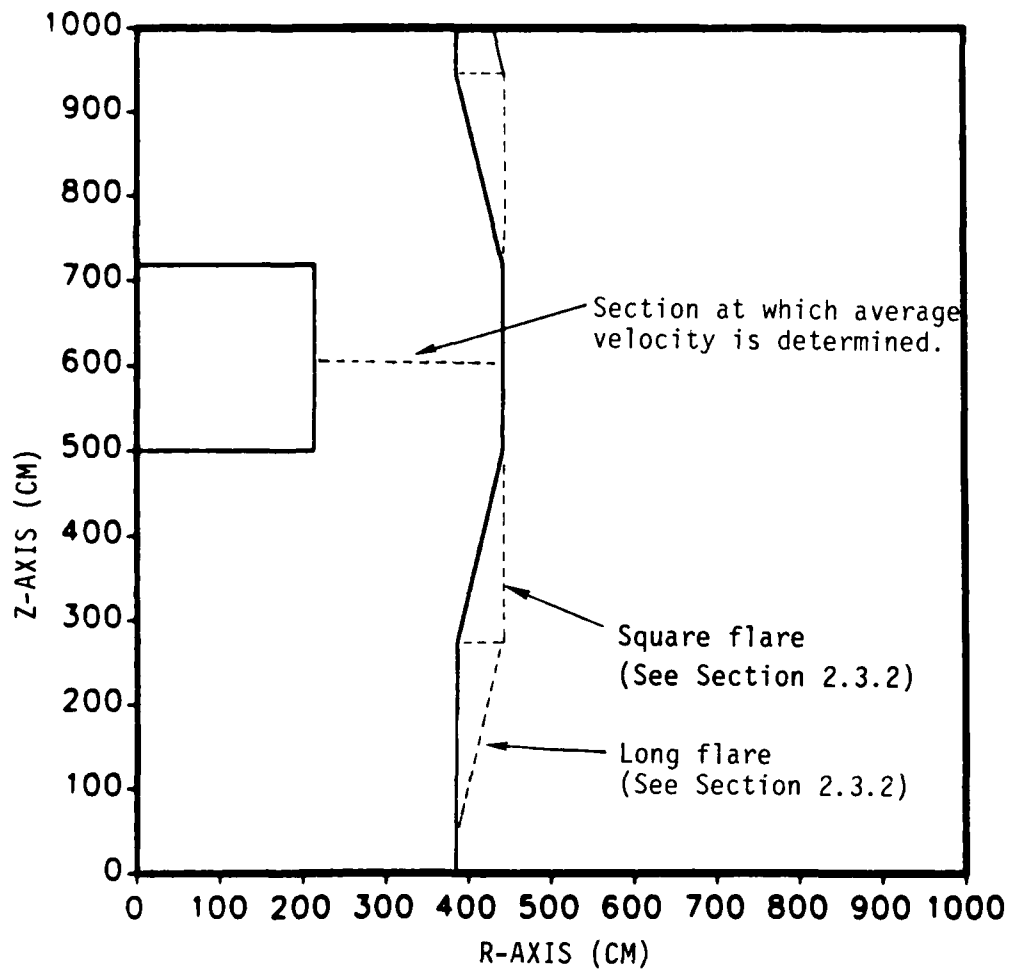
Figure 2.4. This figure illustrates the standard flare geometry used in 30% blockage calculations. A rectangular test object is also shown.

The length of the flared section is equal to the length of the block, and the length of the tapered sections fore and aft is also equal to the length of the block. The annular area between the cylindrical object and the flared wall section is equal to the area upstream and downstream of the object. In the vented configuration, a circular slot is opened in the wall of the straight tube. This slot is centered at the test object, and the width of the slot is 25% of the length of the object. Flow is assumed free to expand into the region outside of the tube. These configurations are idealized to illustrate hydro-dynamic influences as were the related calculations made by BRL (Reference 1). Various mismatches of the test object size and loca-tion would obviously arise if a flared or vented configuration were used in a blast simulator.

Average velocity is another quantity which will be discussed from time to time. This is the volume average velocity of the stream measured between the axial midpoint of the object and the tube wall.

The curves in the many figures which follow are identified by 6 digit problem numbers. In an effort to minimize possible confusion Table 2.1 lists these problem numbers and describes what was calcu-lated in each case.

2.3.1   30 psi, 10% Blockage Results

The first series of comparisons will describe the results for a relatively strong, 30 psi overpressure, blast in a configuration of 10% blockage. Data from straight, flared, and the vented straight calculations are compared with a reference calculation for a 2% blockage case in Figures 2.5 through 2.12. The net force data is shown in Figure 2.5. In each case, the heavy line is the reference calculation which is assumed a reasonable approximation to the free-field condition. Note that in the straight pipe the net force is in perfect agreement with the reference calculation until about 30 ms. This shows that the diffraction phase and early parts of the drag

21

Table 2.1. This table gives a brief description of the several configurations calculated and referred to in this report.

Problem	Shock Overpressure (psi)	Sample Shape	Blockage (%)	Comment
8306.21	10	Rectangle	2	Reference
8306.23	30	Rectangle	2	Reference
8306.24	30	Triangle	2	Reference
8306.25	10	Triangle	2	Reference
8307.30	10	Triangle	30	Standard flare
8307.31	30	Triangle	30	Standard flare
8307.32	30	Rectangle	30	Standard flare
8308.04	30	Rectangle	30	Square flare
8308.05	10	Rectangle	30	Square flare
8308.06	10	Rectangle	30	Long flare
8308.17	10	Rectangle	30	Straight tube
8309.10	30	Rectangle	30	Straight tube
8309.28	30	Triangle	30	Straight tube
8309.29	10	Triangle	30	Straight tube
8310.24	10	Rectangle	30	Standard flare
8311.02	30	Rectangle	10	Standard flare
8311.03	30	Rectangle	10	Straight tube
8311.04	30	Rectangle	10	Vented straight tube
8311.18	30	Rectangle	30	Vented straight tube
8311.28	30	Rectangle	30	TRS and Standard flare
8311.29	30	Rectangle	30	TRS and Standard flare
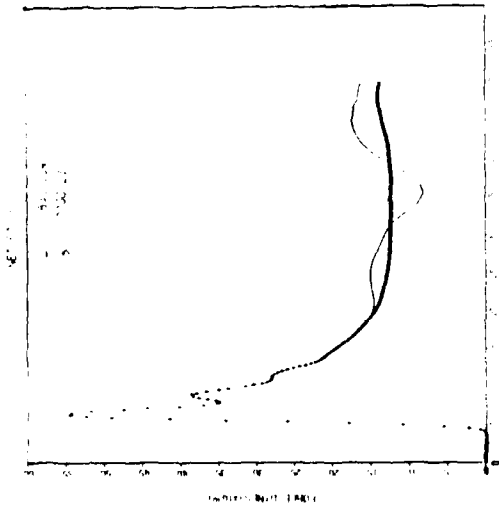
Rectangular sample   30 psi
Vent vs. Ref.
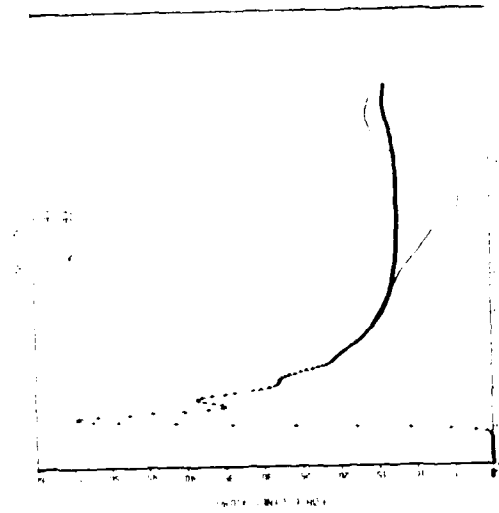
Rectangular sample   30 psi
Std. flare vs. Ref.
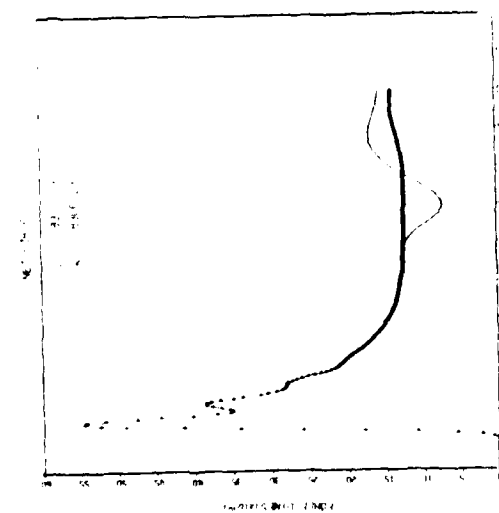
Rectangular sample   30 psi
Straight vs. Ref.

Figure 2.5.   Net force comparisons for 30 psi shocks and 10% blockage. The net force results for
a straight, standard flare, and vented test chamber are compared with nominal free field
conditions, 2% blockage.

phase are perfectly represented in the 10% blockage case. At later
times the force decreases and then increases above the reference
value. On the other hand, small perturbations are observed in the
flared case roughly 10 ms earlier. Departures from the reference
curve are more pronounced than they were in the standard case. The
net force for the vented calculation is qualitatively similar but
slightly different in detail. The top force for these three cases is
shown in Figure 2.6. Note again that the straight tube provides the
best fidelity until 30 ms during the diffraction and the early part of
the drag phase. The rarefaction originating at the upstream flare can
be seen to significantly influence the top force in the flared case
before 15 ms whereas the rarefaction is delayed until almost 20 ms in
the vented case. The prominent reflection from the wall is seen in
each case arriving between 36 and 38 ms. Interestingly, it is most
prominent in the flared case probably because of reinforcement from
reflections at the downstream flare. Figures 2.7 and 2.8 show the net
force and top force impulses as a function of time. In each case, the
impulse delivered within 50 ms is within 15% of the reference value
for all configurations.

Figure 2.9 shows the average velocity for these three cases.
The straight tube shows a slowly increasing average velocity whereas
the flare and vented case have essentially constant average veloci-
ties, the first somewhat below, the second somewhat above the
reference value.

Further insight into these flow fields is provided by Figure 2.10
which shows pressure contours around rectangular objects in the several
flow conditions at a time of 50 ms. Note that the contours generated
by the several configurations are qualitatively similar but different
in detail. This is further illustrated in Figure 2.11 which shows
axial (vertical) velocity component contours. The size of the reverse
flow vortex at the top corner of the object is smaller in the straight
tube than in either of the others. In both figures and in all follow-
ing contour plots identical contour values are used. This helps with
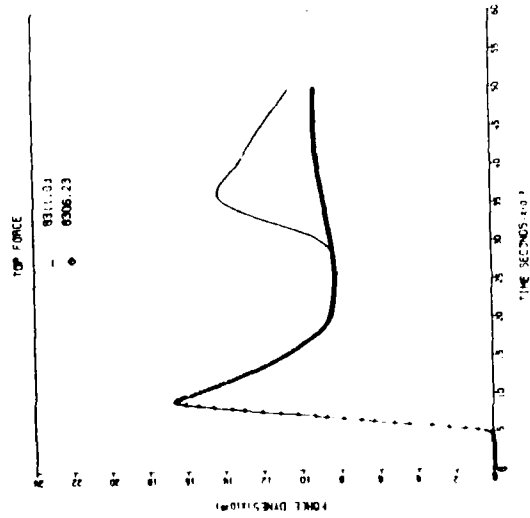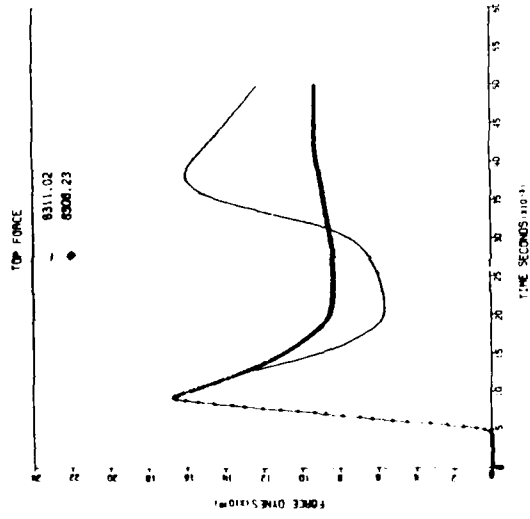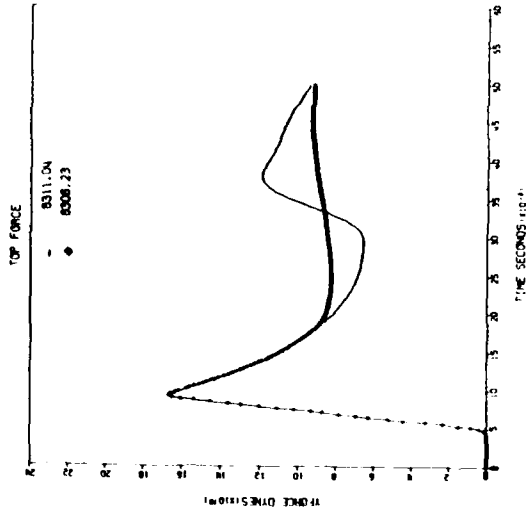
Figure 2.6. Top or hold down force comparisons for 30 psi shocks and 10% blockage.
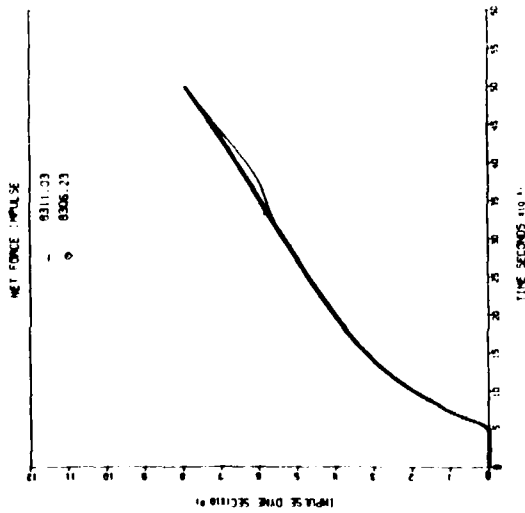
Rectangular sample, 30 psi
Straight vs. Ref.
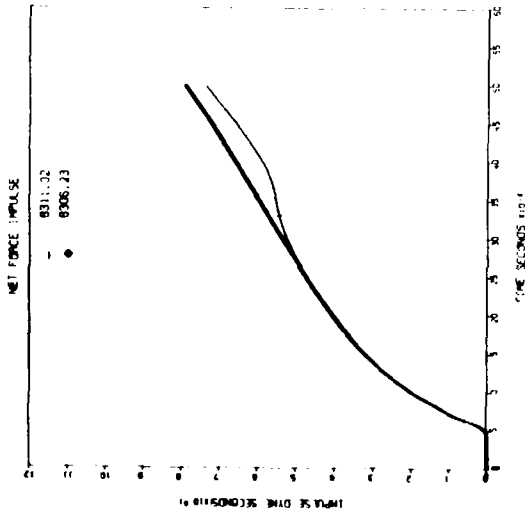
Rectangular sample, 30 psi
Std. flare vs. Ref.
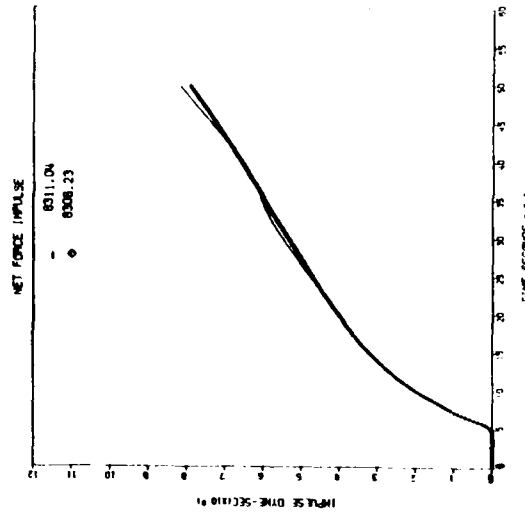
Rectangular sample, 30 psi
Vent vs. Ref.

Figure 2.7. Net force impulse comparisons for 30 psi shocks and 10% blockage.
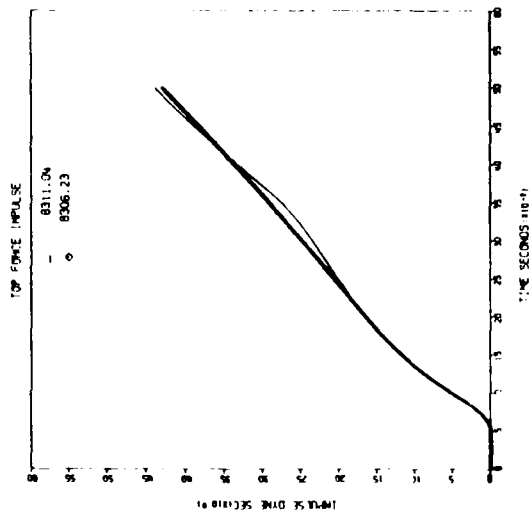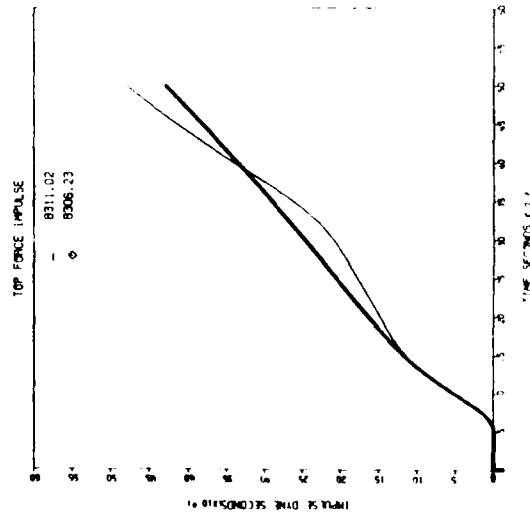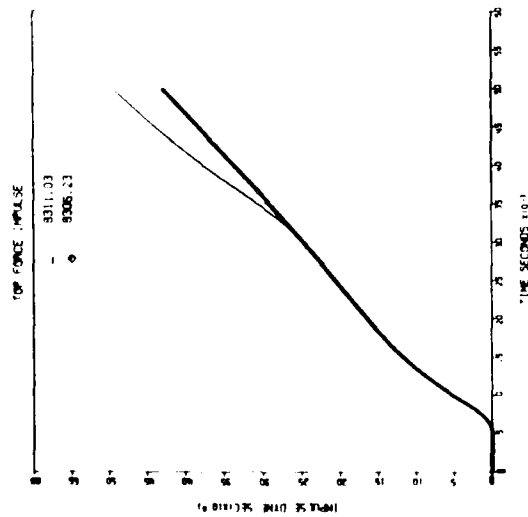
Figure 2.8.   Top force impulse comparisons for 30 psi shocks and 10% blockage.
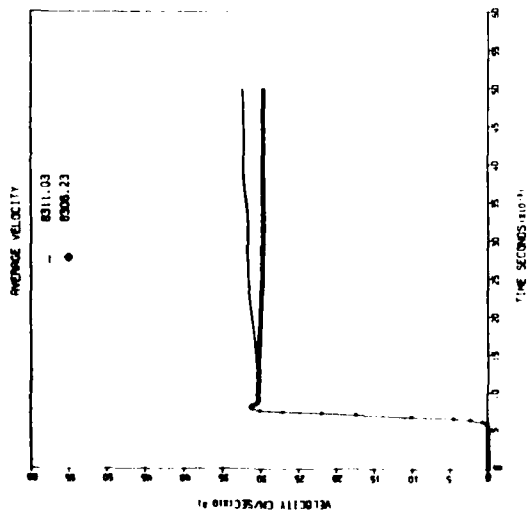
Rectangular sample, 30 psi
Straight vs. Ref.
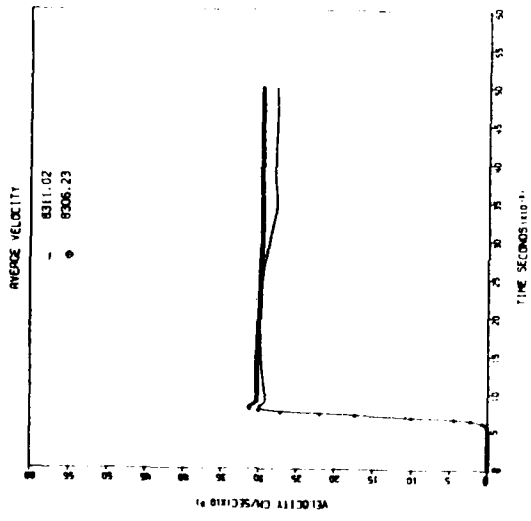
Rectangular sample, 30 psi
Std. flare vs. Ref.
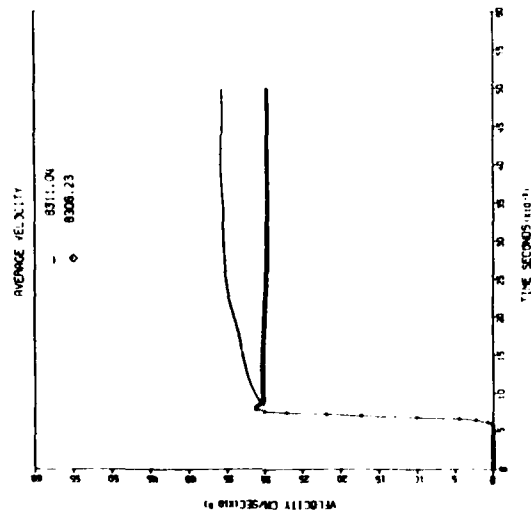
Rectangular sample, 30 psi
Vent. vs. Ref.

Figure 2.9. Average velocity comparisons for 30 psi shocks and 10% blockage.

28
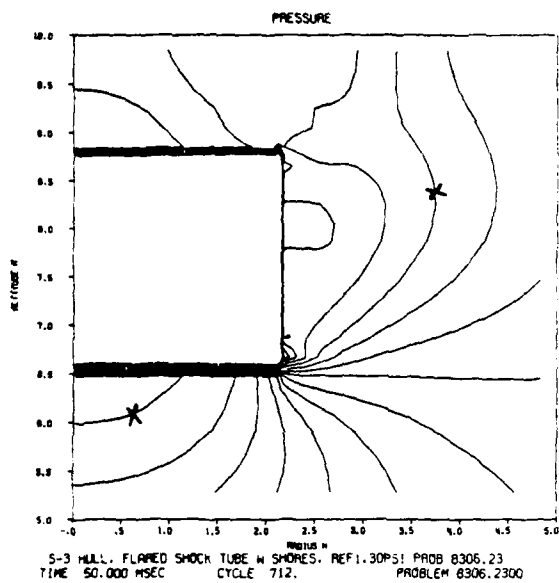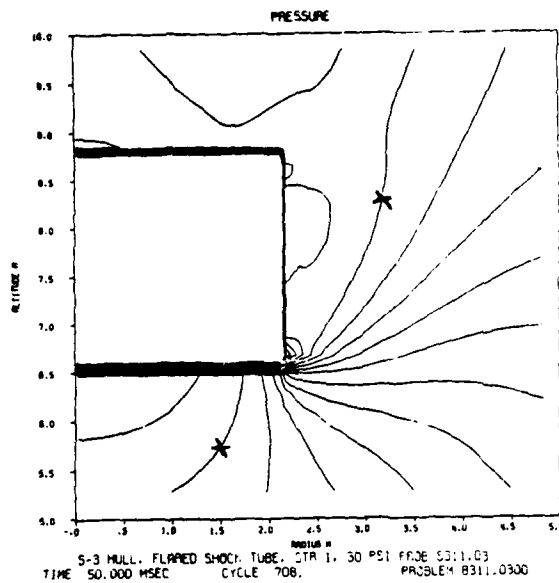
Reference

Straight Tube
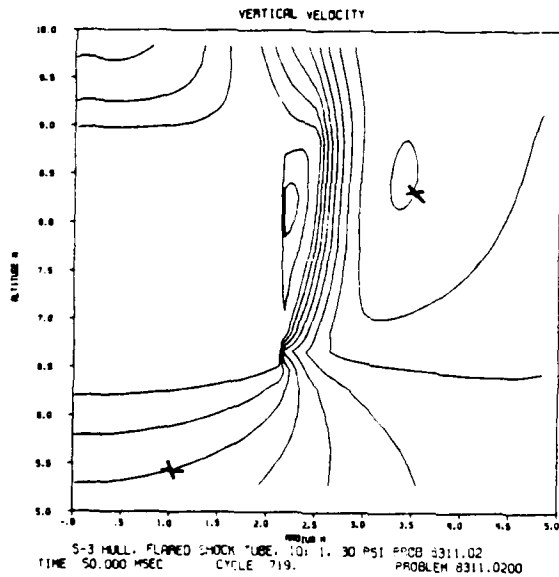
Standard Flare

Vented Tube

Figure 2.10. Pressure contours at 50 ms for the several configurations
studied at 30 psi and 10% blockage. Comparable contour
values are indicated by the symbols in each figure.

29

VERTICAL VELOCITY

S-3 HULL. FLARED SHOCK TUBE W SHORES. REF1.30PSI PROB 8306.23
TIME 50.000 MSEC   CYCLE 712.   PROBLEM 8306.2300

Reference

VERTICAL VELOCITY

S-3 HULL. FLARED SHOCK TUBE. STR 1. 30 PSI PROB 8311.03
TIME 50.000 MSEC   CYCLE 708.   PROBLEM 8311.0300

Straight Tube

VERTICAL VELOCITY

S-3 HULL. FLARED SHOCK TUBE. 10: 1. 30 PSI PROB 8311.02
TIME 50.000 MSEC   CYCLE 719.   PROBLEM 8311.0200

Standard Flare

VERTICAL VELOCITY

S-3 HULL. FLARED SHOCK TUBE. VNT 1. 30 PSI PROB 8311.04
TIME 50.000 MSEC   CYCLE 706.   PROBLEM 8311.0400

Vented Tube

Figure 2.11. Axial velocity contours at 50 ms for the several configurations
studied at 30 psi and 10% blockage. The velocities are quite
comparable.

30

qualitative interpretation. The only quantitative information comes from the symbols which indicate selected pressure contours, and the obvious zero velocity interval in which a contour is not plotted. This also explains why the object outline is not shown in the velocity figures.

Figure 2.12 summarizes the pressure histories at the stations indicated in Figure 2.3. It is interesting to note the arrival of various reflected shock and rarefaction waves in the several configurations. This suite of results tends to confirm the conclusion of the BRL study (Reference 1) that flow perturbations produced by 10% blockage were not excessive. Note, however, that a 10% blockage for a 30 psi blast should produce choked conditions according to the curves of Figure 2.1. No dramatic evidence of such conditions was seen in these calculated results. Note also that the flared configuration gave the poorest overall pressure traces of any of the cases considered.

2.3.2   10 psi 30% Blockage Results

A more interesting question concerning the potential utility of a flared or vented test chamber deals with higher blockage ratios. In this section, 10 psi, 30% blockage conditions will be considered.

Figures 2.13 through 2.17 show comparisons between the net force and top force, their moments and average velocities for the 10 psi 30% blockage cases for the straight tube and standard flare examples as well as for two alternative flare geometries. The curves labeled "square flare" refer to a calculation in which the tube diameter was abruptly increased to its full diameter; the curves labeled "long flare" refer to a calculation in which the length of the test chamber itself was increased threefold, that is, the expanded section was continued for one body length upstream and downstream of the object. Both of these configurations are illustrated in Figure 2.4. The flare transition shape was the same as in the standard calculations. Note

31
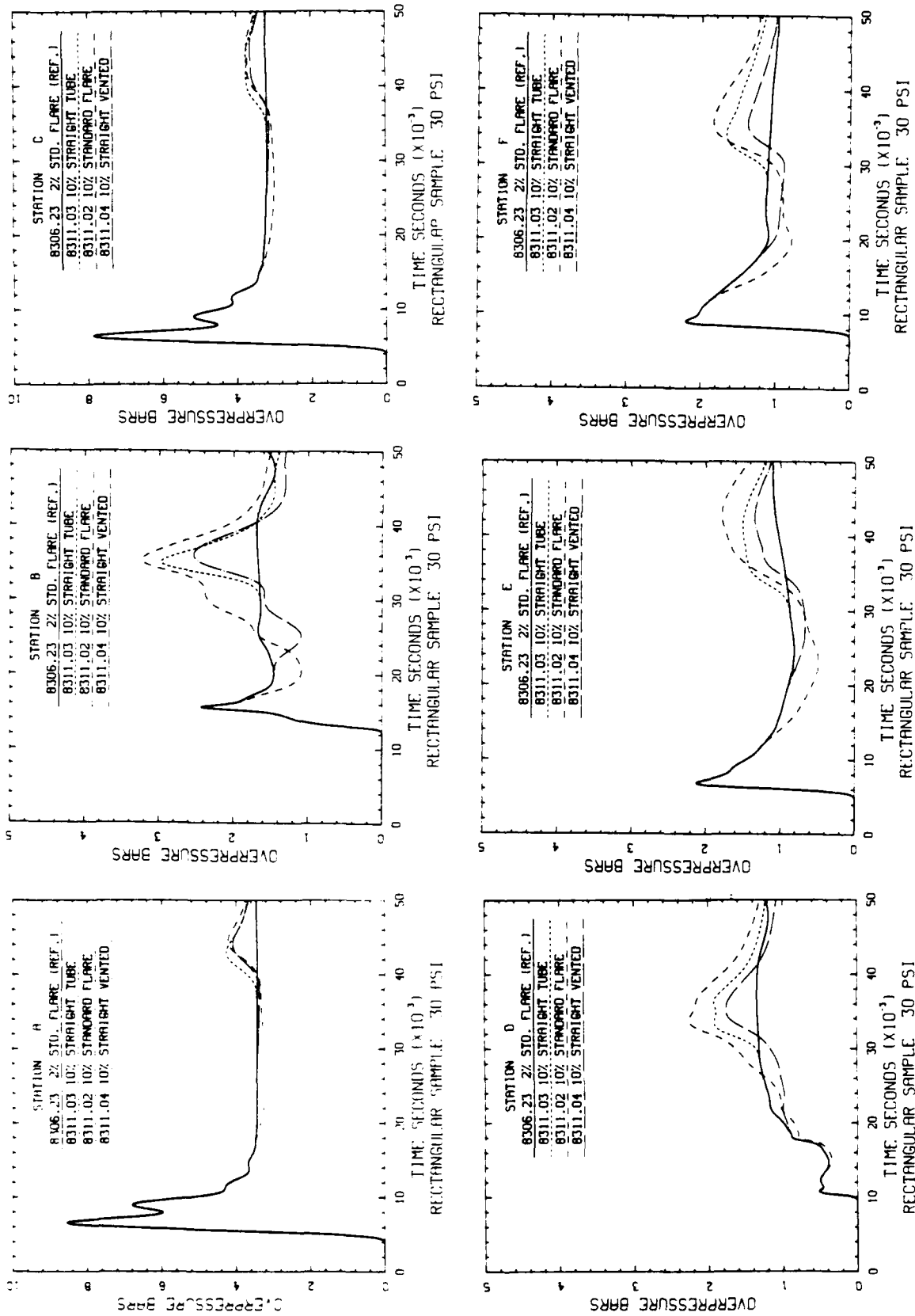
Figure 2.12. Pressure as a function of time at the several stations indicated in Figure 2.3 for the configurations studied at 30 psi and 10% blockage.

NET FORCE

— 8308.17
◇ 8306.21

FORCE DYNES(X10⁹)

TIME SECONDS(X10⁻⁹)

NET FORCE

— 8310.24
◇ 8308.21

FORCE DYNES(X10⁹)

TIME SECONDS(X10⁻⁹)

Rectangular sample, 10 psi
Straight vs. Ref.

Rectangular sample, 10 psi
Std. flare vs. Ref.

NET FORCE

— 8308.05
◇ 8306.21

FORCE DYNES(X10⁹)

TIME SECONDS(X10⁻⁹)

NET FORCE

— 8308.06
◇ 8306.21

FORCE DYNES(X10⁹)

TIME SECONDS(X10⁻⁹)
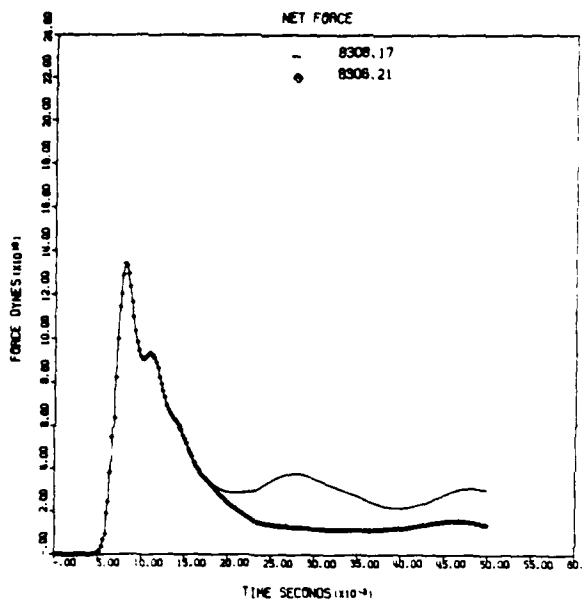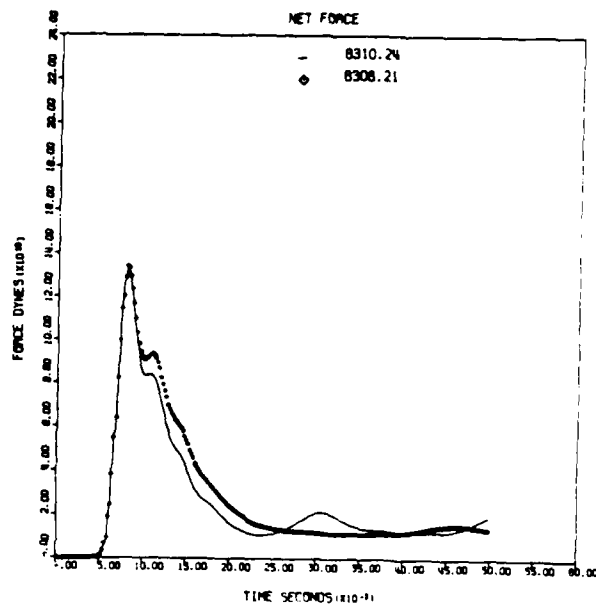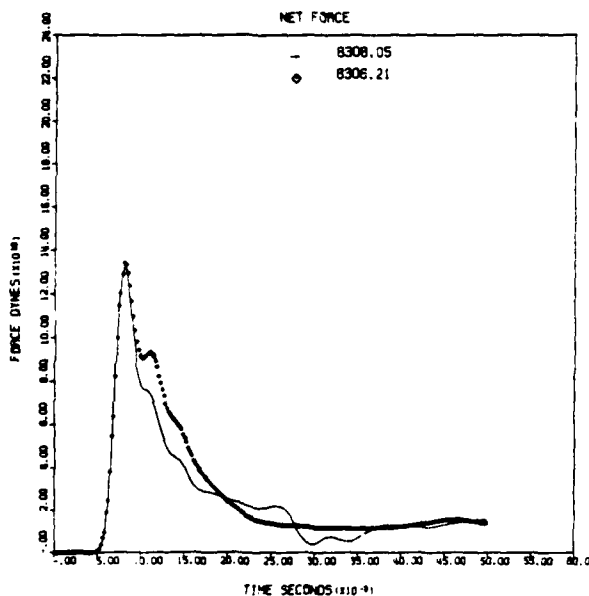
Rectangular sample, 10 psi
Square flare vs. Ref.
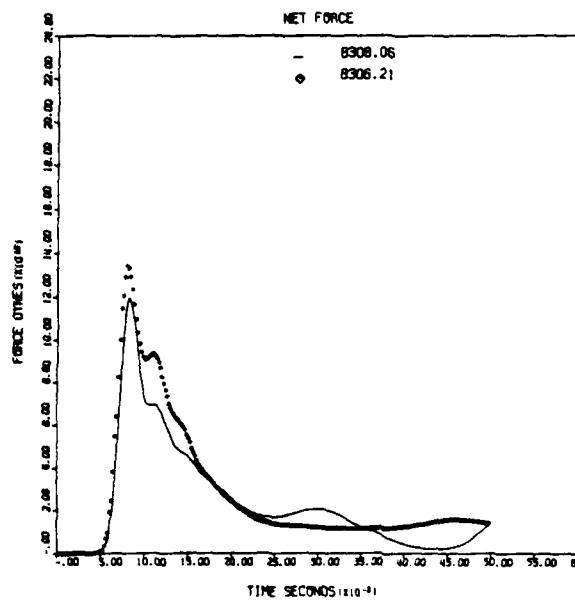
Rectangular sample, 10 psi
Long flare vs. Ref.

Figure 2.13.   Net force comparisons for 10 psi shocks and 30% blockage.
The net force results for a straight tube, standard, square
and long flares are compared with nominal free field
conditions, 2% blockage.
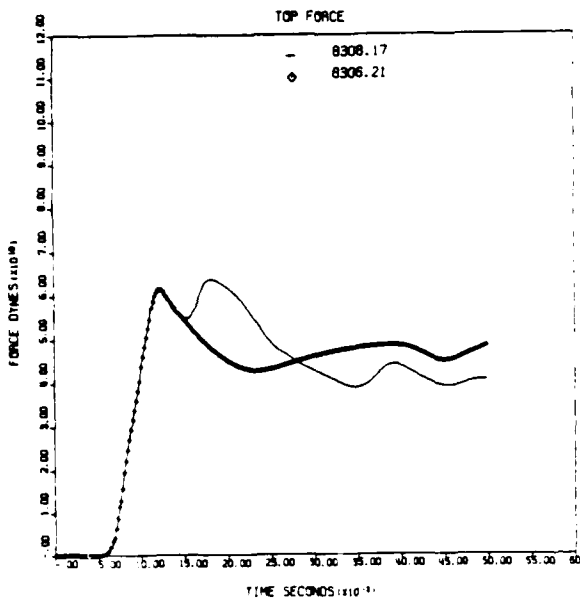
33

Rectangular sample, 10 psi
Straight vs. Ref.
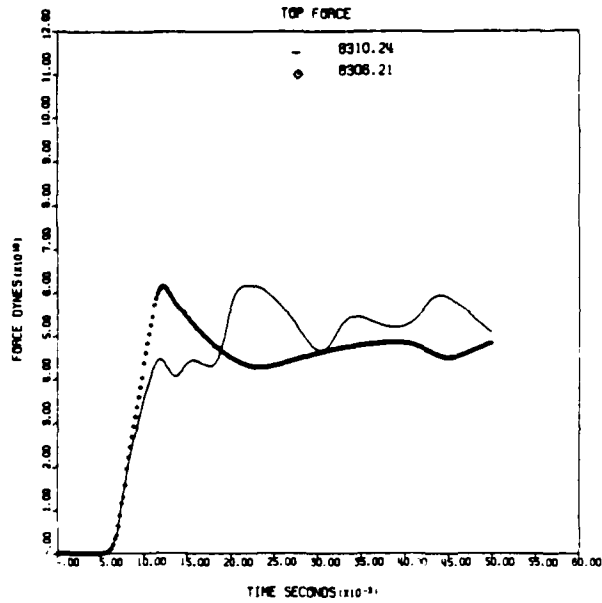
Rectangular sample, 10 psi
Std. flare vs. Ref.
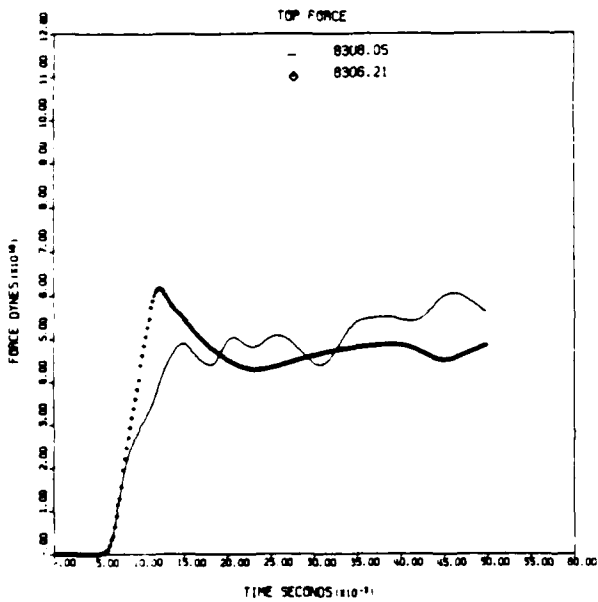
Rectangular Sample, 10 psi
Square flare vs. Ref.
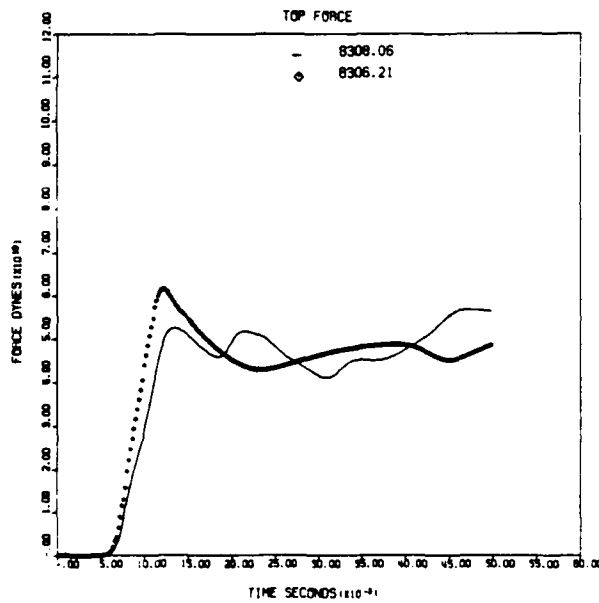
Rectangular sample, 10 psi
Long flare vs. Ref.

Figure 2.14.   Top or hold down force comparisons for 10 psi shocks and
30% blockage.
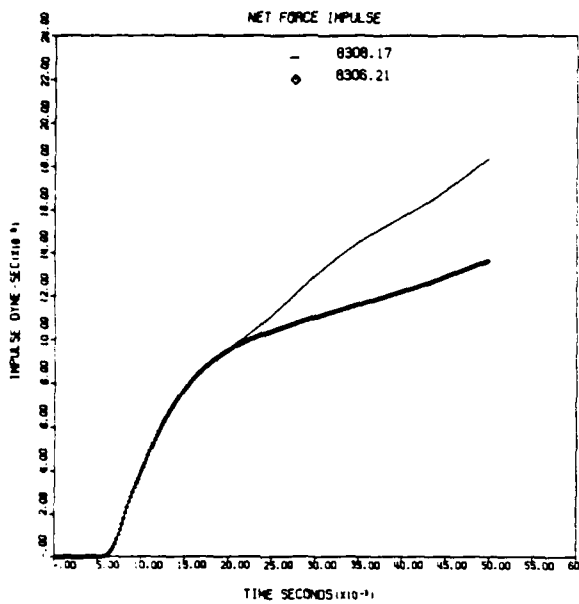
34

Rectangular sample, 10 psi
Straight vs. Ref.
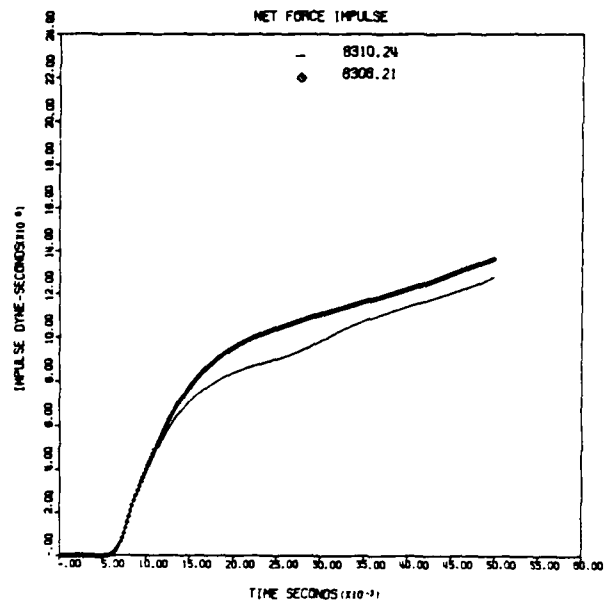
Rectangular sample, 10 psi
Std. flare vs. Ref.
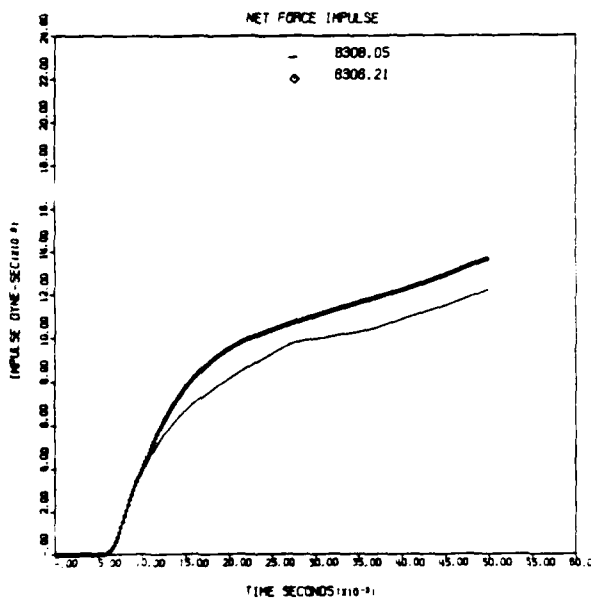
Rectangular sample, 10 psi
Square flare vs. Ref.
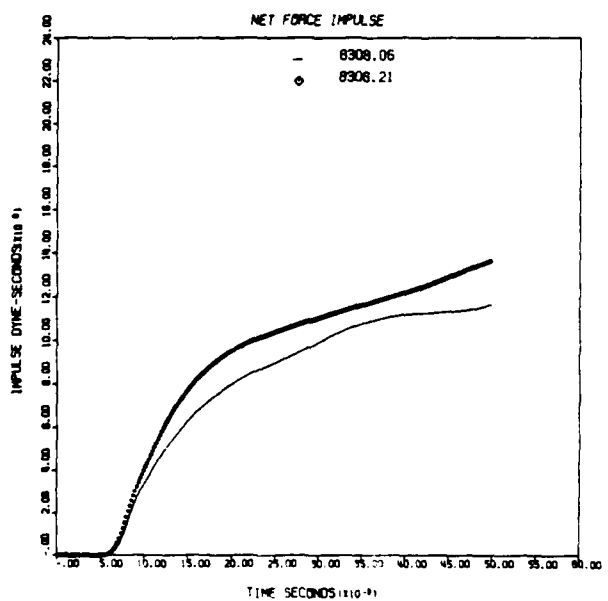
Rectangular sample, 10 psi
Long flare vs. Ref.

Figure 2.15. Net force impulse comparisons for 10 psi shocks and
30% blockage.
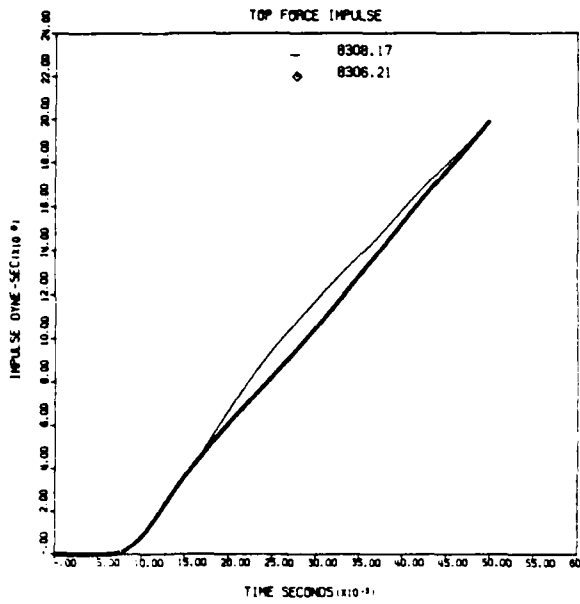
35

Rectangular sample, 10 psi
Straight vs. Ref.
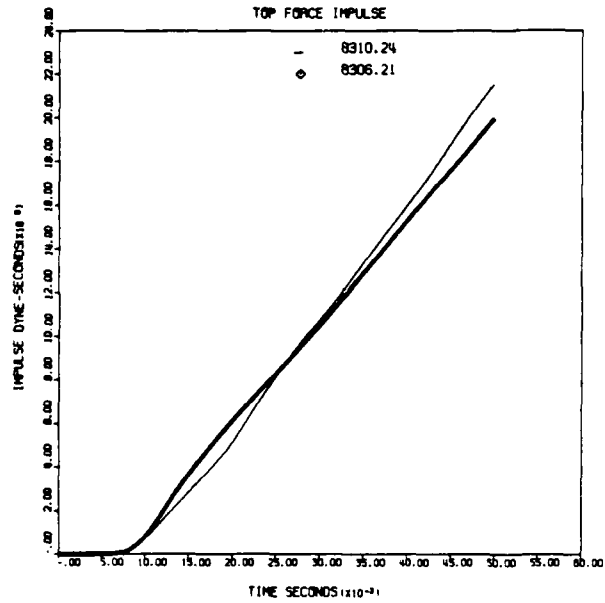
Rectangular sample, 10 psi
Std. flare vs. Ref.
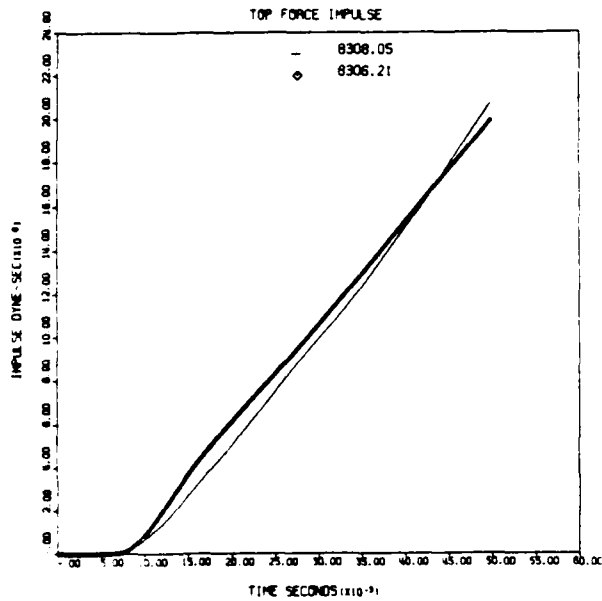
Rectangular sample, 10 psi
Square flare vs. Ref.
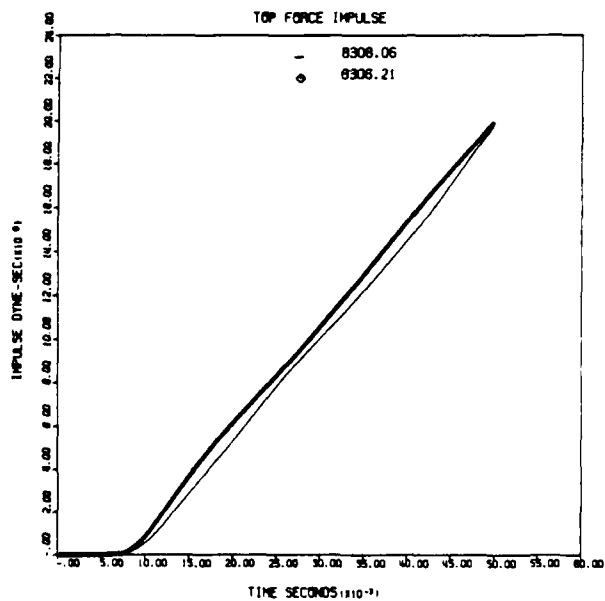
Rectangular sample, 10 psi
Long flare vs. Ref.

Figure 2.16.   Top force impulse comparisons for 10 psi shocks and
30% blockage.
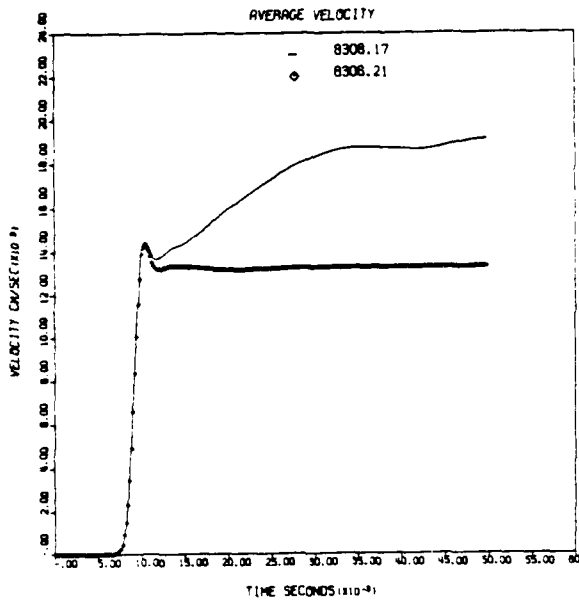
Rectangular sample, 10 psi
Straight vs. Ref.
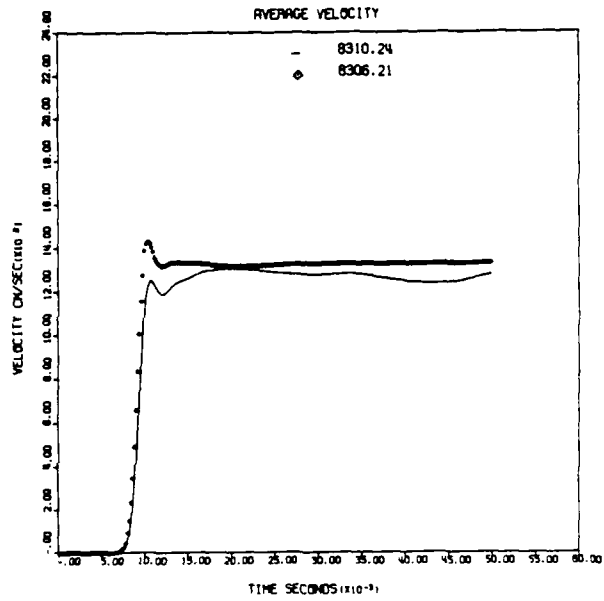
Rectangular sample, 10 psi
Std. flare vs. Ref.
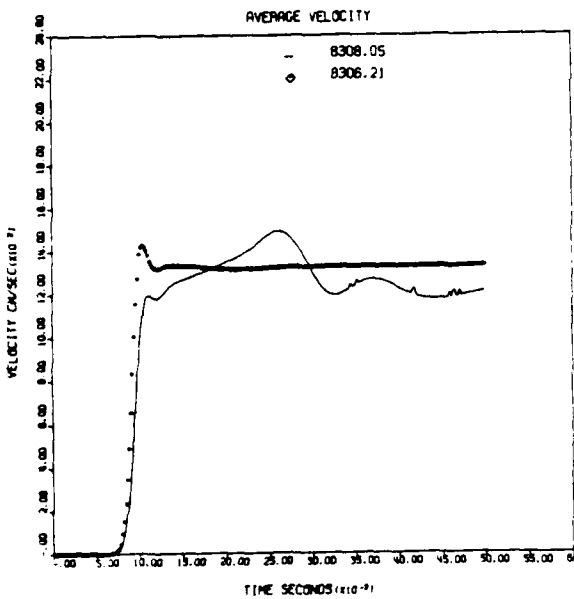
Rectangular sample, 10 psi
Square flare vs. Ref.
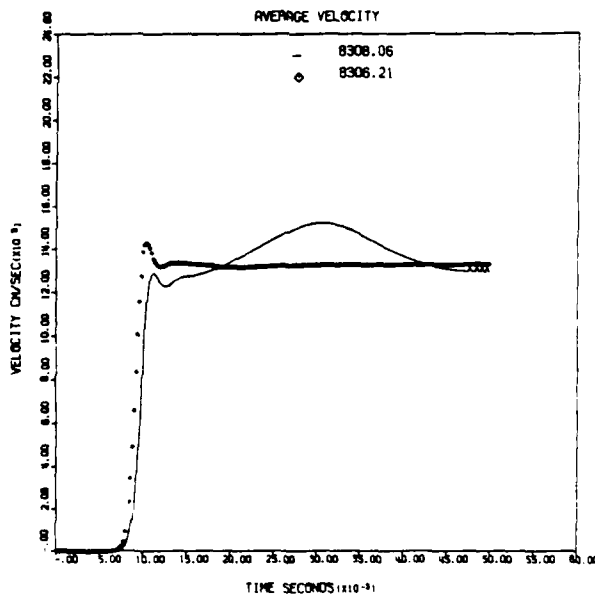
Rectangular sample 10 psi
Long flare vs. Ref.

Figure 2.17. Average velocity comparisons for 10 psi shocks and 30 % blockage.

that zero time in the long flare case has been adjusted by approximately 4 ms to account for the longer pipe section ahead of the object. The net force curves show that for these relatively weak shock conditions the major loads occur during the diffraction phase. The late-time drag force is only about 10 % of the peak diffraction load. The curve also shows that the drag force is approximately doubled in the straight tube compared to the quasi-free-field reference calculation. The rarefaction which is generated in the flared test chamber modifies the late stage of the diffraction loading of the object but produces approximately the correct drag phase. The square flare configuration gives a net force which is qualitatively similar but different in detail from the standard case. The long flare is less attractive in that the entire diffraction phase is modified by the flare-generated rarefaction, and late-time force oscillations are more severe.

The top force curves shown in Figure 2.14 again demonstrate the efficacy of the straight tube in preserving the diffraction phase and the influence of the rarefaction in modifying the diffraction phase in the flared cases. The rarefaction influence of the standard flare is clearly less significant than either of the alternatives considered. At late times, the details of the top force loads differ as various waves reflect within the configuration, however, in general, the forces are within 10 to 20% of reference values.

The net force impulse shows the impulse in the straight tube to be high at late times, and in all of the flared configurations it is low. It is probably true that a partial flare, a compromise between a straight tube and a fully flared configuration, might well produce a net force impulse in excellent agreement with the free-field expectation at blockages as high as 30% .

The top force and hold-down impulses in all cases are quite close to the free-field values.

38

Figure 2.17 shows that the average velocity increases dramatically in the straight tube, agrees almost perfectly with expectation in the standard flare, and oscillates about the expected value for the two alternate flare configurations considered.

The pressure profiles shown in Figure 2.18 shows that the late time flow fields are qualitatively similar in each case. In particular, at 50 ms the standard flare and free-field pressure contours are in quite good agreement. The straight tube gives poorest agreement.

The vertical velocity contours shown in Figure 2.19 for these five different configurations at nominal 50 ms are again very similar. Each shows a reverse flow region above the object. All of the flared configurations and the free-field case show this region to cover almost all of the block top, whereas in the case of the straight tube only a very small reverse flow region exists.

In general, the pressure as a function of time at various stations along the test object presented in Figure 2.20 show the expected trends. On the front face, the free-field pressure is high at early time during the diffraction phase, and after about 15 ms approaches a constant value. In the other configurations, wall reflections can be seen which raise the front face loading as expected. The long flare shows the influence of the early rarefaction which reduces the strength of the incident shock before it reaches the object.

The loads at the lower rear corner demonstrate that the straight tube produces the best agreement with the reference calculation, whereas the various flared configurations provide results within roughly 50% of the free-field values because these discrepancies are related to the arrival of various reflected shock and rarefaction waves.

The flow conditions at the upper rear corner are all in reasonable agreement with the free-field case. Again, the influence of various shock and rarefaction waves is apparent in the straight and

39
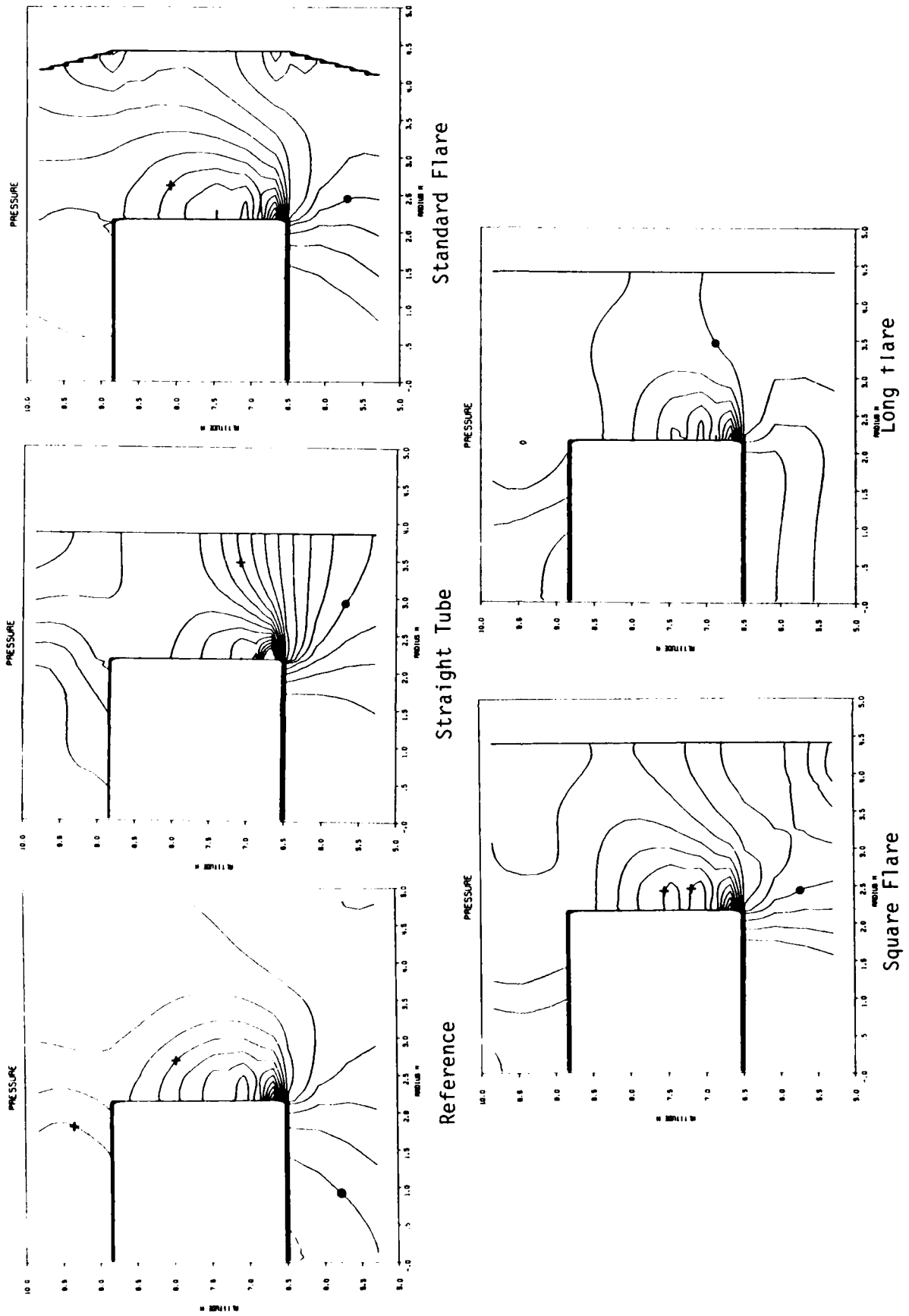
Figure 2.18. Pressure contours at 50 ms for the several configurations investigated at 10 psi and 30% blockage. Corresponding contours are indicated on each figure.

40
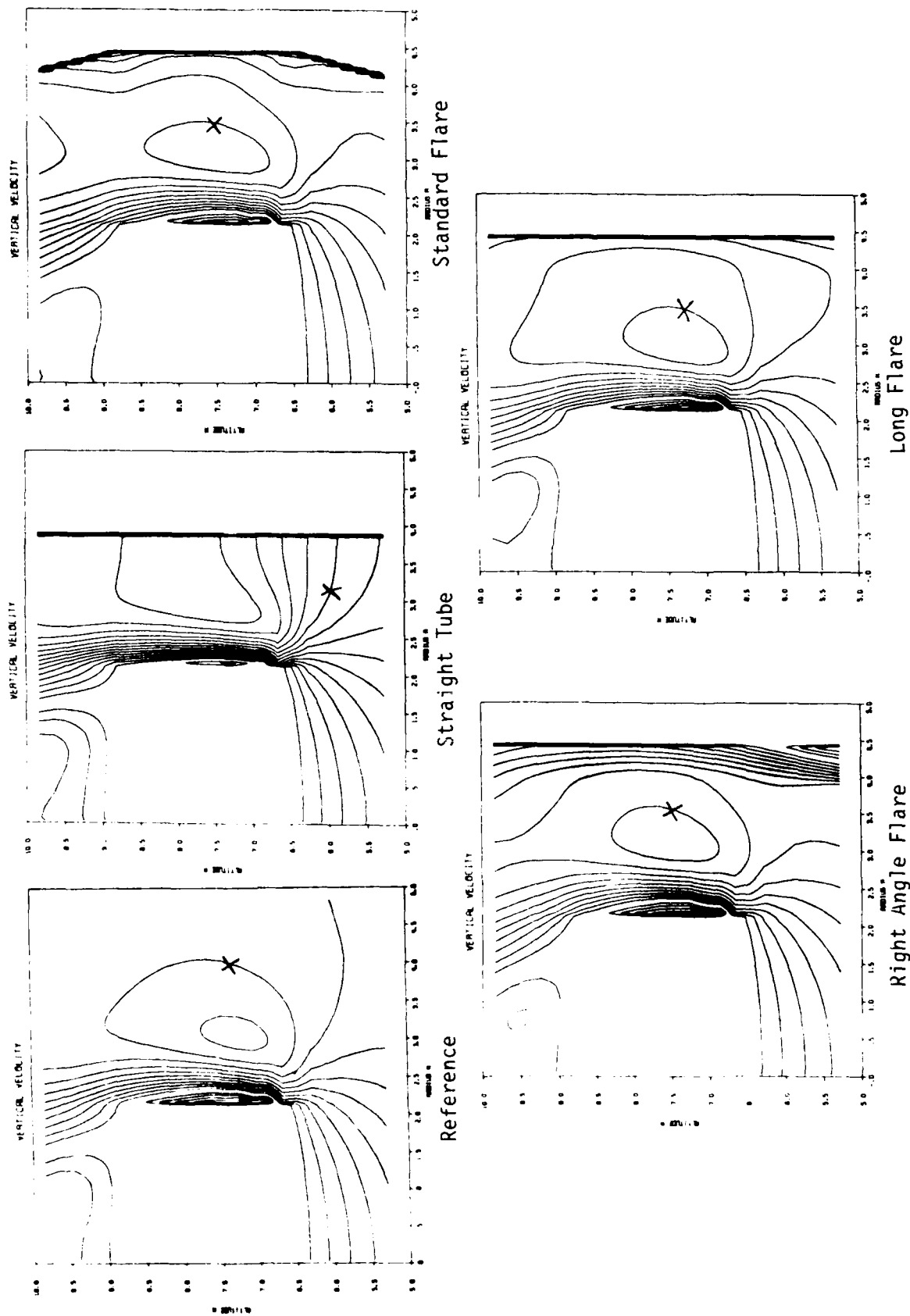
Figure 2.19. Vertical or axial velocity contours for the several configurations studied at 10 psi and 30% blockage. All of the flared configurations give results in good qualitative agreement with the reference calculation.

41
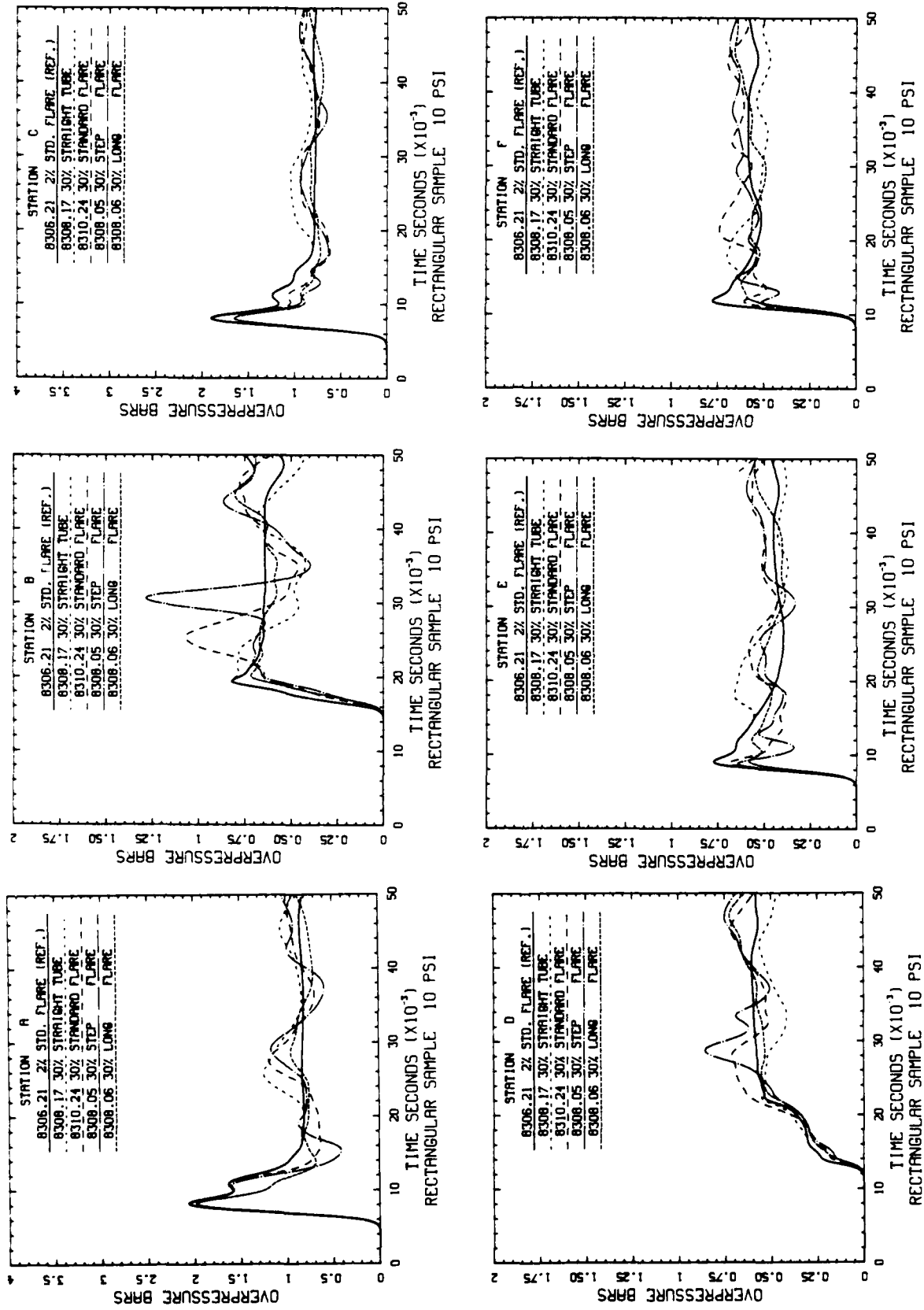
Figure 2.20. Pressure as a function of time at the several stations indicated in Figure 2.3 for the configurations studied at 10 psi and 30% blockage.

42

flared configurations. The top forces again demonstrate the expected pattern. The straight tube provides early time diffraction loading in excellent agreement with the free-field case, the flared examples are influenced by the rarefaction wave from the flare corners at early time, but during the drag phase the flared loadings are closer to free-field than is the straight case.

Since the flow Mach number behind a 10 psi blast wave is relatively low (0.36), extreme blockages can occur before flow choking is to be expected in even the steady state case. For the 30% blockage considered above, the expected steady state flow Mach number is only 0.5%, a value far from the transonic range. The straight tube provides good fidelity during the d raction phase, and during the drag phase. The increase in axial force is consistent with that expected from the calculated increase in dynamic pressure shown in Figure 2.2 for this case. On the other hand, the flared configurations do less well in the diffraction phase but better in the drag phase. All things considered, the standard flare configuration seems more attractive than either the square cornered or lengthened flares considered. Finally, it appears for this shock strength that an alternate configuration with a flare of less severe expansion might provide even better flow simulation than any of the configurations considered here. These results also point out that the simulation facilities required for a particular application depend critically upon that application. Blockage is a minor perturbation for diffraction sensitive targets, but of more concern for drag targets.

2.3.3   30 psi Blast Waves and 30% Blockage Results

For a variety of reasons the simulation domain in which the flared concept is of most potential interest is that of high pressures and high blockages. This would be true in the HML case where 30 psi environments and higher are expected and in the upper end of the Army requirements at 35 psi. In each case large targets are of interest. Large targets lead to large blockages. High pressure facilities are

more costly to construct than low pressure facilities for engineering reasons, and anything reasonable which can be done to reduce the overall physical size of such facilities will be economically attractive. Therefore, a series of calculations was run for 30 psi blasts and 30% blockage configurations. These calculations will be summarized in the following figures and discussion. The sequence of discussion will follow the pattern set above. The net force experienced in the straight tube, standard flare, the vented tube, and the right-angled flare configurations are shown in Figure 2.21. The net force fidelity during the diffraction phase for the straight and the vented straight pipe is dramatically illustrated. The influence of the flared corner rarefactions in the two flare cases is also apparent, and the magnitudes are as expected. On the other hand, the two straight configurations produce drag forces which are approximately 60% high, whereas the flared configurations produce drags a few percent low. Again, a flare of, say, 25% in a 30% blockage case might produce a drag force in excellent agreement with expectations.

Top force summaries shown in Figure 2.22 are particularly interesting. The fidelity of the straight tube in the early diffraction phase is again evident, but significant departures associated with reflected waves occur throughout the drag phase. Both of the flared cases show reduced loadings during the diffraction phase and drag phase vertical forces as high or higher than in the straight tube. On the other hand, the vented straight tube looks quite attractive in this context. The rarefaction from the vent decreases the load just behind the peak, but it also reduces the late-time loading during the drag phase so that at 50 ms the top force loads associated with the vented straight pipe are identical with those of the reference calculations.

The impulses are consistent with the above observations as shown in Figures 2.23 and 2.24. They are high in the straight tube configurations and low in the flared pipes. Again, a compromise between the
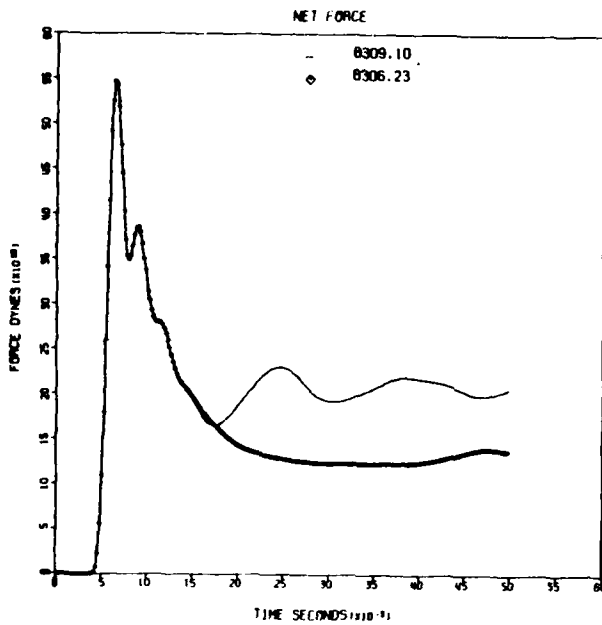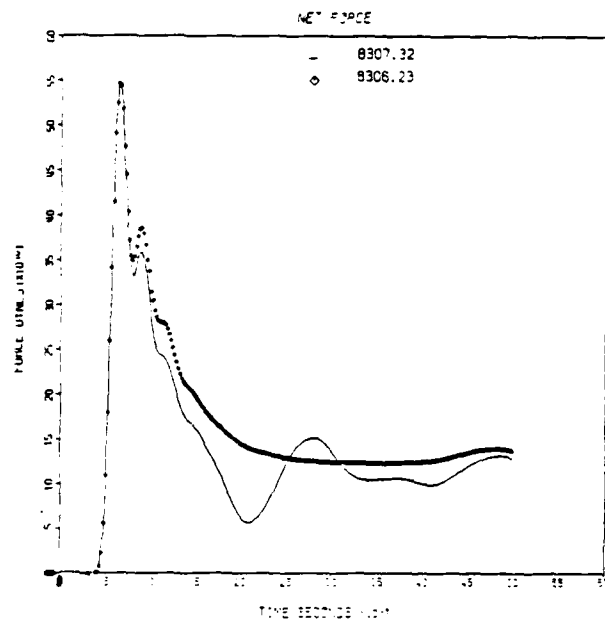
44

Rectangular Sample, 30 psi,
Straight tube vs. reference.

Rectangular sample, 30 psi
Std. flare vs. reference.
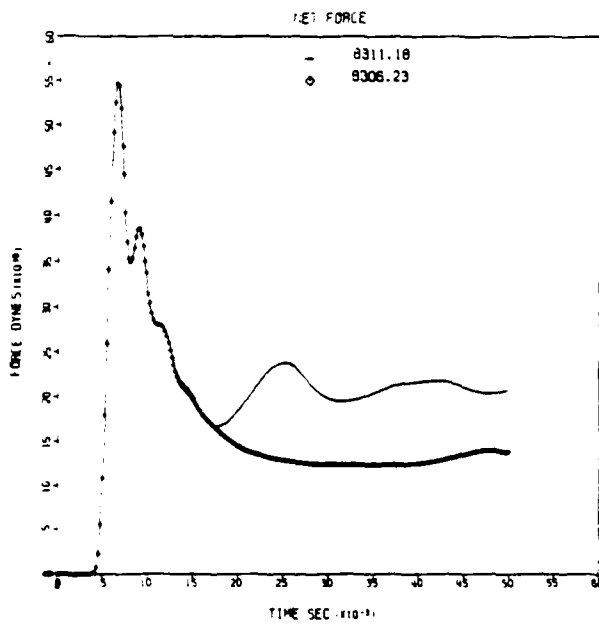
Rectangular sample, 30 psi,
Vent vs. reference.
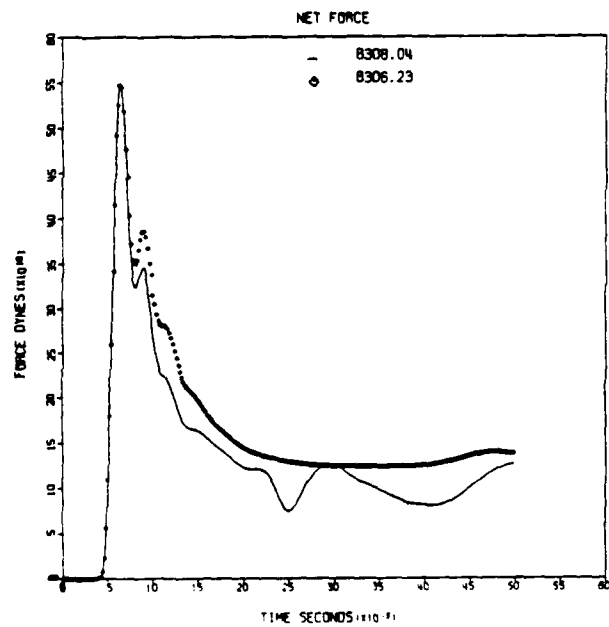
Rectangular sample, 30 psi,
Square flare vs. reference.

Figure 2.21. Net force comparisons for 30 psi shocks and 30% blockage.
The net force results for a straight, standard flare, square
cornered flare and vented test chamber are compared with
nominal free field conditions, 2% blockage.
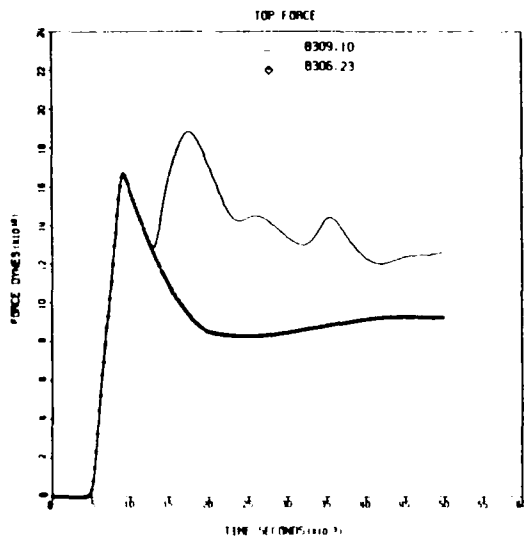
Rectangular sample, 30 psi,
Straight tube vs. reference.
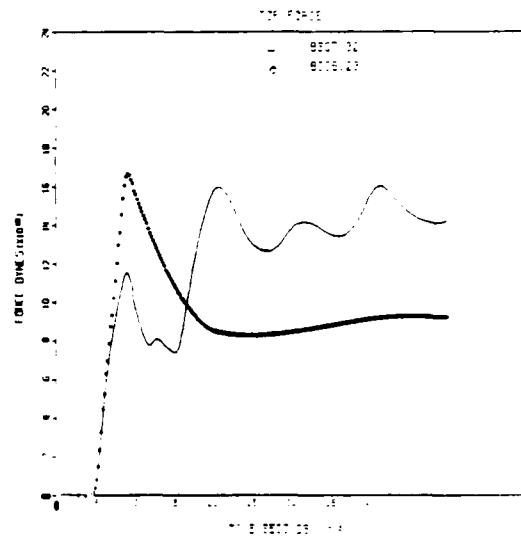
Rectangular sample, 30 psi
Std. flare vs. reference.
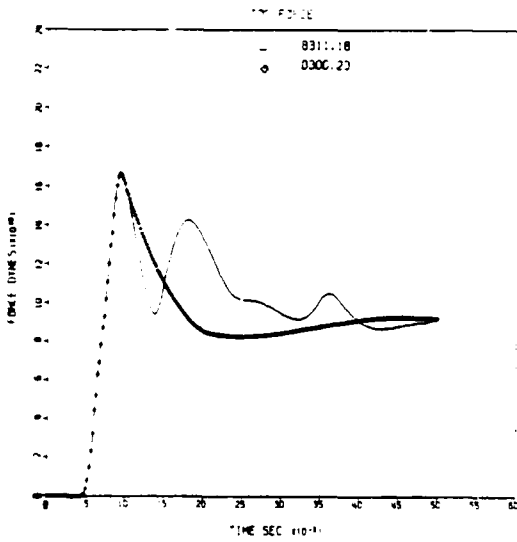
Rectangular sample, 30 psi,
Vent vs. reference.
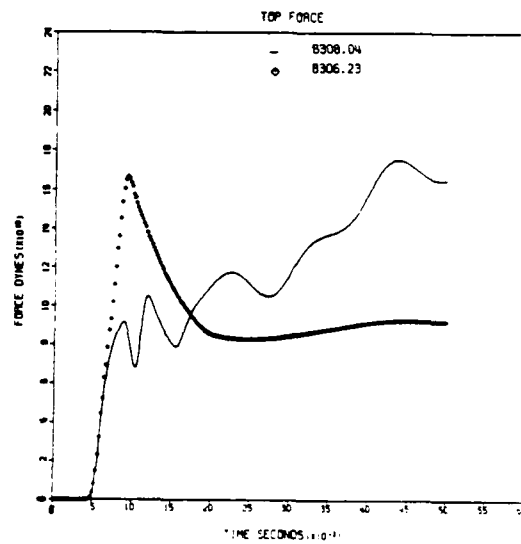
Rectangular sample, 30 psi,
Square flare vs. reference.

Figure 2.22.   Top force comparisons for 30 psi shocks and 30% blockage.
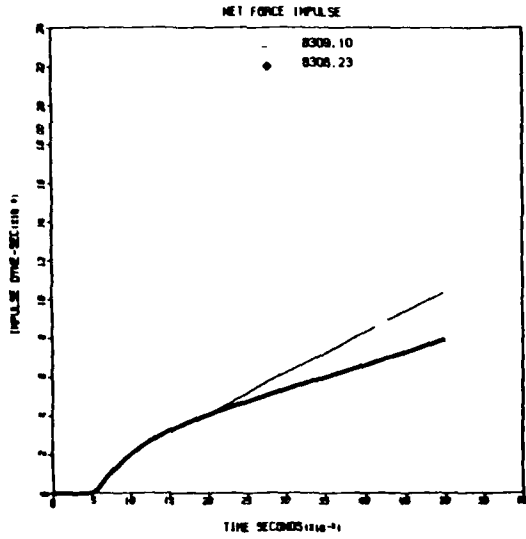
Rectangular sample, 30 psi
Straight tube vs. reference.
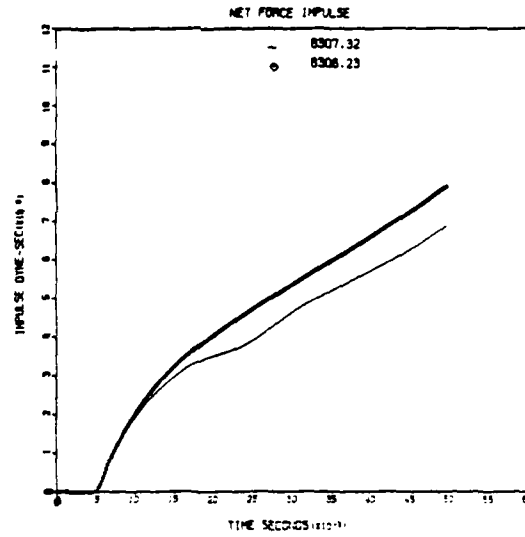
Rectangular sample, 30 psi,
Std. flare vs. reference.
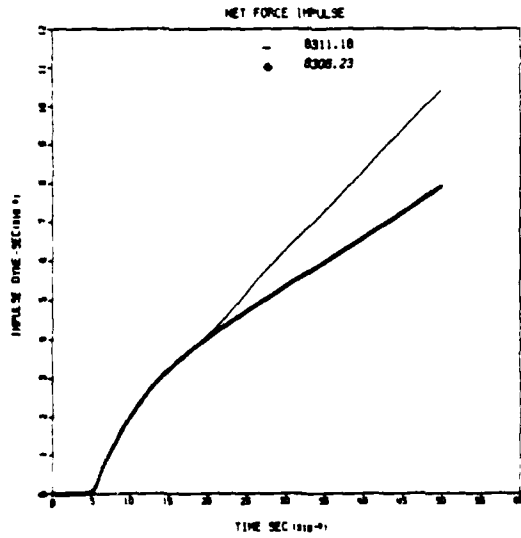
Rectangular sample, 30 psi,
Vent vs. reference.
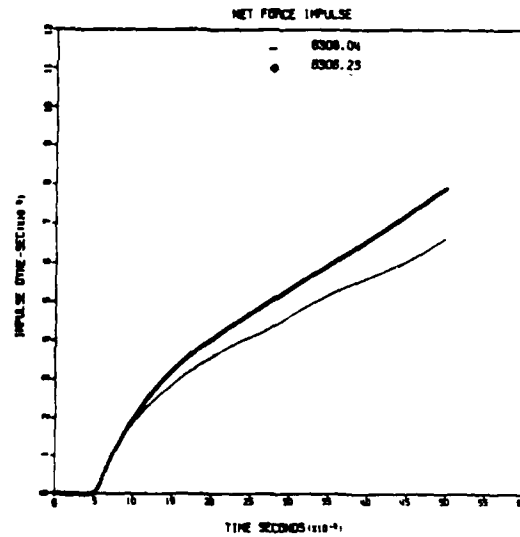
Rectangular sample, 30 psi,
Square flare vs. reference.

Figure 2.23. Net force impulse comparisons for 30 psi shocks and 30% blockage.
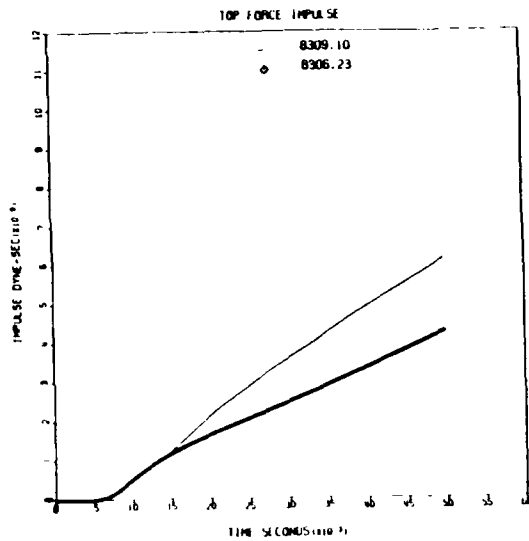
Rectangular sample, 30 psi
Straight tube vs. reference.
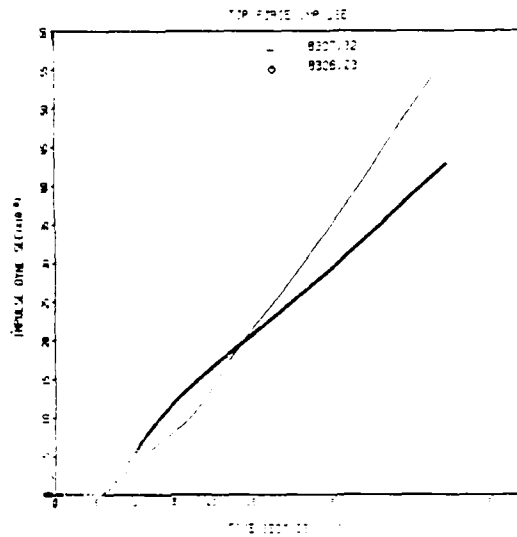
Rectangular sample, 30 psi,
Std. flare vs. reference.
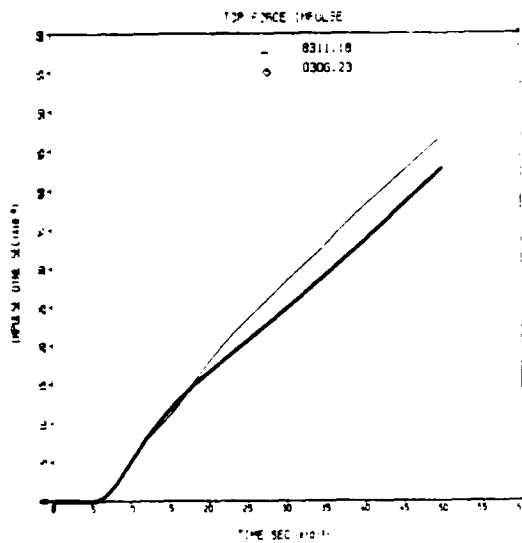
Rectangular sample, 30 psi,
Vent. vs. reference.
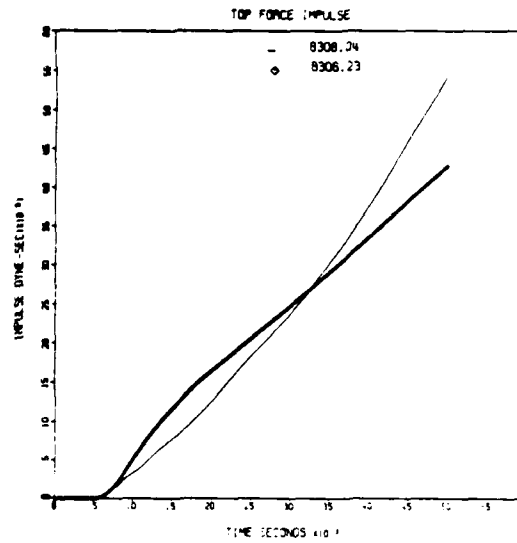
Rectangular sample, 30 psi,
Square flare vs. reference.

Figure 2.24.   Top force impulse comparisons for 30 psi shocks and
                30 blockage.

48

two configurations possibly including the vent option could provide
the best simulation environment. As expected the vented configuration
produces the best agreement with the reference calculation.

In Figure 2.25, which shows the average velocity, again illus-
trates that the flared configuration does the best job of producing an
average velocity in agreement with the free-field prediction.

The pressure contours at 50 ms for the various configurations
are presented in Figure 2.26. It is clear that none agrees very well
with the reference calculation, but all are qualitatively similar.

Figure 2.27 shows a comparison of axial velocity contours. The
flared configurations produce much better agreement with the reference
calculation at 50 ms than do either of the straight tubes. In particu-
lar, note that the reverse flow vortex is properly generated by the
flares but is completely absent in the straight tubes. This could be
very important in influencing blast damage on complex targets.

All of the configurations provide good simulations of the front
face loading as shown in Figure 2.28. The reflected waves arrive as
expected, but in each case the calculated forces agree with the
reference calculation to within 50% .

The back face loads seem best simulated in the straight tube
with the vent a reasonable second. Both flared cases produce low
pressures during the diffraction and high pressures during the drag
phase. This is probably the main reason that the net force presented
in Figure 2.21 is lower than for the straight tube. The high
pressures generated in the flared configuration compensate for the
reflected pressures on the front of the block. The top forces are
better replicated moment by moment in the straight tubes, the vented
version being best. The flared configurations generate high late time
hold down forces as shown in Figure 2.27 and 2.28.
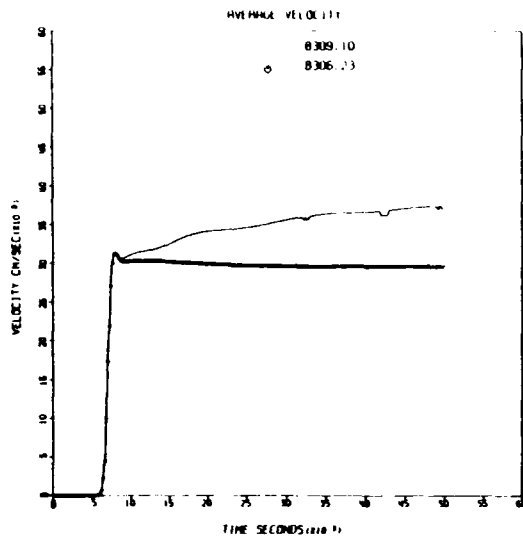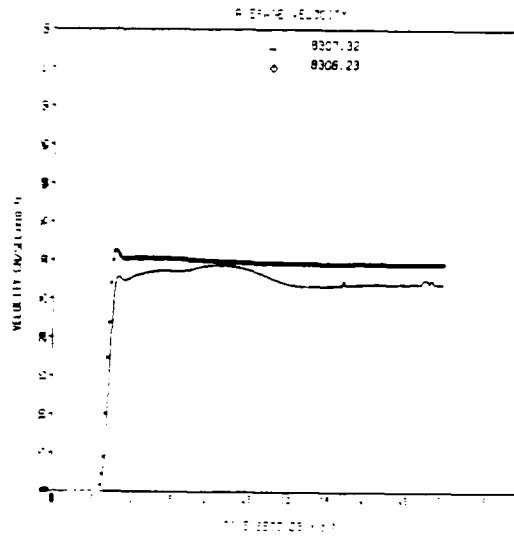
49

Rectangular sample, 30 psi
Straight tube vs. reference.

Rectangular sample, 30 psi,
Std. flare vs. reference.
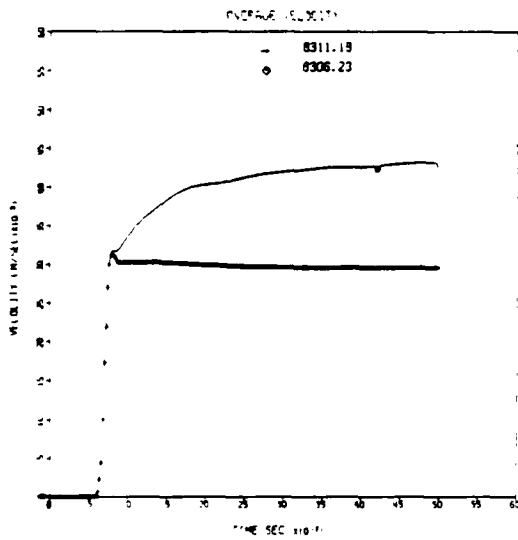
Rectangular sample, 30 psi,
Vent vs. reference.
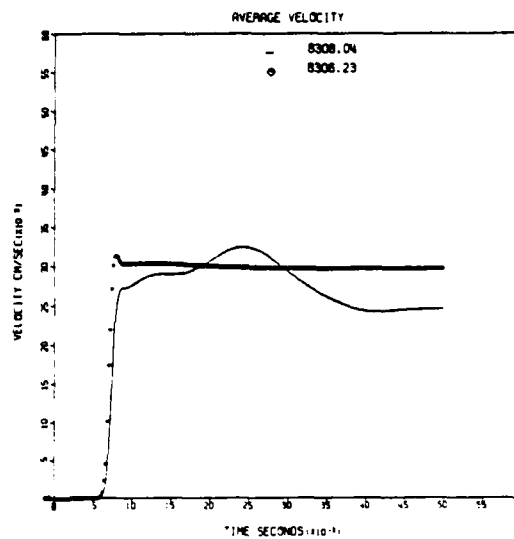
Rectangular sample, 30 psi,
Square flare vs. reference.

Figure 2.25. Average velocity comparisons for 30 psi shocks and 30% blockage.

50
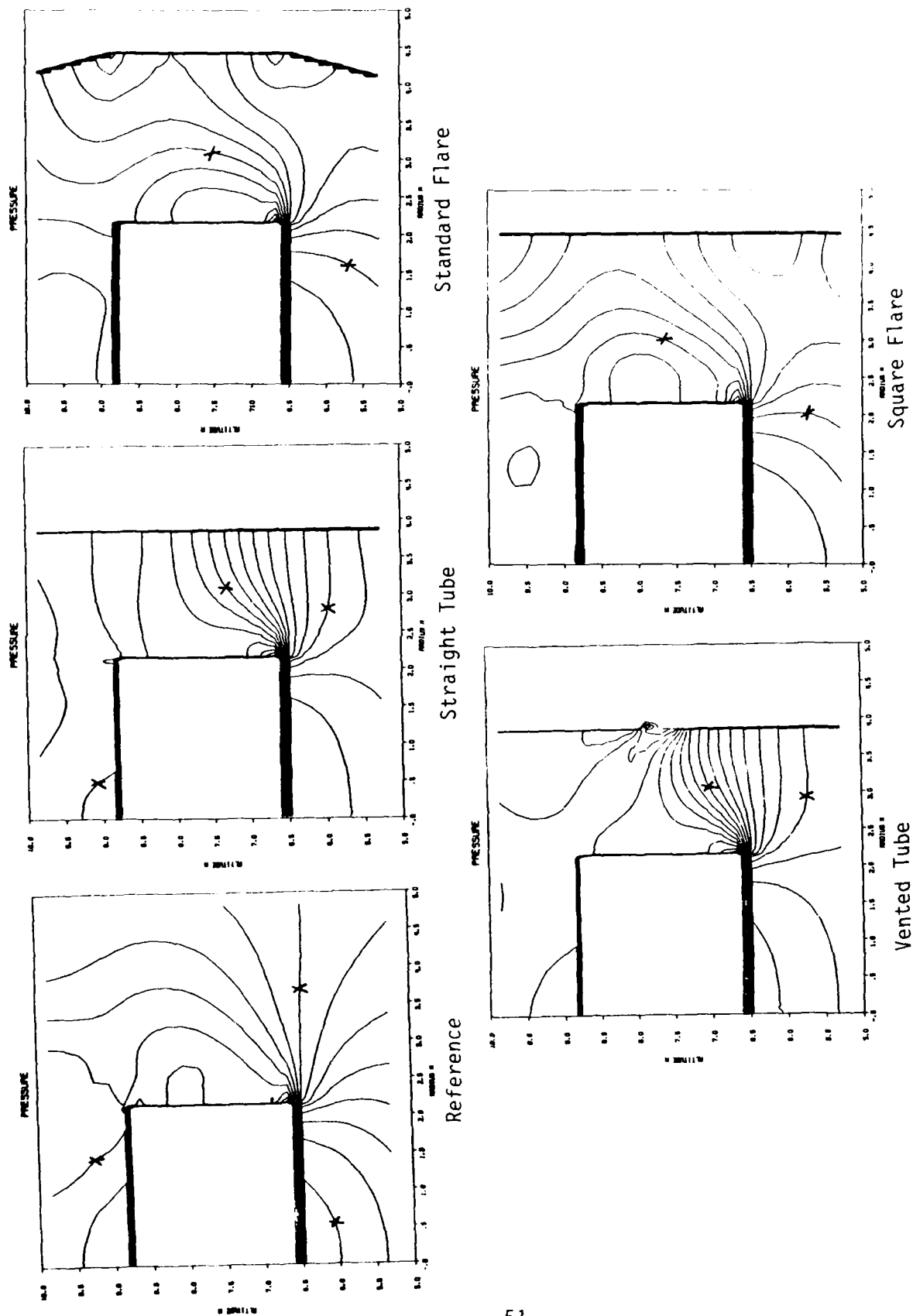
Figure 2.26. Pressure contours at 50 ms for the configurations studied at 30 psi and 30% blockage. The loadings are qualitatively similar, but the magnitudes differ.
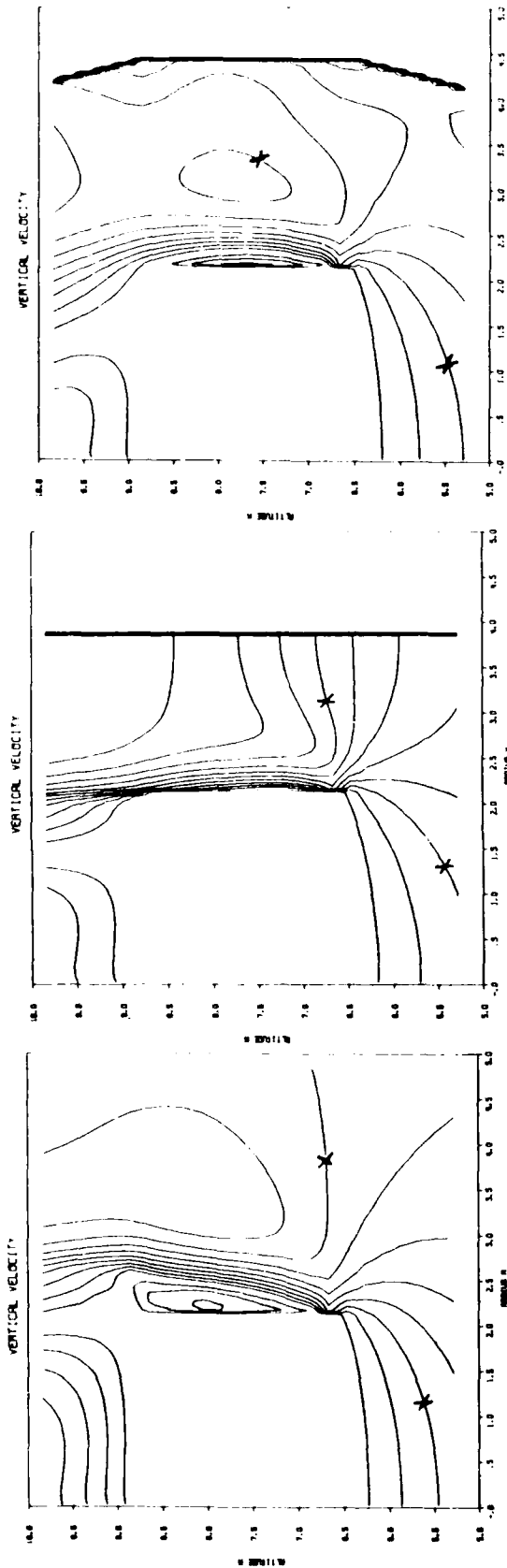
51
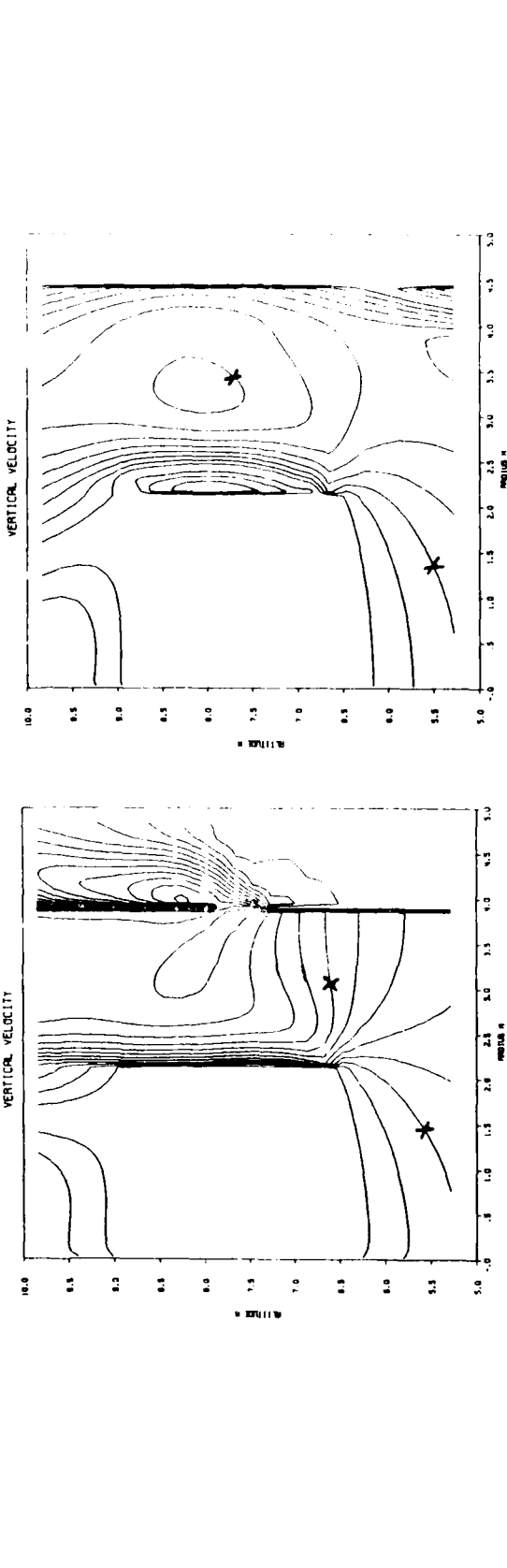
Figure 2.27. Axial velocity contours at 50 ms for the configurations investigated at 30 psi and 30% blockage. Note that the recirculation region is missing in the straight and vented straight cases.

52
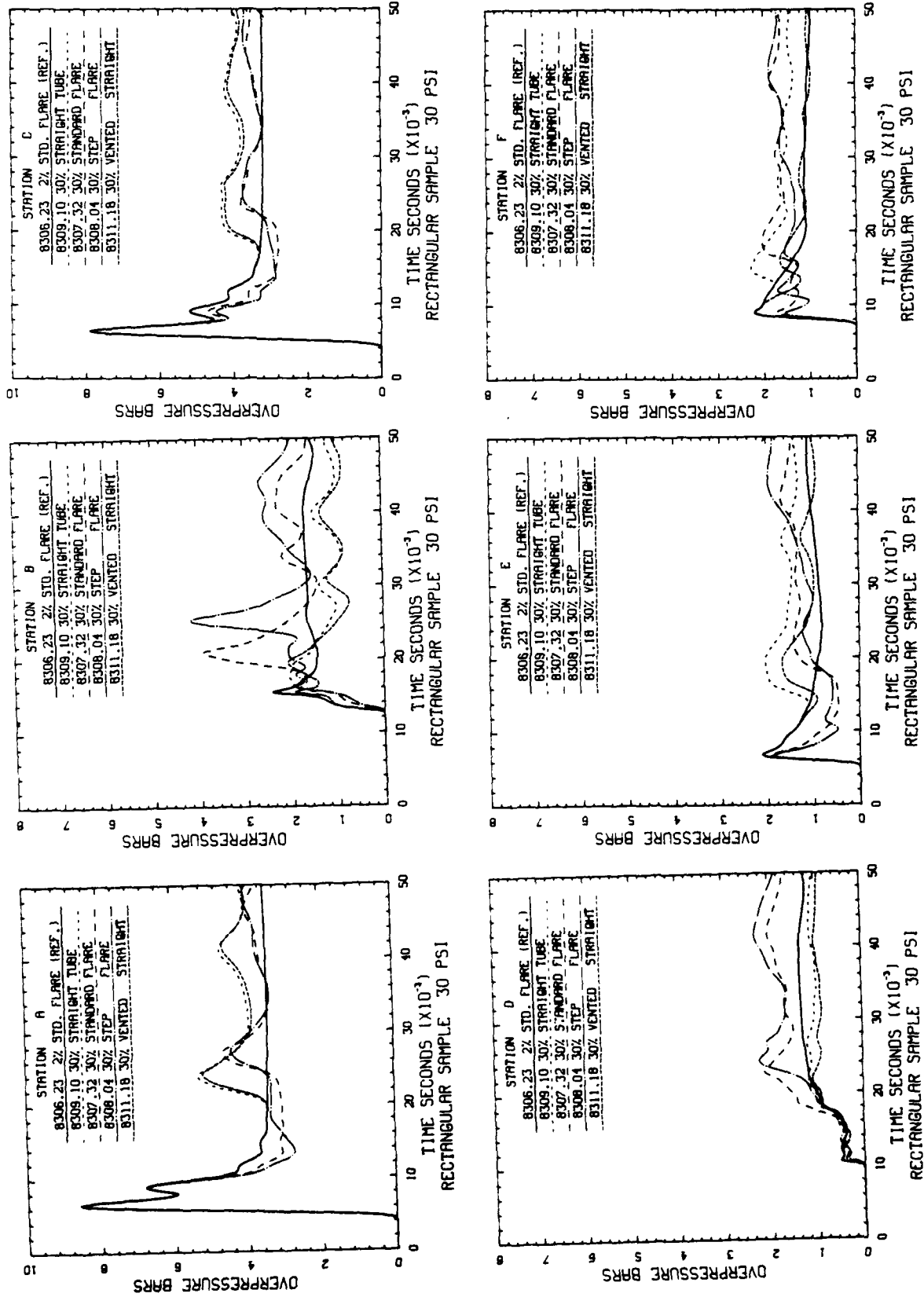
Figure 2.28. Pressure as a function of time at the several stations indicated in Figure 2.3 for the configurations studied at 30 psi and 30% blockage.

2.3.4   Thermal Radiation Source Influence

Two additional calculations were performed to estimate the influence of TRS operation on blast simulator performance. These calculations were for the straight tube and the standard flare, 30 psi 30 % blockage cases. It was assumed that a ᵀRS system existed 1.5 meters in front of the test object. The reaction products were assumed vented from the tube before blast arrival, leaving behind a modestly heated region between 1 and 2 meters in front of the test object. The temperature in this region was assumed to be twice ambient so that the heated region appeared as a half-density region of air with which the blast interacted before reaching the test object.

In this case, the comparisons to be presented are between the calculated results with and without the TRS present for a given config-uration. Figure 2.29 shows the results for the net force. Note in both cases the blast arrives slightly earlier because of the high sound speed in the heated region. Its amplitude is slightly reduced because of the impedance discontinuities, but the overall trend of the data and, in particular, the late-time characteristics, are very simi-lar. In both cases the amplitude of the oscillations is reduced. The perturbation on the hold down forces are also small as shown in Figure 2.30.

The careful examination of other graphic output from these calcu-lations shows no change in qualitative flow features which can be attributed to the heated layer assumed left in front of the test object by TRS operation. In every case the perturbations seemed small compared to the difference in calculated results arising from config-urational changes. Qualitatively similar calculations were made by Kitchens et al (Reference 4). More dramatic results were obtained presumably because a more extensive heated region was assumed.

54
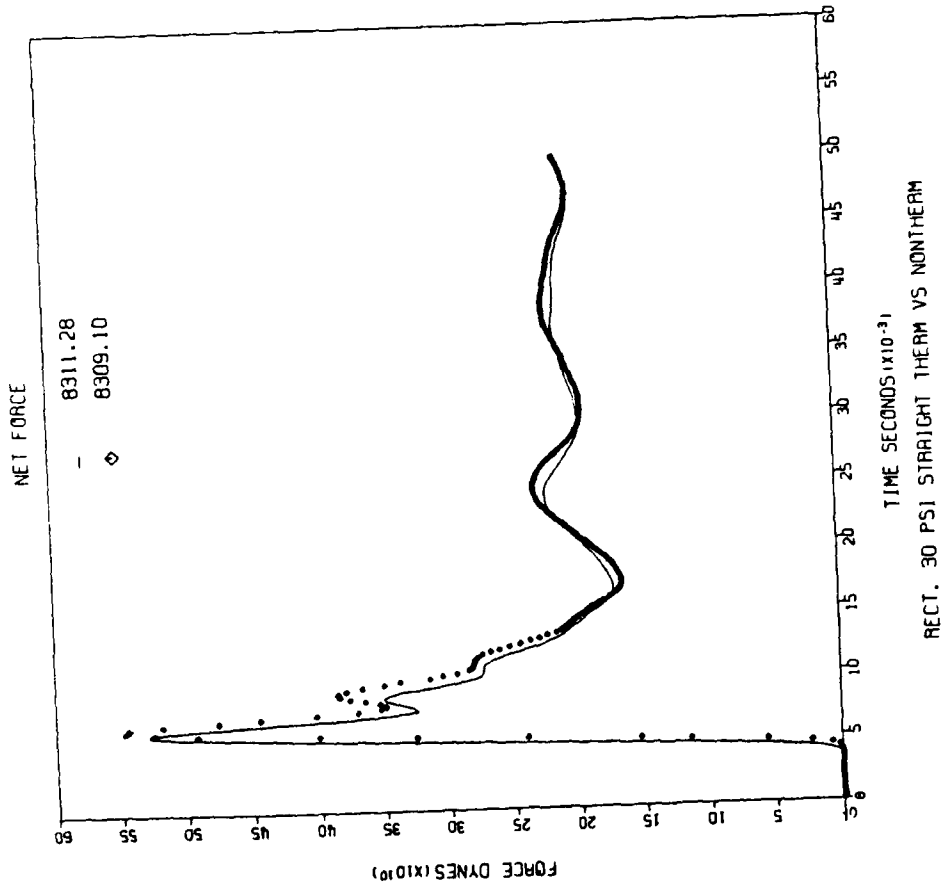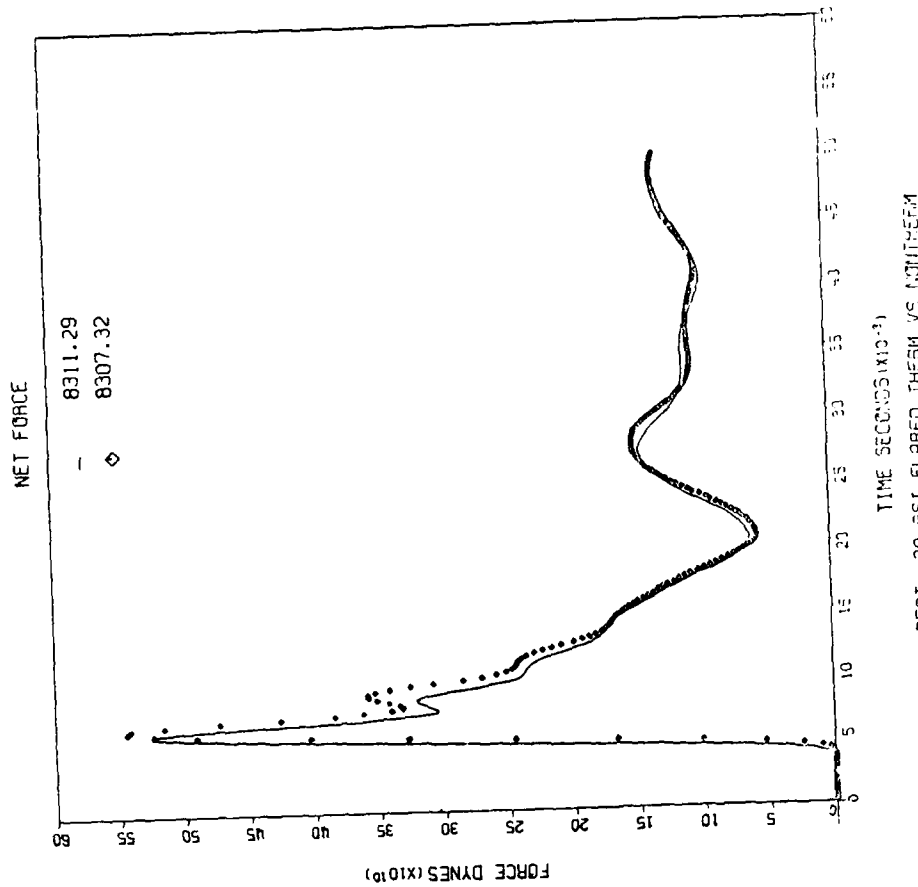
Figure 2.29. Comparisons of net force for 30 psi shocks and 30% blockage with and without a residual hot layer from a TRS present. The heated case is shown by the light line.
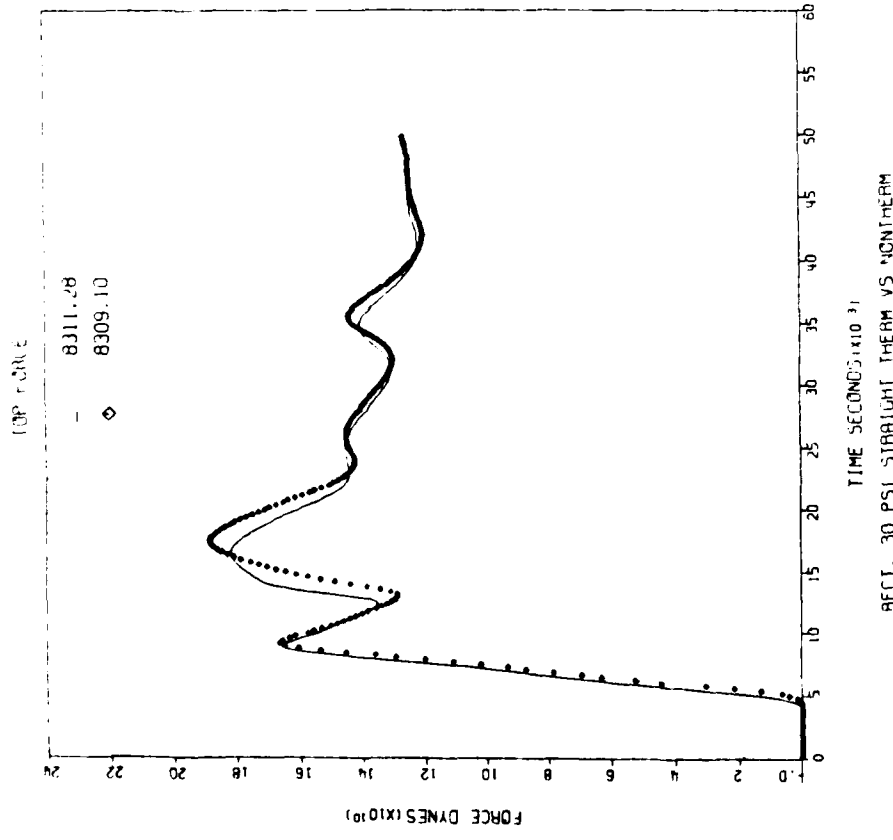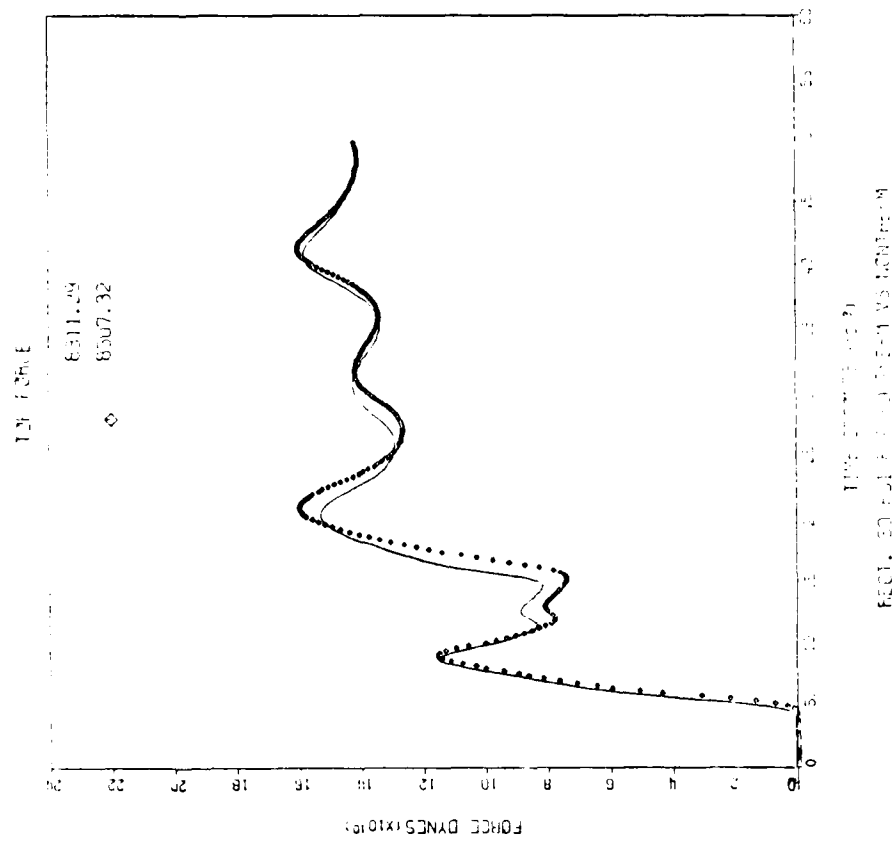
Figure 2.30. Top force comparisons for 30 psi shocks and 30% blockage with and without a residual hot layer from a TRS present. The heated case is shown by the light line.

56

2.3.5 Other Test Shapes

All of the results presented to date have assumed the test object to be a rectangular cylinder on the axis of an axisymmetric tube. This was interpreted as a semicircular cylinder on the floor of a semicircular simulator for consideration of hold-down forces. In an effort to demonstrate that the conclusions described above were not dependent upon a particular assumed test object shape, additional calculations have been done. In one set, the test object was assumed to be an isosceles triangular cylinder with the same base and height as the rectangle used previously as shown in Figure 2.3. The flare was identical with the standard flare decribed above. Summary plots are presented in Figures 2.31 through 2.38 which show a comparison of the straight tube and flared tube calculations with the reference or free-field results for 30 psi blast conditions and 30% blockage. As before, the straight tube obviously gives a good representation of the loading during the diffraction phase. The rarefaction associated with the flare corner is quite evident in the early part of the net force figure in the flared configuration. The top force and average veloci- ties show similar patterns. This is another example in which a compromise between a full flare and the straight tube might provide more nearly optimum simulation conditions insofar as loads are concerned. The pressure and axial velocity contours show that the qualitative flow features are again much better preserved in the flared than in the straight tube geometry. Quantitatively, the straight tube may be better.

Calculations were also done for 10 psi, 30% blockage condi- tions using the triangular obstacle. The qualitative results are identical with those presented above, and, in the interest of brevity, will not be presented in detail. For the straight tube, the net force impulse is high at late time; for the flare it is low. In both cases the top force impulses are in excellent agreement with free field expectations.
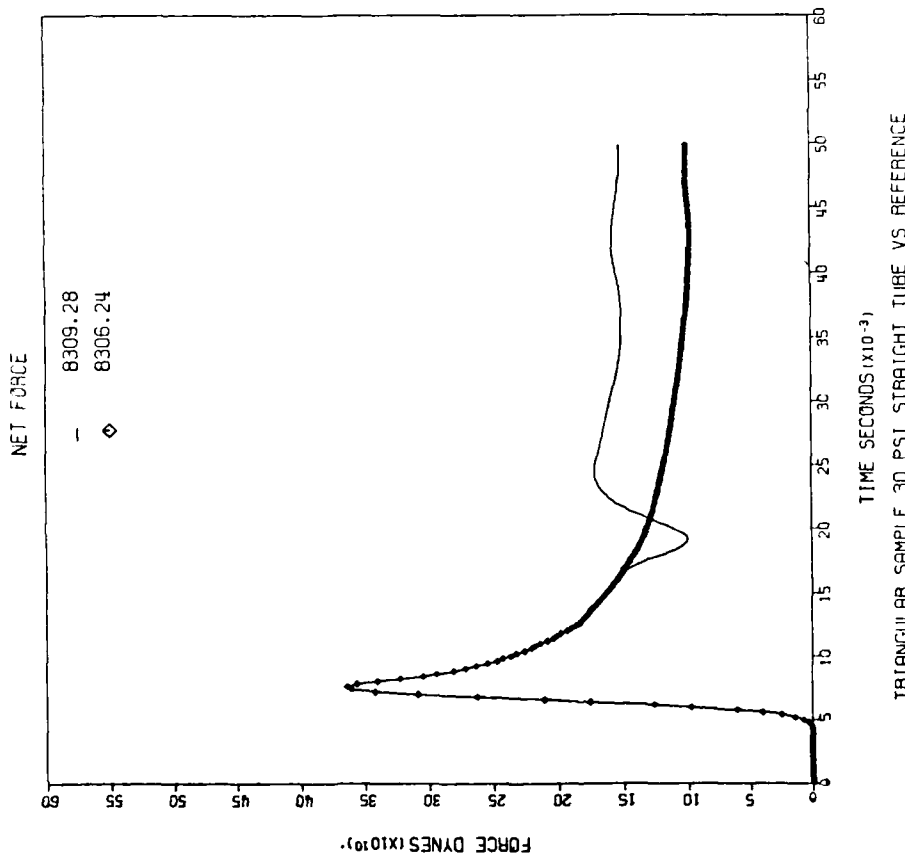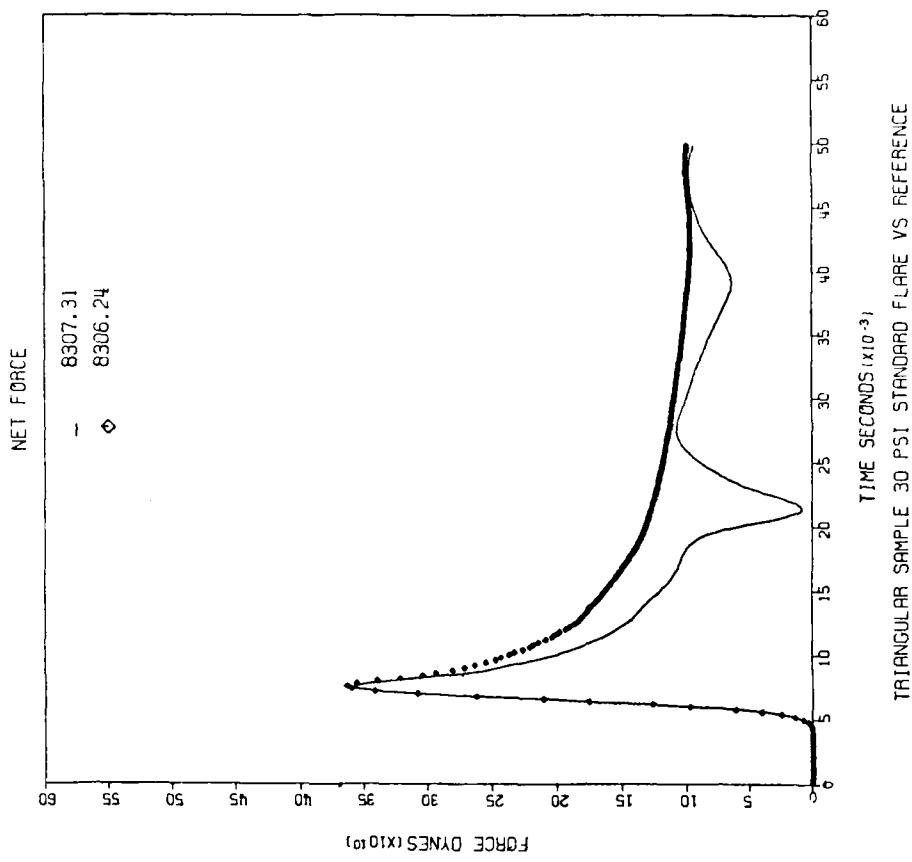
Figure 2.31. Net force comparisons for triangular obstacles, 30 psi shock and 30% blockage. Results from straight and flared test sections are compared with nominal free field conditions, 2% blockage.

58
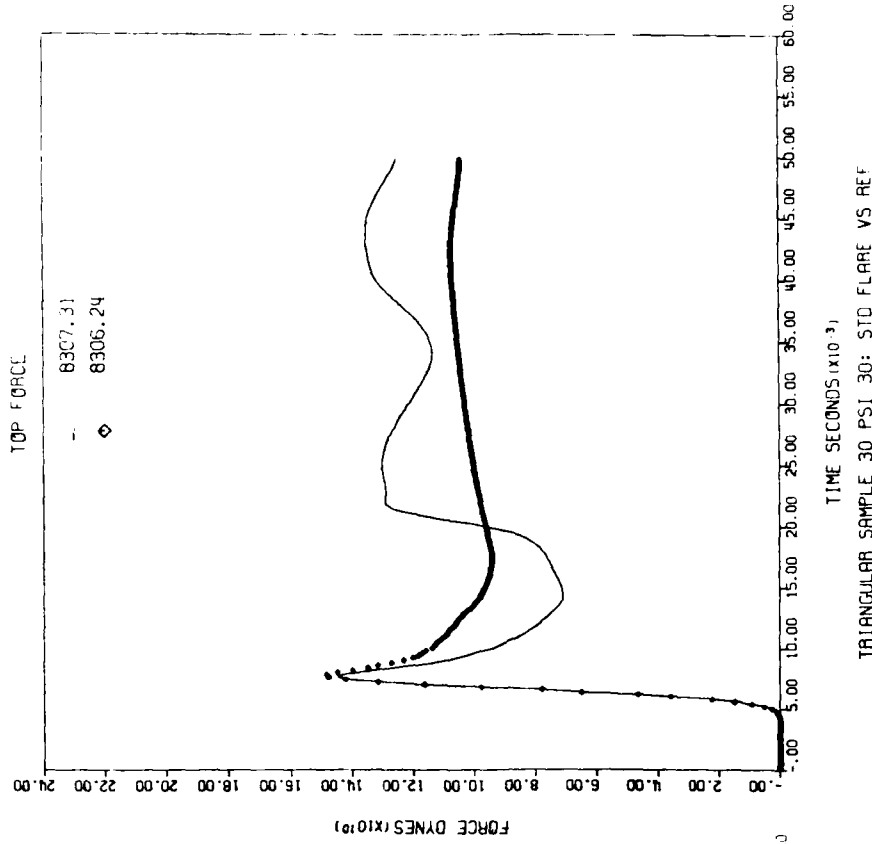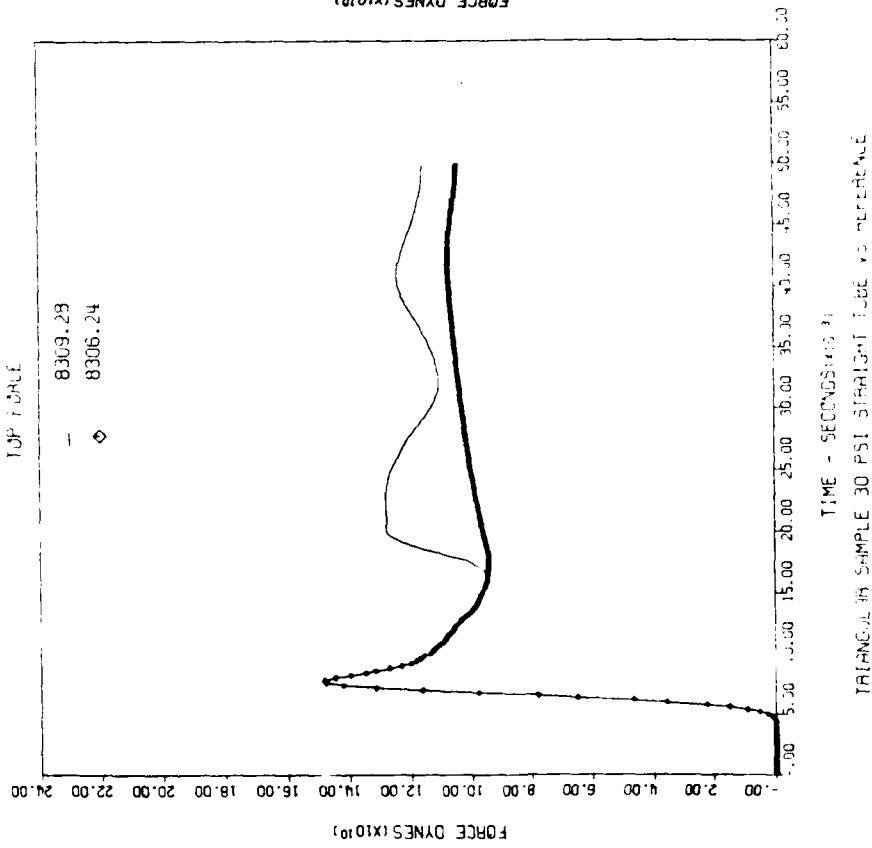
Figure 2.32. Top force comparisons for triangular obstacles, 30 psi shocks and 30% blockage.
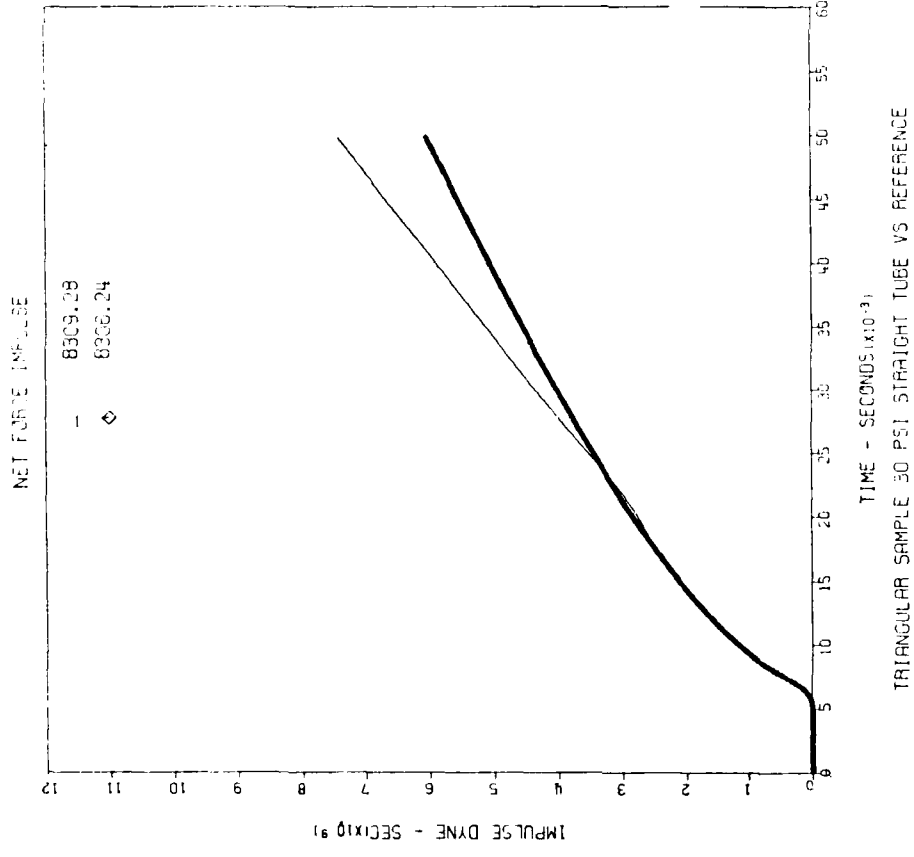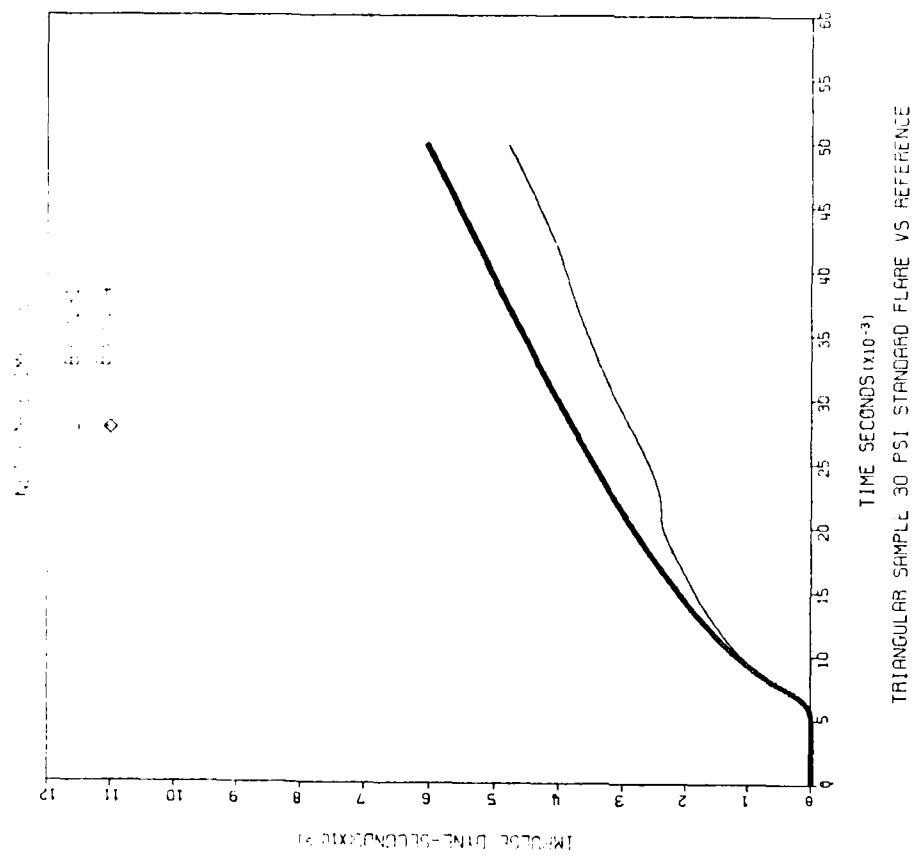
Figure 2.33. Net force impulse comparisons for triangular objects, 30 psi shocks and 30% blockage.
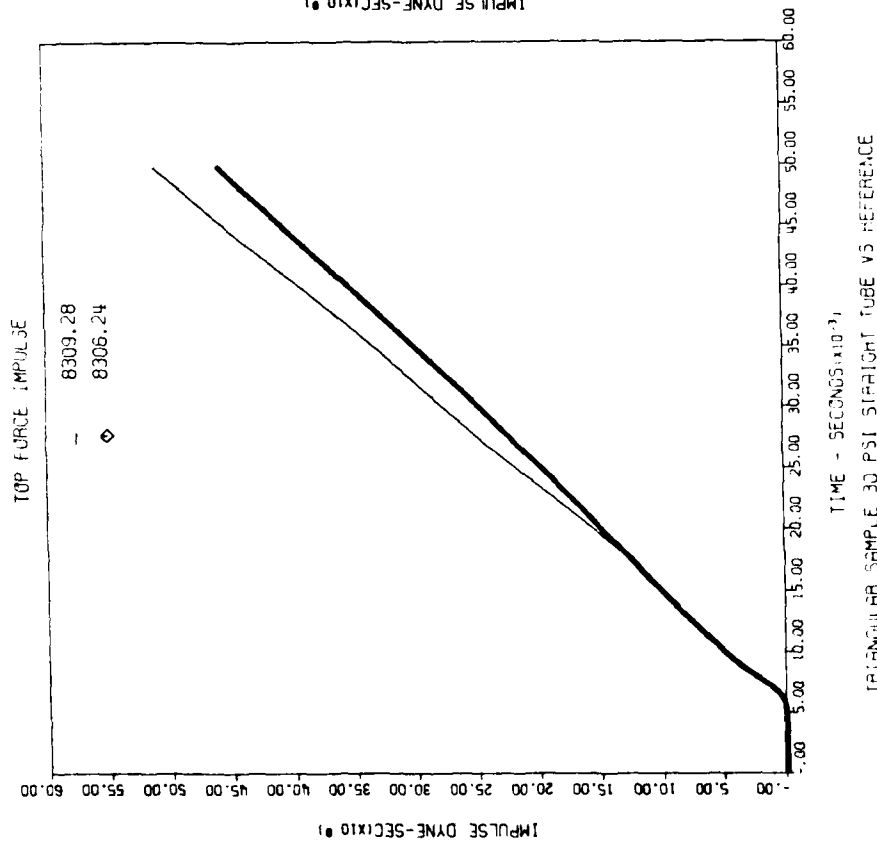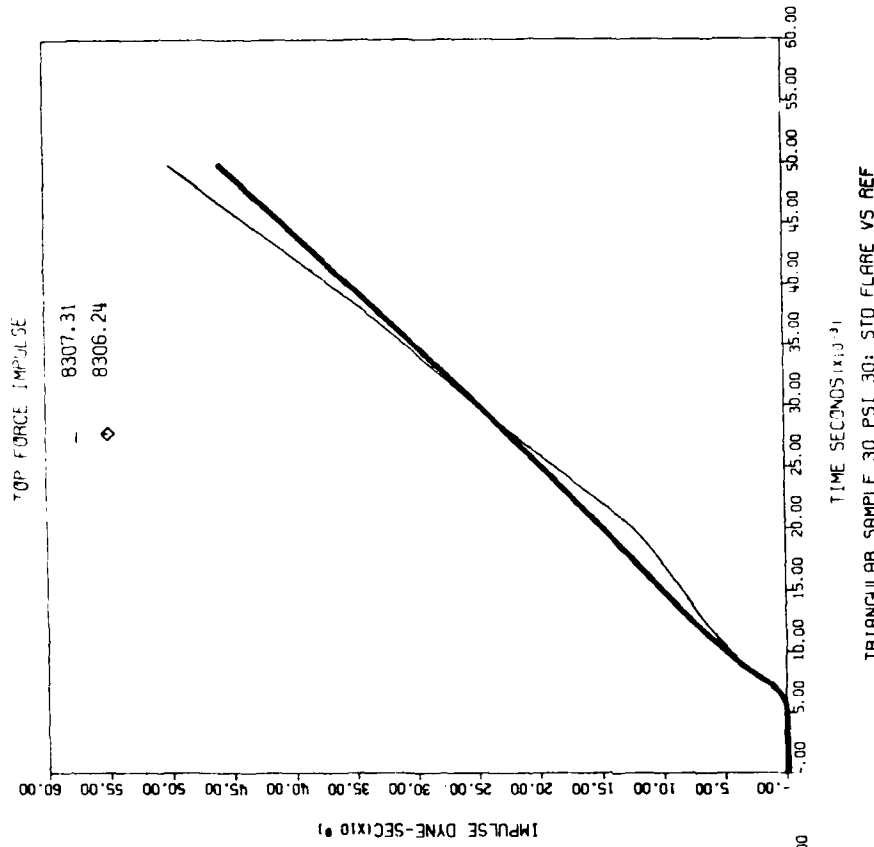
Figure 2.34. Top force impulse comparisons for triangular objects, 30 psi shocks and 30% blockage.
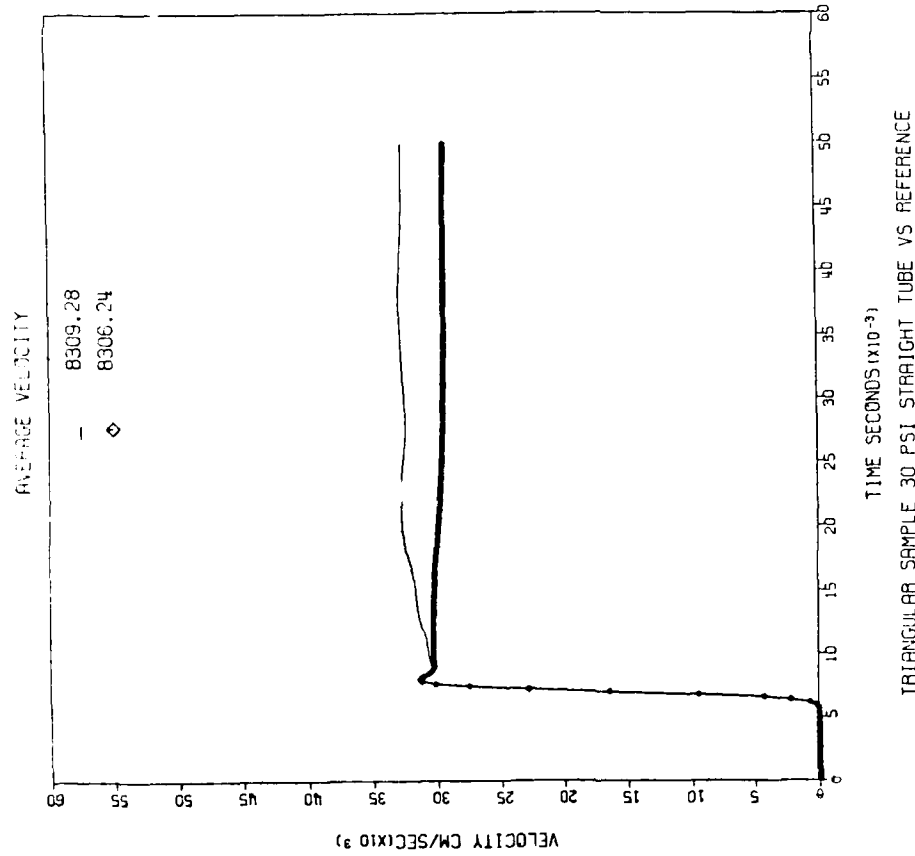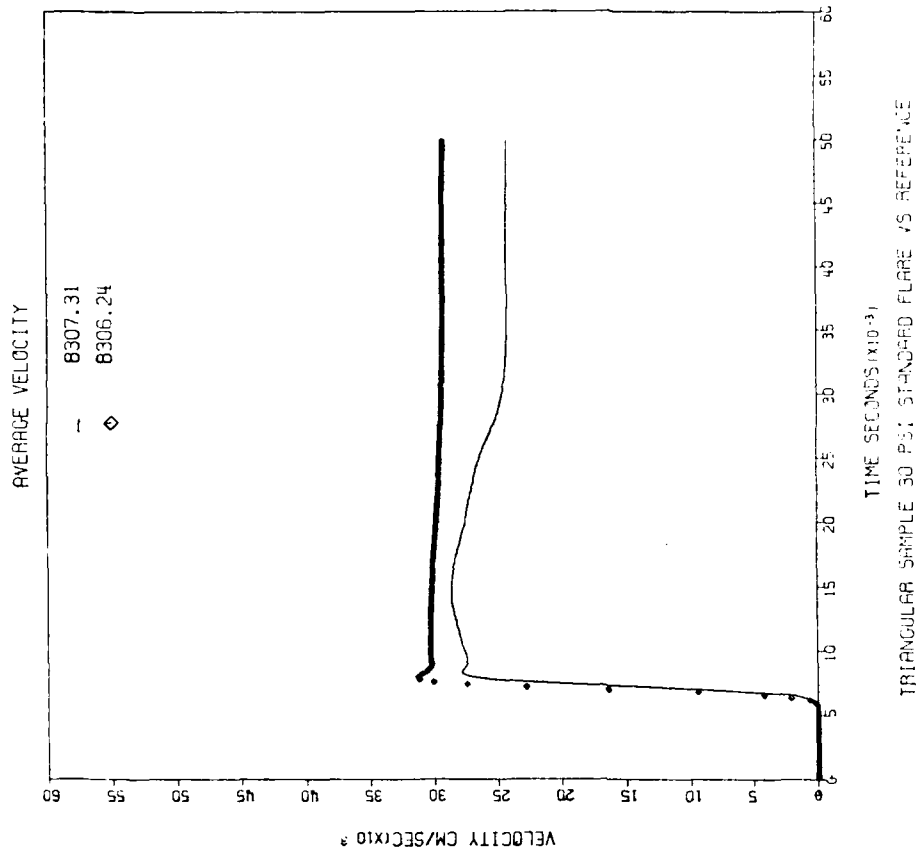
Figure 2.35. Average velocity comparisons for triangular objects, 30 psi shocks and 30% blockage.

Figure 2.36. Pressure contours at 50 ms for the triangular obstacles studied at 30 psi and 30% blockage.

63

Figure 2.37. Axial velocity contours at 50 ms for the triangular configurations investigated at 30 psi and 30% blockage.
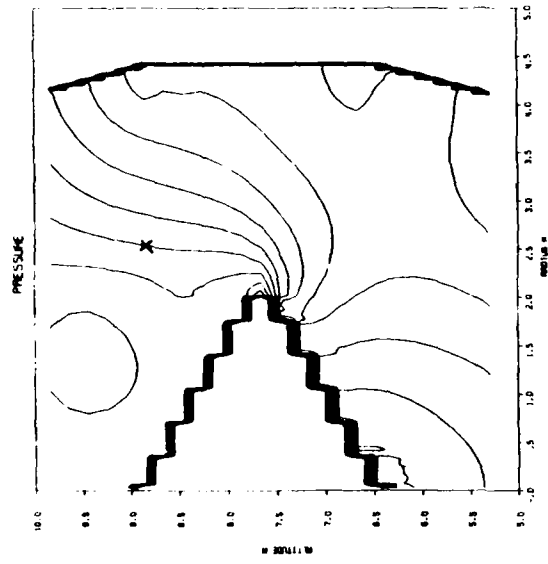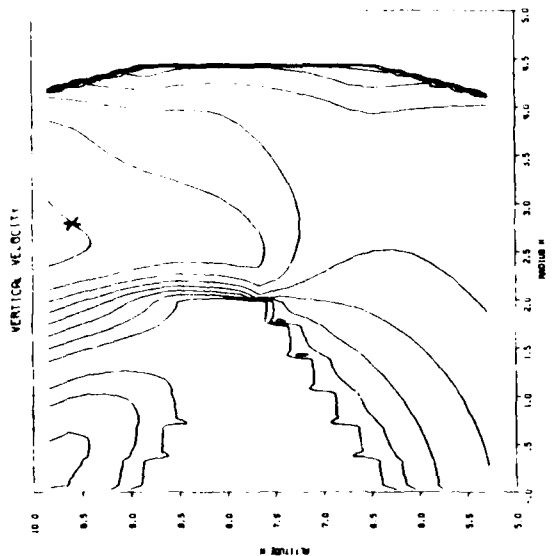
Standard flare
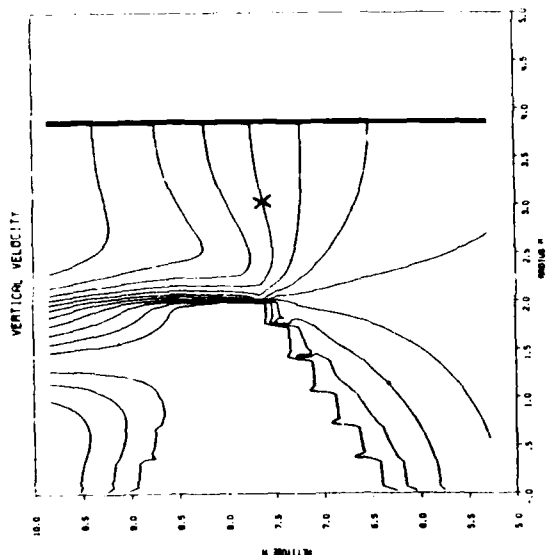
Straight tube

Reference
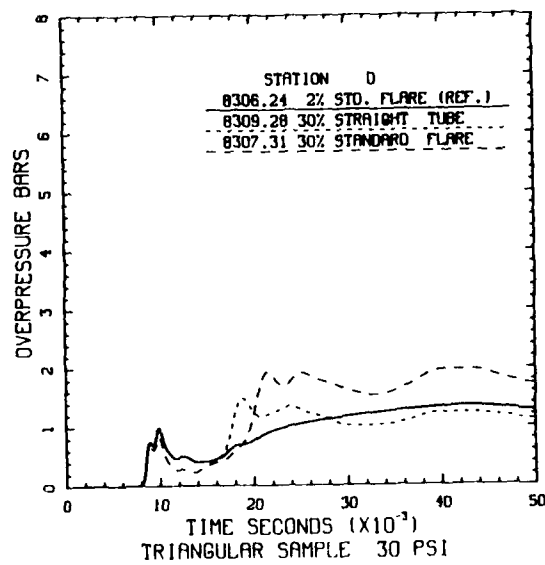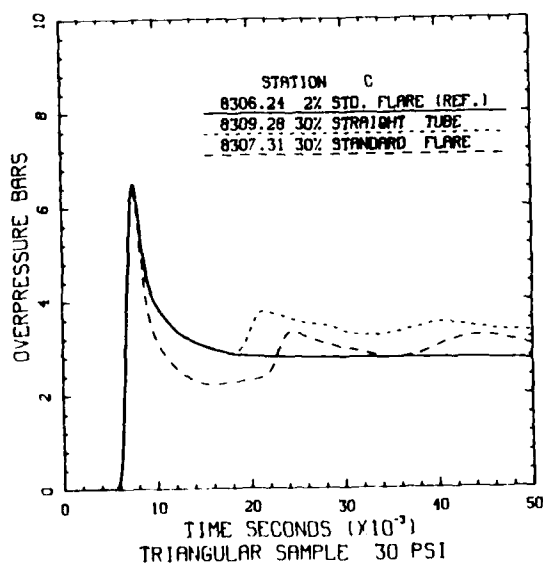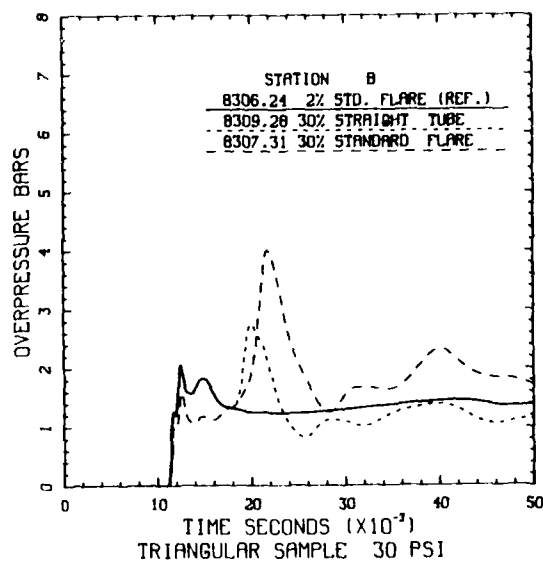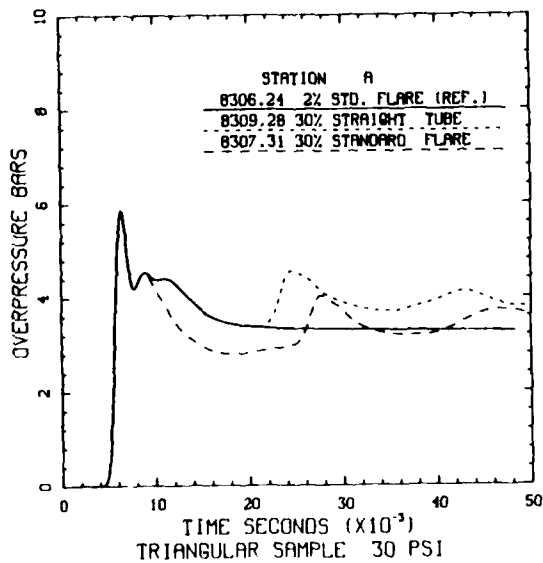
Figure 2.38.   Pressure as a function of time at the several stations
shown in Figure 2.3 for the triangular target and the
configurations studied at 30 psi and 30% blockage.

A very limited calculational investigation was made of an irregular shape, jocularly called the "truck" which is shown in Figure 2.3. The free field and flared cases were compared at 10 and 30 psi driving conditions. Conclusions quite similar to those quoted above were obtained. The net force for the flared case was somewhat low at late time, the top force was somewhat high. No detailed results are presented here.

The calculations with triangular and "truck" shapes have confirmed the general conclusions derived in the more extensive rectangular block calculations.

2.4 CONCLUSIONS

In the earlier sections, a number of conclusions and summary statements were made as specific points were discussed. At this time a number of more general and global conclusions will be presented.

● Calculations of the sort presented here provide a great deal of insight into the nature of the flows to be expected in a blast simulator. They can be performed quickly and are relatively inexpensive. Insofar as they adequately represent reality and insofar as a credible two-dimensional approximation can be defined for a case of interest, such calculations can be very valuable in data interpretation from simulator tests which, by their very nature, must deviate from true, free-field conditions. The calculations can also be very valuable in designing the simulation experiments so as to maximize the anticipated data return.

● It appears that drag coefficients and free field flow concepts are of limited value in interpreting simulator results because the "free field" simply does not exist in the usual sense. It seems better to consider actual forces as described above.

66

• Flow blockage in a simulator is an important perturbation to a flow field as shown in many of the cases presented above and in several BRL reports. However, even in the case of a 30 psi blast and a 30% blockage for a steady non-decaying wave, blockage can be considered a perturbation to the flow field. The qualitative features of the late-time loadings seem independent of whether or not sonic conditions are predicted in steady state theory.

• The Army has decided on the basis of other arguments that 10% blockage is acceptable for a large blast simulator. These calculations support that conclusion even up to 30 psi blast conditions. Without question, flow details are changed in the 10% blockage case, but the qualitative features of the flow field are preserved. In most cases, calculations of the sort presented here can quantify the blockage effects and help to compensate for them either in experimental design or in data analysis.

• A test section flare appears useful, particularly for drag sensitive targets, but it does not solve all blockage problems. Additional geometric configurations might be profitably investigated. In particular, a longer downstream flare before returning to the nominal tube dimensions may be desirable to retard the wave reflection and reduce the top force. This change is also expected to increase the net force in a given situation which appears desirable.

• Perforations in the vicinity of the test chamber also appear beneficial to simulator performance. This possibility has not, however, been investigated in sufficient detail in this series of calculations. In particular, variations in open area and hole location were not considered.

• The thermal radiation source perturbations as modeled here do not appear to introduce significant flow effects in a straight simulator or in a flared simulator for the 30 psi-30% blockage conditions investigated.

●   The calculations performed have shown the influence on
simulator performance of blockage, of the basic flare concept, of
several variants of flare geometry and of test section venting to some
extent. It appears that combinations of test section geometric factors
may be chosen to match particular requirements. This possibility may
be particularly useful in the Hardened Mobile Launcher (HML) context
where non-ideal flow environments are desired.

●   In the author's opinion, a large blast simulator should be
designed with at least 30% blockage anticipated if provisions can be
included to permit geometric options including adjustable flares and
vents in the test chamber. This conclusion is based on comparison of
Figures 2.12 and 2.28 which show pressures as a function of time for
30 psi shocks and 10 and 30% blockage. Performance does not seem
much worse at the higher blockage . Some intermediate test section
configuration may provide excellent results. Obviously, a simulation
facility which includes adjustable flares and vents as suggested here
would be more complex than a conventional design, but it would also be
much smaller. For instance, the reference diameter of a flared
simulator permitting 30% blockage is 1/3 that of a conventional tube
restricted to 10% blockage. To some approximation the construction
cost of anything is related to its mass which goes as the cube of a
reference dimension. This leads to a cost saving of a factor of 27
for the more complex facility. Of course this is ridiculous, however
it suggests an area for serious consideration. Engineering constraints
important at large size might be relaxed for something much smaller.
One could easily buy a good computer and support the competent engineer
required to tune an "adjustable" facility to a particular application
if several tens of millions of dollars could be saved in construction
costs. Also, operating costs are related to facility size. To some
extent the costs of operating complexity for the adjustable simulator
could be offset against the savings related to its small size.

SECTION 3
APPLICATION OF FLARE CONCEPT TO DASACON

As one considers the modification of DASACON by the inclusion of
a flared or ventilated test chamber, the most important question is,
what is the objective of use? Two applications come to mind for
present consideration. The first is as a general purpose blast simu-
lator, and the second is as a special purpose facility for HML applica-
tions. If it is decided to make any structural changes, it appears
that a particular modification could be made which would have applica-
tion to both objectives. It is appropriate to emphasize, however,
that no such modification program should be undertaken until experimen-
tal verification of the anticipated utility was obtained in a small
scale shock tube facility. In other words, it is important to verify
that the calculational results discussed above adequately approximate
reality.

3.1 SUGGESTED MODIFICATION TO DASACON

The most effective way to modify the existing DASACON facility
would appear to be to add a new test chamber just downstream of the
existing 22 ft test chamber. In this way, the existing chamber with
its numerous ports and instrumentation conduits would be preserved for
diffraction sensitive studies and for complete simulation testing of
small objects. The new flared test chamber could be used for large,
drag sensitive targets. Since the two chambers would be physically
close together, the blast conditions to be anticipated would be quite
similar.

It is an open question just how the flared section should be
constructed. In particular, is it necessary to permit variable area
conditions or can a single facility with, say, a 30% flare be used
satisfactorily? From some points of view, the variable area config-
uration would be attractive in that the simulator area could be
tailored to particular requirements. However, the engineering and
operational complications of the variable geometry would be signifi-
cant, and changing the flare area would complicate the ventilation

69

option which might be simultaneously attractive. It could also compli-
cate the problem of venting TRS products if that should be deemed
necessary. An alternative which might be very effective would be to
expand the tube gradually from the existing test chamber to, say, 30%
with the expectation that test objects could be mounted anywhere
between the existing test chamber and the full 30% flare section at a
location where the flow conditions are optimum for the particular
requirement. This alternative is sketched in Figure 3.1. Specific
calculational studies should be undertaken if this alternative
receives further serious consideration.

3.1.1 Potential Effect on Army Blast Simulator Requirements

The area of the large 22 ft diameter test chamber in DASACON
above the existing floor is approximately 32 m^2. If this were
followed by an expanded section to compensate for 30% blockage,
targets of approximately 10 m^2 in cross section could be tested
satisfactorily. This would permit the testing of the M113 A1 armored
personnel carrier, the 5/4 ton truck and S-250 shelter, and the M577
A1 command post carrier. It would not be large enough to adequately
test many of the larger components of present interest to the Army.

3.1.2 Potential Hardened Mobile Launcher Simulator Application

If ongoing simulator design studies should indicate that the
geometric modifications similar to a flared or vented test chamber
were potentially attractive for the large and full scale HML simula-
tors, the DASACON facility could serve as a reasonably scaled demon-
stration facility. Such a course would be much less expensive than
building a dedicated facility for such a demonstration.

3.2 AN ALTERNATE EXTENSION OF THE EXISTING DASACON

An alternative modification to the DASACON facility is sketched
in Figure 3.2. In this case, it is assumed that a new test chamber is
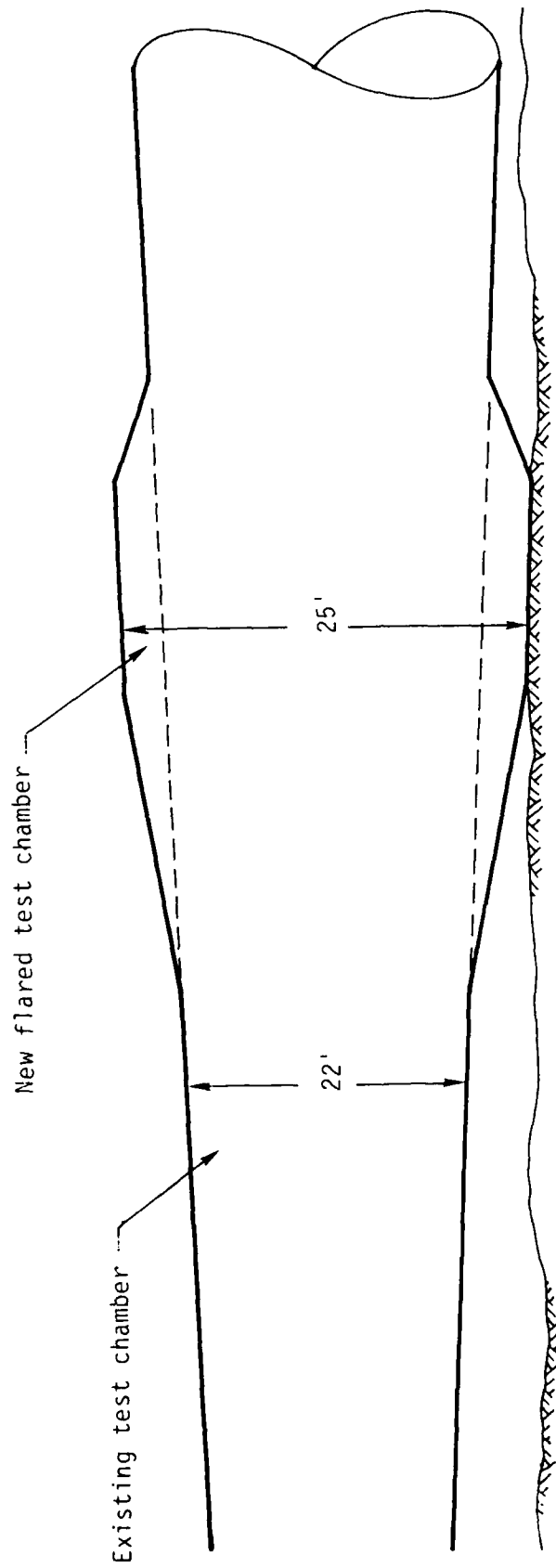
Figure 3.1. Sketch of a possible modification for DASACON in which a new, flared test chamber is constructed adjacent to the existing 22 ft diameter station. The expansion shown corresponds to a 30% increase in tube area.

New flared test chamber

Existing test chamber

25'

22'

71
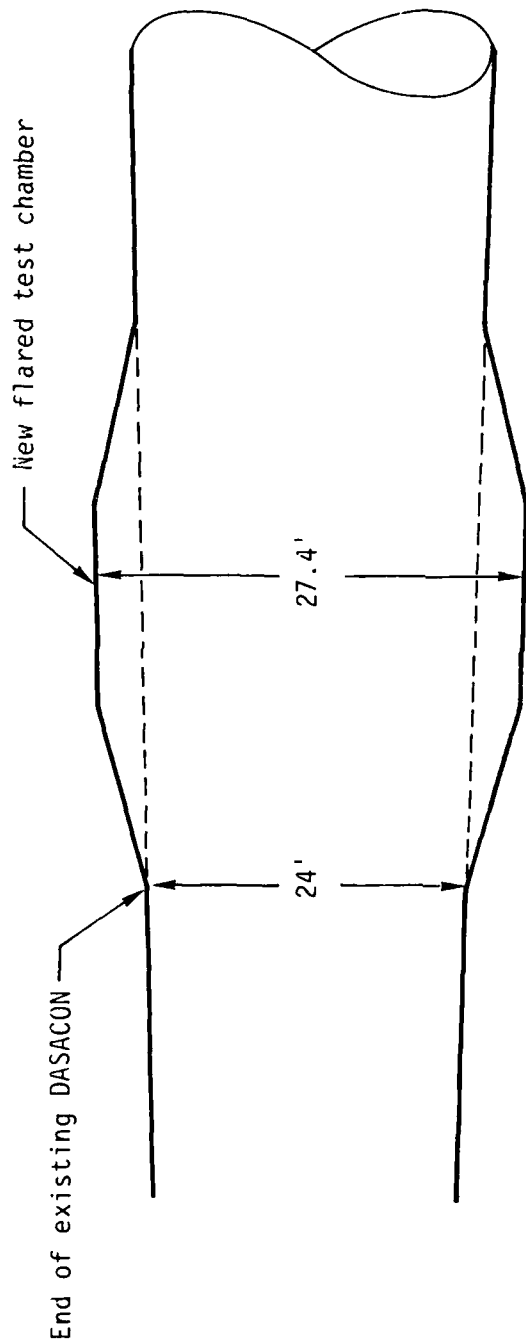
Figure 3.2. Sketch of a possible modification for DASACON in which a new, flared test chamber is constructed beyond the end of the present tube. The expansion shown corresponds to a 30% increase in tube area.

72

installed beyond the open end of the present tube near the 2450 ft station. Such a test chamber would be unconstrained by any existing construction and could, therefore, be optimally designed. It would be approximately 24% larger than an expanded facility near the existing test chamber. This would permit the testing of somewhat larger military equipment such as the M-2 infantry fighting vehicle or the M-109 series self-propelled howitzer. This does not appear, however, to represent a qualitative increase in facility capability, and it is not recommended that this option receive further consideration.

3.3 COMMENTS

If the DASACON blast simulator were reactivated and if it were modified by the addition of a flared and ventilated test chamber, it could become a useful, large blast facility. It would be large enough to test a number of the military systems for which blast criteria have been defined. However, it would not meet all of the Army requirements, and there is no credible way that it could be made to meet these requirements. Therefore, the facility should not be considered as an alternative to the proposed large blast/thermal simulator presently under consideration. Such a facility might also find application in the high-priority simulator development program for large scale HML testing.

It should also be borne in mind that the considerations presented so far have considered only geometric factors. Another major consideration in a blast simulator is the performance envelope which is available. This question is discussed in the following section.

SECTION 4
DRIVER OPTIONS FOR DASACON

As originally designed and used DASACON was driven by a solid TNT cylinder mounted on the axis of four 16 inch gun barrels near the apex of the cone. This system was not satisfactory for a variety of reasons. Loading the explosive was difficult and time consuming. It was actually accomplished by floating the charges into the barrels on water and subsequently draining the water from the barrels. It was impossible, however, to remove all the water, and this led to energy inefficiencies and to excessive rust development. TNT is known to be an oxygen-deficient explosive which leaves carbon as a reaction product. In DASACON the residual carbon settled as a dust which was entrained by succeeding shots, and sometimes dust explosions occurred which led to unexpected and irreproducible blast conditions.

The problems of DASACON operation were considered by a Navy review panel in the 1970's (Reference 5). A number of alternate driver systems were identified and described briefly, but no work was done to implement any of them. The possibility of driving the system with a gaseous detonation was one of the alternatives suggested. This possibility and several variants of it will be considered in the following sections.

4.1 CHARACTERISTICS OF DETONABLE SYSTEMS

Two important classes of problems must be treated in the consideration of a gas detonation driver for DASACON. These are the prediction of the performance envelope which might be expected in the facility and the problems of engineering involved in modifying the present facilities to permit the detonation driver to be used effectively.

Performance calculations have been made assuming the conical flow to be a segment of a one-dimensional spherical system. Configurations were investigated in which the detonation was assumed to run from the

apex out or from the outer boundary towards the center. (The later case gave results not significantly different from the former.) Partial or truncated conical and vented driver systems were also studied. Finally, a number of constant volume explosion calculations were made. The detonation work was augmented by studies of a combustion driver system which will be described later. Most of the calculations to be described ignore the potential influence of boundary layer development. This issue was studied in a limited way using a quasi-one-dimensional pipe flow code called FLIP which had been calibrated primarily in the nuclear line of sight flow domain. The boundary layer influences were found to be negligibly small which is consistent with observations of DASACON performance (Reference 6).

The engineering problems which have been investigated to some extent include studies of the bursting strength of the DASACON pipe, the problems of installing a diaphragm to separate the detonable mixture from the remainder of the tube, and the injection, mixing and initiation of the driver mixture. A major consideration in all of the engineering investigations has been a question of safety as it may influence personnel, the facility and experiments being conducted.

4.2   DETONATION CALCULATIONS

4.2.1   Initial Conditions

Detonation systems can be most simply and completely described through the determination of the Chapman-Jouget conditions. These are the hydrodynamic and thermodynamic conditions which are assumed to exist at the end of the chemical reaction zone at the head of a detonation wave.* Most of the calculations have been made for an

---

*   It is well known that the C-J conditions are appropriate only for a steady, one-dimensional flow, but no free running detonation is either steady or one-dimensional, so the C-J conditions are only a very close approximation to physical reality. That approximation is an excellent one for all questions of an engineering nature.

ethane, C_2H_6-air mixture. C-J conditions for this mixture were calculated with the ORAKL code, a variant of the well known TIGER code (Reference 7). Figure 4.1 shows how detonation conditions vary with the fuel-air mass ratio. That figure also shows a similar calculation for a propane, C_3H_8-air mixture. Note that pressures are essentially identical for the two mixtures, so they could be used interchangeably. The effective adiabatic exponent was determined by calculating isentropes from Chapman-Jouget states of interest. This, together with the knowledge of pressure and temperature permitted an adequate definition of the initial flow conditions.

4.2.2 Hydrodynamic Calculations

The hydrodynamic calculations were made with the SKIPPR code. This is a one-dimensional, Lagrangian calculating system which can handle spherical, cylindrical, or slab problems. A detonation subroutine exists which reproduces the previously calculated Chapman-Jouget conditions and the appropriate flow field behind the detonation wave.

For convenience, calculations were made assuming the interface between detonable mixture and air was at 1 cm, and a complete conical detonation would assume initiation at zero and propagation until 1 cm range. Implicit in this assumption is the neglect of any potential contribution from driver gas in the gun barrels. This is a trivial effect which has no importance to the results to be presented. In other cases, different initial conditions were used. As mentioned earlier, in some calculations the detonation was replaced by a constant volume explosion. Some calculations were run in an effort to significantly reduce the explosive mass used in the given experiment. From simple cube root scaling considerations, a factor of 8 reduction in explosive mass is required to produce a factor of 2 change in range for a given blast condition. In a spherical system 1/8 of the volume is located between the radii of 0.957 and 1. Calculations were made in which detonation was initiated at 0.957 and terminated at 1.

76
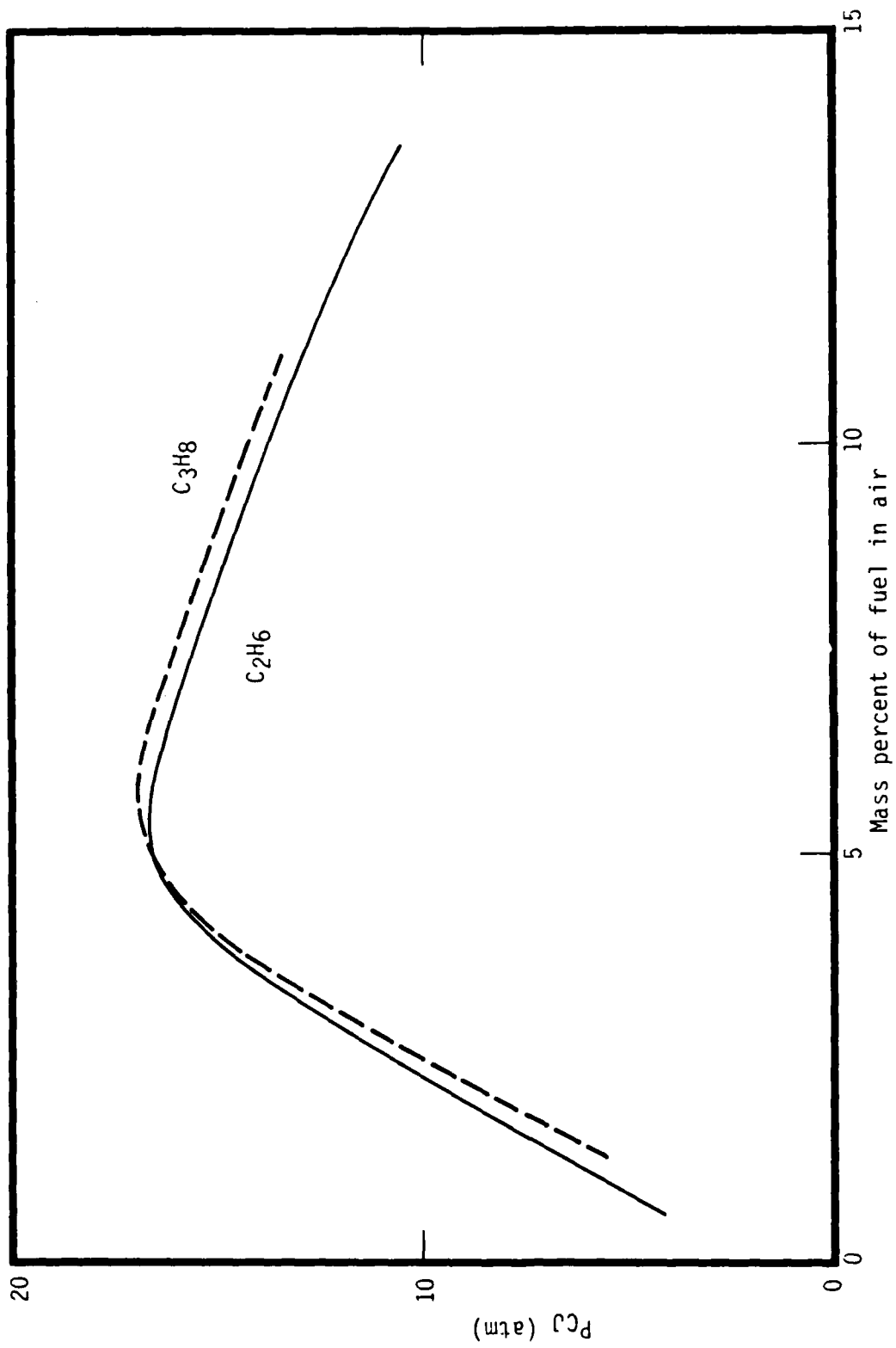
Figure 4.1. Detonation C-J pressure in C_2H_6 and C_3H_8 - air mixtures as a function of weight percent fuel in air. For present purposes the curves are assumed to be identical.

See note on Page 109.

Additional calculations were made in which the explosive mixture was assumed to react at constant volume. In each case the calculations were scaled to DASACON dimensions in a straight-forward manner to be described in more detail below.

Additional calculations were made with the FLIP code (Reference 8). This quasi-one-dimensional system assumes the flow variables are uniform across the tube section, but arbitrary area changes can be included. This code was used in the study of vented initiator systems, for the investigation of rarefaction wave eliminators, and for the estimation of boundary layer influence by including wall stress terms, as mentioned earlier.

4.2.3   Calculational Scaling

A procedure whereby given calculational results can be scaled to the DASACON configuration and an equivalent nuclear yield determined will be described below. Calculations were done, as mentioned above, with, for instance, a detonation starting at the apex and running to a dimension of 1 cm. This is followed by a spherical shock driven into air. Calculations were often extended to a final radii of 10 cm. At a number of radial stations, pressure, velocity, dynamic pressure and positive phase impulse were calculated from the numerical results and graphically summarized as a function of range. For an example of the scaling process, assume the test chamber location is known and that a particular peak pressure is desired at that chamber. Look at the peak pressure-range curve shown in Figure 4.2 and find the R value at which that pressure occurs. Then the diaphragm location is at

$$R_{Dia} = \frac{R_{TC}}{R}$$

Linear scaling between the diaphragm location in DASACON and the calculation gives the scale factor for time and for positive phase impulse.

78
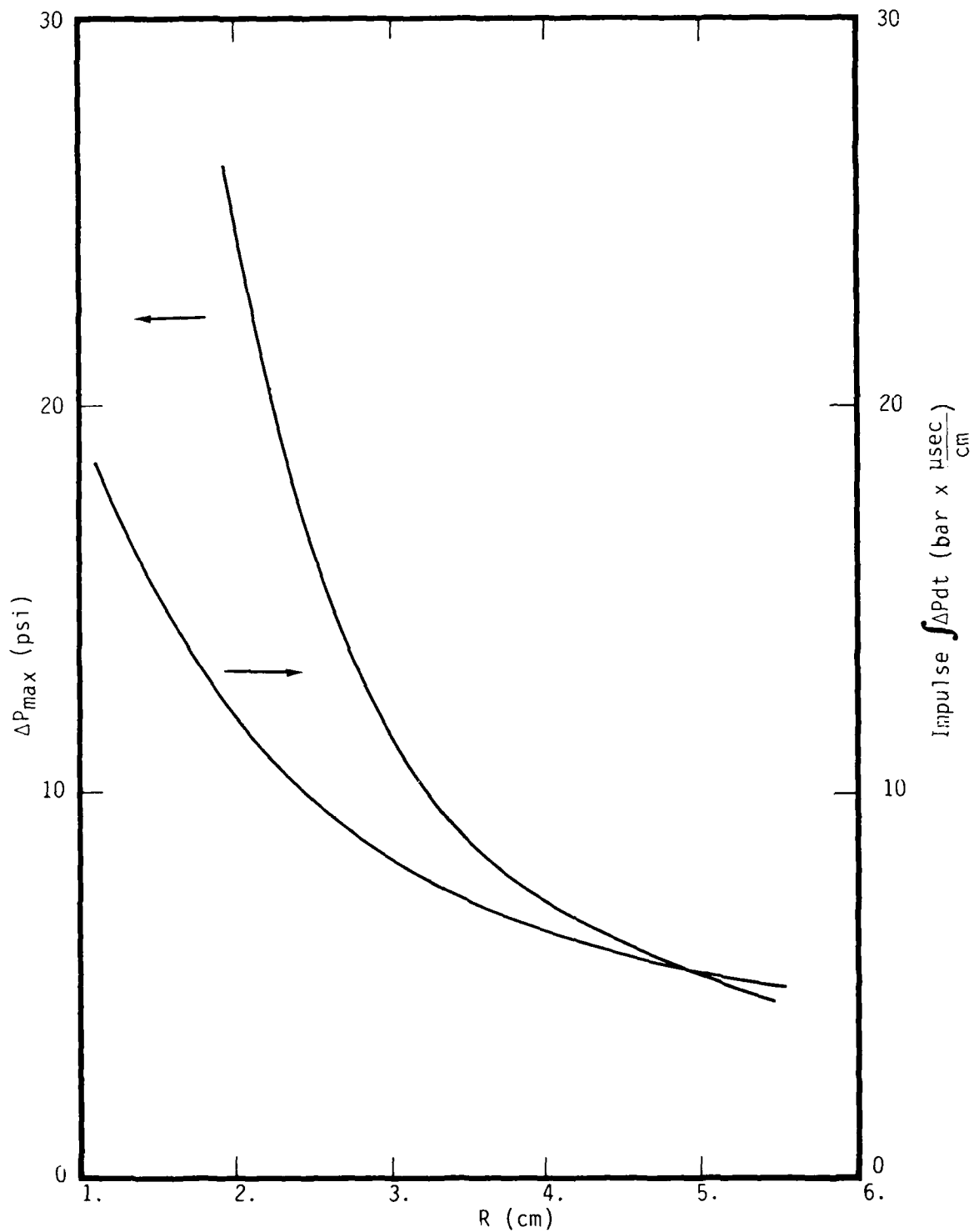
Figure 4.2. Calculated peak pressure and positive phase impulse
as a function of range for a propane-air detonation
driver running from the apex to 1.0.

The equivalent yield was estimated from positive phase impulses from nuclear surface bursts, deduced from Speicher-Brode (Reference 9) fits to empirical blast wave data. The result is shown in Figure 4.3 as a function of peak pressure for a 1 KT explosion. The equivalent yield in KT is the cube of the ratio of the scaled calculated impulse to the Speicher-Brode impulse. Obviously, other techniques could be used to estimate equivalent yields. For instance, positive phase duration, dynamic pressure impulse, or an overall fit to the wave shape could be used to estimate the yield.

4.2.4 Calculated Results

Representative calculated results for a stoichiometric ethane-air mixture are presented in Figure 4.4. Both static and dynamic pressure are shown at several different radii. Note that the calculated wave shapes are excellent approximations to ideal blast waves. This is true of essentially all of the detonation-driven results obtained. An X-t diagram for this configuration is shown in Figure 4.5. For this case the detonation products are not expected to expand beyond an R of 1.75. In the results shown in the earlier figure, the interface arrival at R = 1.5 is seen at 19 μs as a decrease in the dynamic pressure. For comparison with an alternate driver see Figure 4.15. The present result follows from the fact that the reaction products are thermodynamically quite similar to air, and the driver was heated, so after expansion its temperature is still higher and density lower than that of shocked air.

A portion of the performance envelope available through this particular driver system is shown in Figures 4.6 and 4.7 as the curves labeled "C_2H_6-air det, 0-1". Each point represents a different diaphragm location, and the test chamber is assumed to be at 2200 ft. Based on an ever changing diaphragm location it is interesting to observe that high pressures go with high yields in this facility driven in this way.

80
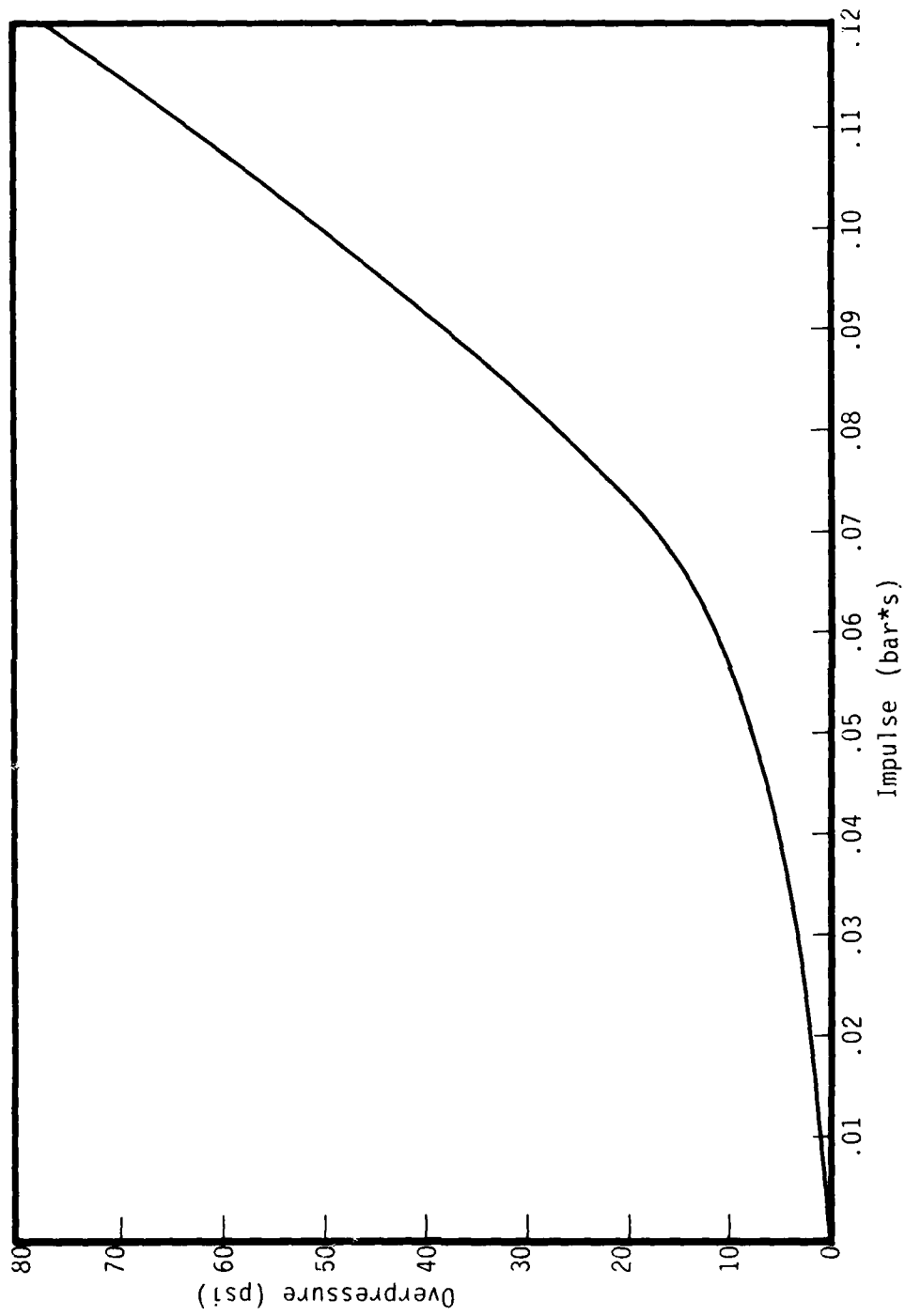
Figure 4.3. Peak pressure - positive phase impulse relationship for nuclear surface bursts based on the Speicher-Brode fits to experimental and theoretical data.
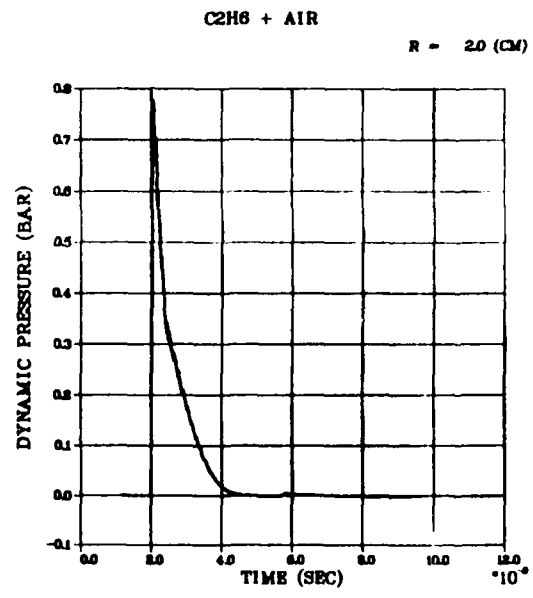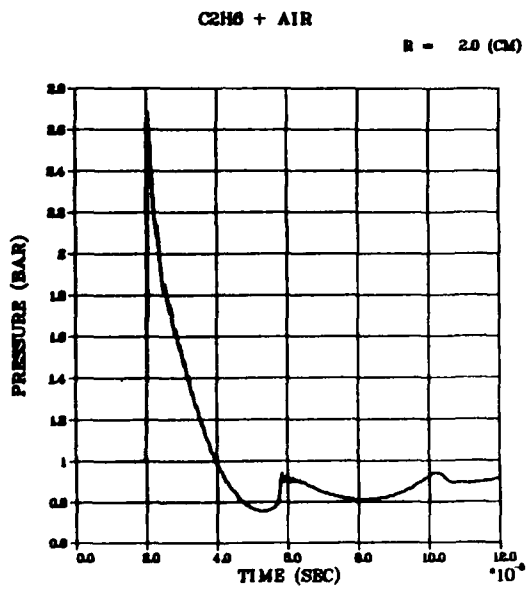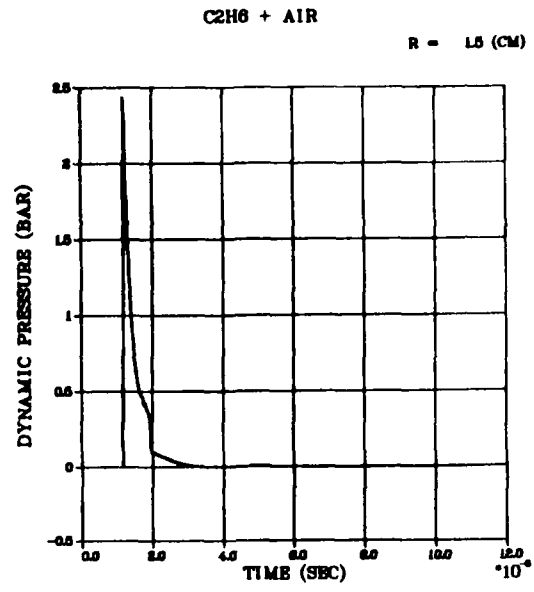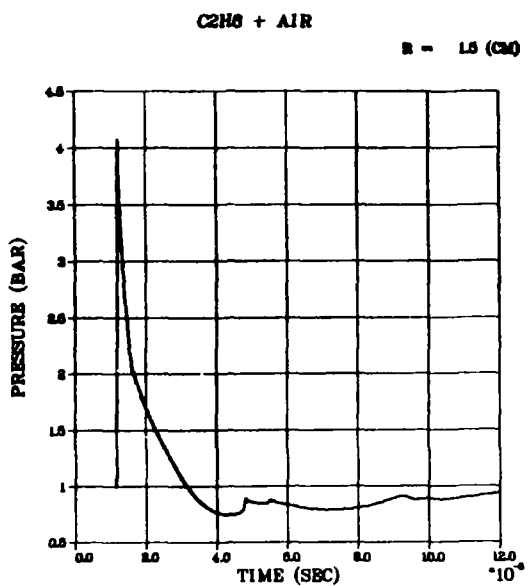
Figure 4.4. Static and dynamic pressure profiles at several ranges driven by a 0-1 ethane (or propane)-air detonation in spherical geometry. The roughness on the wave profiles, especially at large ranges, is a numerical artifact.

82
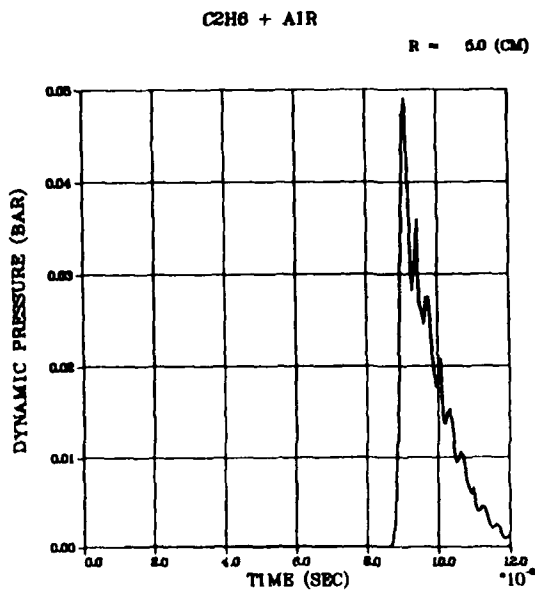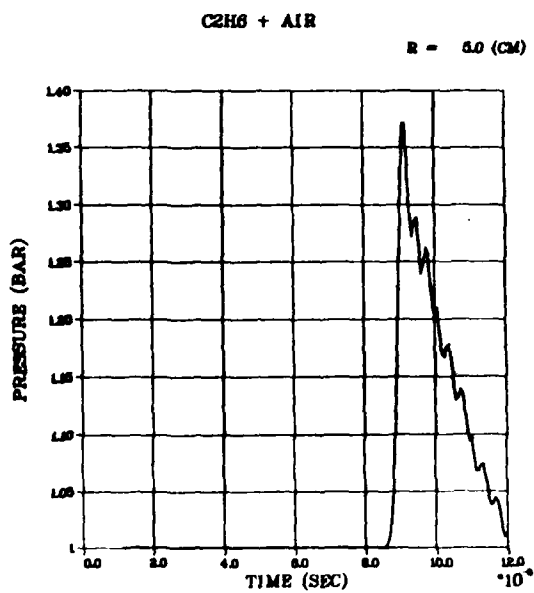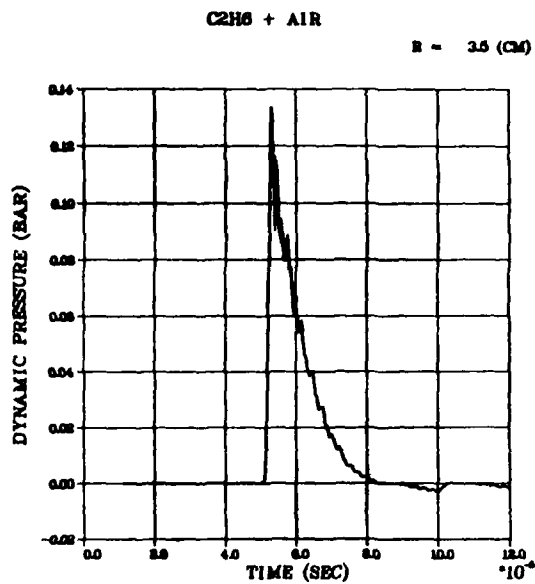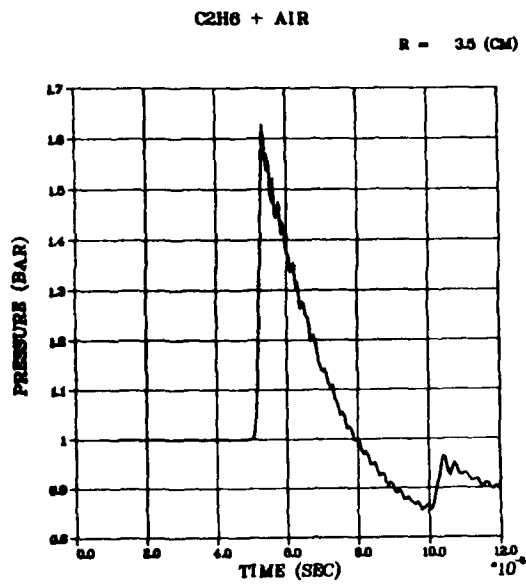
Figure 4.4. (Continued)
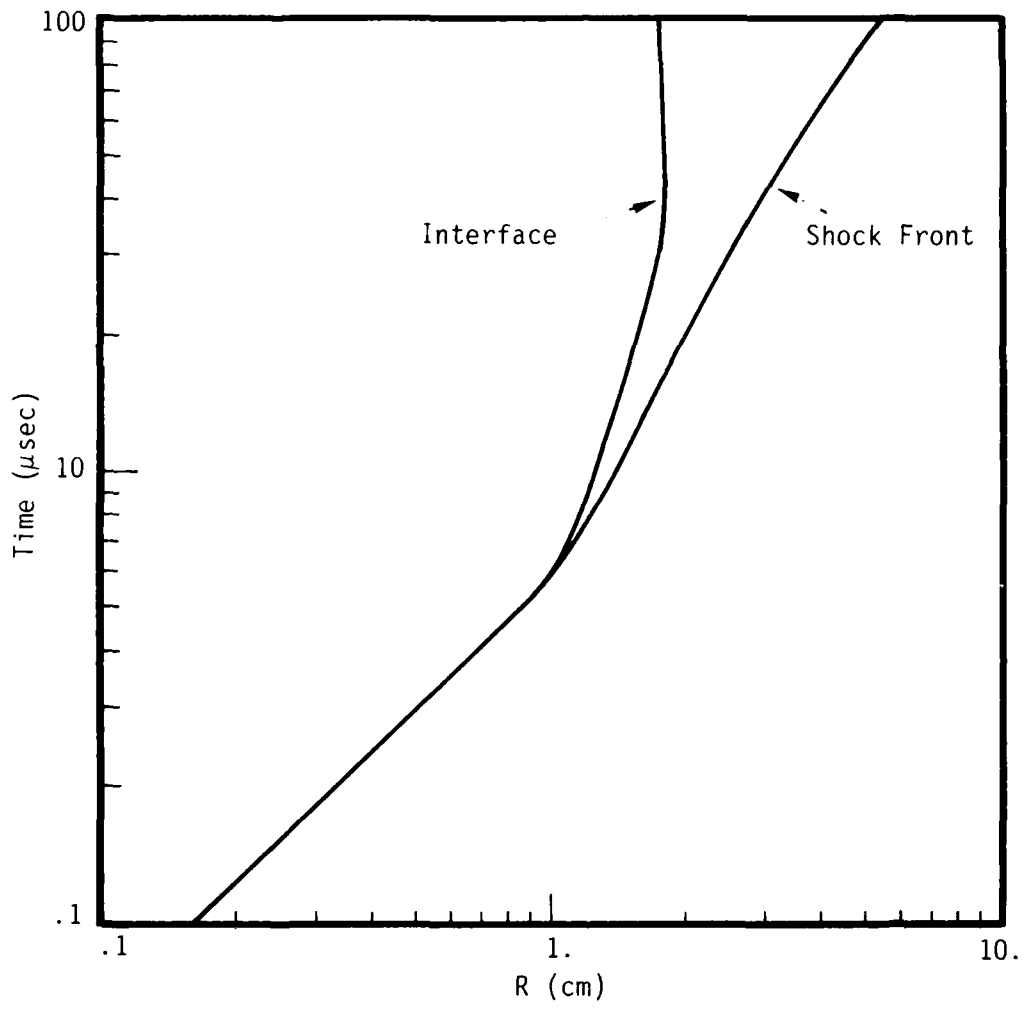
Figure 4.5. Shock front and interface range time curves for the
flow system driven by a spherical ethane-air detonation,
0 - 1.0. Note that the reaction products are not calculated
to expand beyond R = 1.75.

84
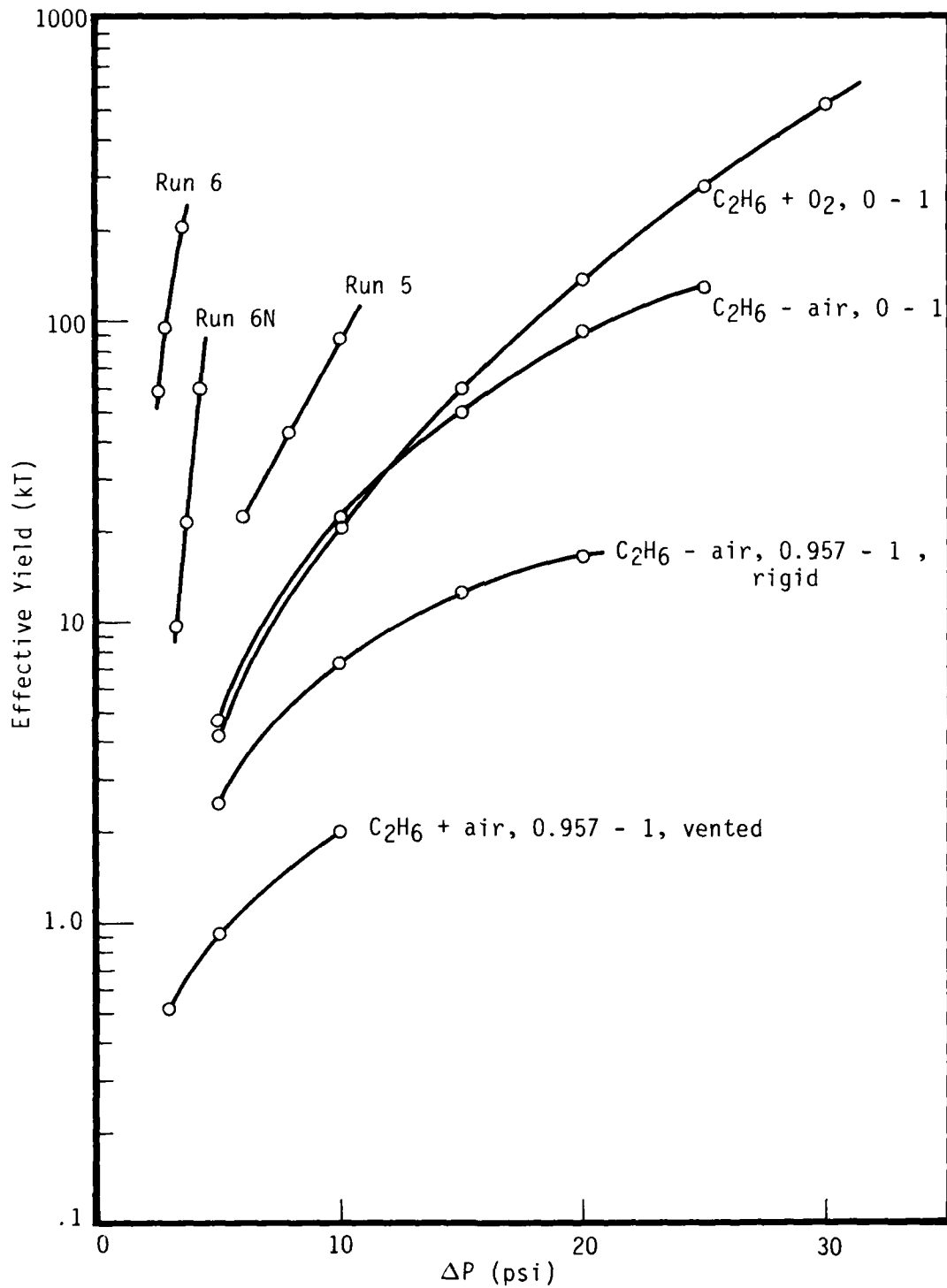
Figure 4.6. Performance envelope for a gas detonation driven DASACON. The effective yield is based on positive phase pressure integrals from Speicher-Brode fits to nuclear surface burst data. The test chamber was assumed to be at 2200 ft.
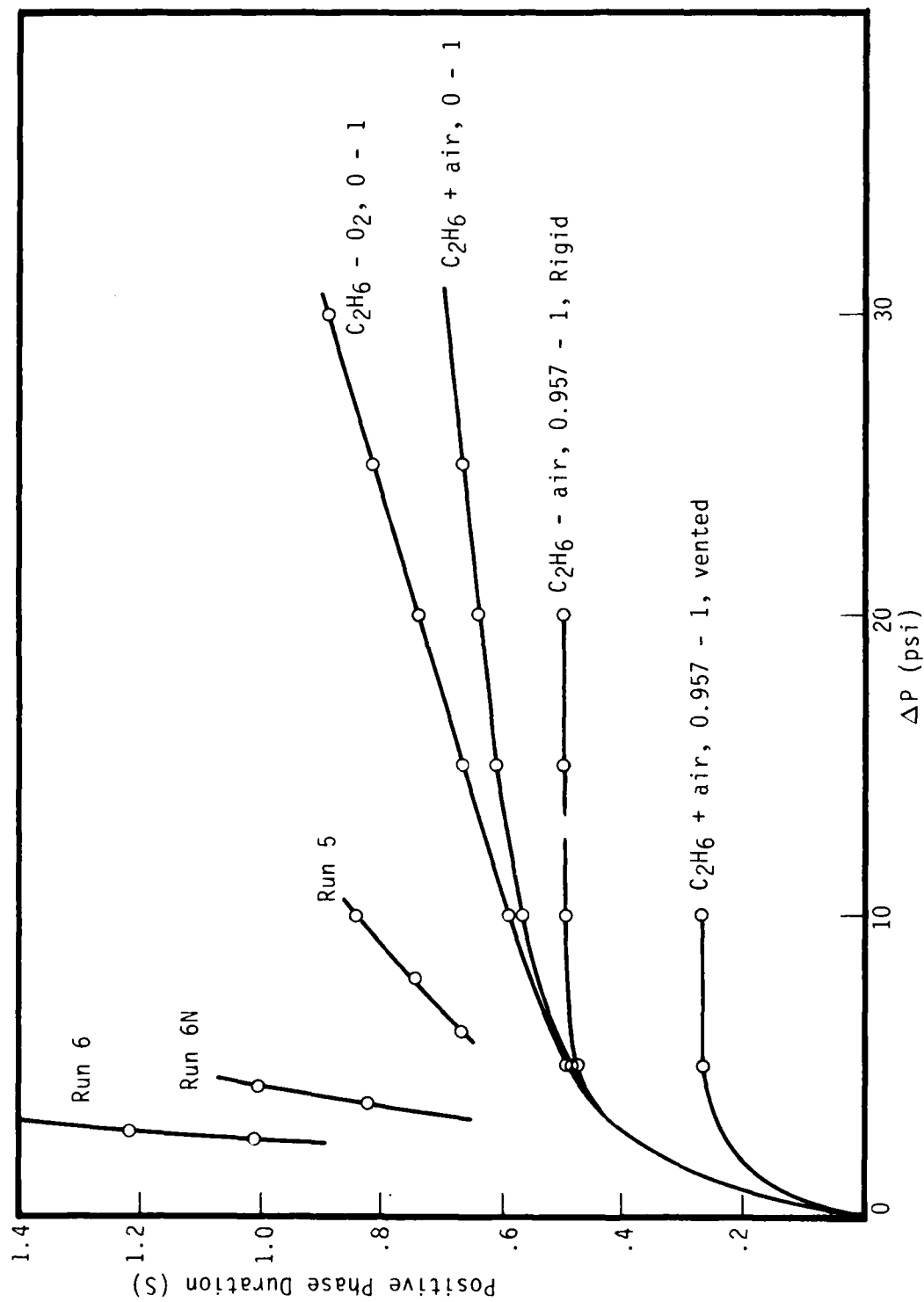
Figure 4.7. Performance envelope for a gas detonation driven DASACON. Positive phase duration at the 2200 ft. test chamber is presented as a function of overpressure for a number of detonation conditions.

Additional calculations were done for an ethane-oxygen and an acetylene-oxygen driver system. Such drivers would be more difficult to obtain in practice, but calculations were performed to illustrate the potential of more energetic detonation driver systems in this application. The results in terms of overpressure and positive phase duration for the $C_2H_6 + O_2$ case are included in Figures 4.6 and 4.7. Some specific results derived for particular test chambers and diaphragm locations are included in Table 4.1.

The potential influence of driver geometry on simulator performance was investigated in additional calculations. These results are most easily illustrated in Figure 4.8 which shows the pressure as a function of range for some of the configurations investigated. The full detonation case was compared with a calculation using 1/8 as much explosive distributed between radii of 0.957 and 1. In one case a rigid wall was assumed to exist at R = 0.957; in the other the tube flared open at a 26° angle* at R = 0.913 thus generating a strong rarefaction at the rear of the driver. Other calculations were done comparing a detonation driver with an assumed constant volume explosion of the gas. The results were essentially identical. This simply illustrates the fact that the far field shock conditions depend primarily on the energy released and not on the details of source characteristics.

The conclusion mentioned above should be reiterated. The calculations clearly show that high blast pressures go with high yields and vice versa in a detonation driven DASACON facility. This is a straightforward result for a fixed test chamber location. A small explosion will produce a small pressure at a given range, a large explosion will give a larger pressure at that range. Within this general constraint changing the gas mixture by adjusting the fuel

---

*An additional calculation showed the results to be essentially independent of this expansion angle probably because a nozzle throat existed in the problem.

Table 4.1. Approximate blast conditions in DASACON at the 2200 ft test chamber driven by three different gas mixtures and using three diaphragm locations. Locations are given in feet, overpressures in psi, positive phase durations in seconds, and the equivalent yields in kT are scaled as described in the text. Almost identical results should be obtained if C_3H_8 were used instead of C_2H_6.

See note on Page 109.

Diaphragm Location	C_2H_6 + Air			$C_2H_6 + O_2$			$C_2H_2 + O_2$		
	Δp	τ	Y	Δp	τ	Y	Δp	τ	Y
400	5	0.44	5.5	8	0.56	19	8.5	0.57	23.1
700	11	0.58	28.4	21.5	0.75	160	23.8	0.73	177
1000	20	0.64	95.5	39.4	0.98	813	46.2	0.94	830
C-J detonation pressure	245			510			616		
"Safe location" for diaphragm without tube strengthening	1010			570			470		

88
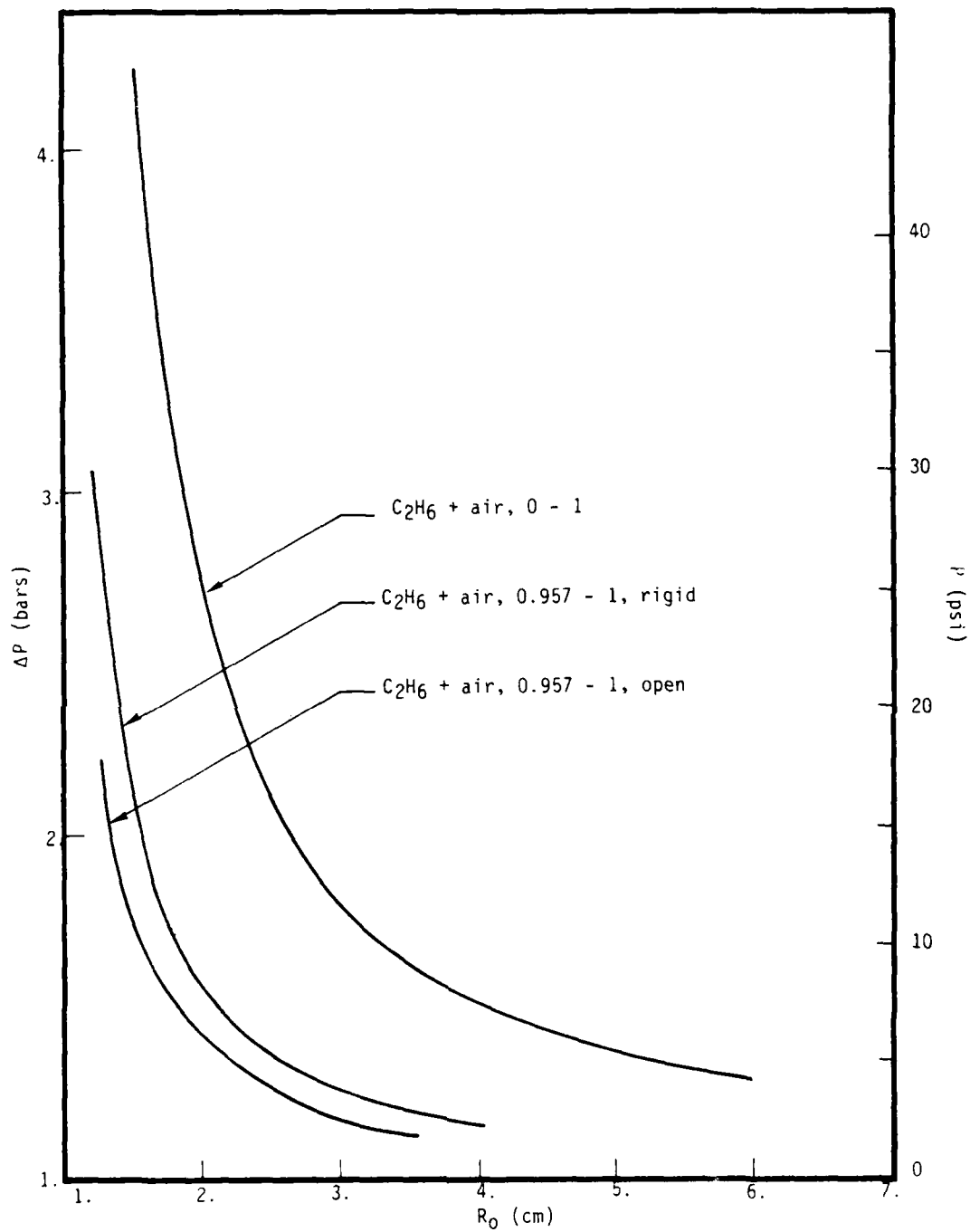
Figure 4.8. Peak pressure-range curves for several configurations investigated using C_2H_6 + air drivers.

The curve labels read:

C_2H_6 + air, 0 - 1

C_2H_6 + air, 0.957 - 1, rigid

C_2H_6 + air, 0.957 - 1, open

The vertical axes are ΔP (bars) and P (psi); the horizontal axis is R_0 (cm).

concentration or by adding oxygen can modify conditions somewhat, but it cannot produce conditions equivalent to large yields and low pressures or low yields and high pressures. More dramatic variations are required for this purpose.

As described above one such variation assumed that the driver region was opened at one end; in particular, it was assumed that a constant volume explosion occurred in the interval between 0.957 and 1.0, and the tube was open at 0.913 on the apex side of this interval. The results of this calculation are shown in Figures 4.6 and 4.7. It is clear that by significantly modifying the one-dimensional, spherical nature of the assumed simulator significantly different flow conditions can be obtained. In particular, higher pressures at lower yield equivalents are expected. However, overpressures higher than 10 psi or so do not appear available. This variant does not address the problem of producing low blast pressures at large equivalent yields. That is a significant part of the performance envelope required by the Army (See Section 4.4).

4.3 ENGINEERING CONSIDERATIONS

The preceeding sections have considered gas dynamic aspects of blast simulation and DASACON rehabilitation. It is now appropriate to consider engineering aspects of this problem. The following sections will discuss structural questions, modifications required to permit the inclusion of a detonation system, and instrumentation required for efficient operation.

4.3.1 Structure

Obviously the first task to be undertaken is a detailed investigation of the current state of the facility. It was designed and built in the 1960's and was abandoned as a blast simulator in the

90

early 1970's. Nevertheless, superficial examination shows the struc-
ture to be in remarkably good shape, but a more careful investigation
is required to make certain that it can be operated safely with the
contemplated gas detonation driver.

The items presently believed to be required in an examination
and rehabilitation of the facility include the evaluation of the
concrete structures and the pipe and its supports, the movable
sections must be reinserted, the buckled section must be evaluated and
repaired or replaced if necessary, the tube should be sandblasted and
painted, and no doubt other things must be accomplished before the
facility can be used. It is important to realize an important detail
however. There is no need or expectation that the driver section be
made vacuum tight. All that is required is a reasonably closed
vessel.

Another feature of the rehabilitation effort will be a detailed
calculation of the strength of the existing system. Figure 4.9 shows
the thickness and material used to construct the tube as determined
from design drawings. Simple estimates of the bursting strength of
the tube at various stations are also included. These estimates must
be reviewed and refined to determine safe operating limits for the
tube. If any aspect of the tube appears inadequate for use with the
detonation driver, the required upgrade must be designed and
accomplished.

Table 4.1 summarizes some blast conditions expected for several
different driver gas compositions. It appears that the detonation
pressures associated with the oxygen-rich systems would exceed the
strength characteristics of parts of the existing tube inside of the
1000 ft range. Therefore, if an effort were made to use the DASACON
as a blast simulation facility for blast conditions approaching 50 psi
overpressures at the 2200 ft chamber, significant strengthening of the
existing structure would be required.

91
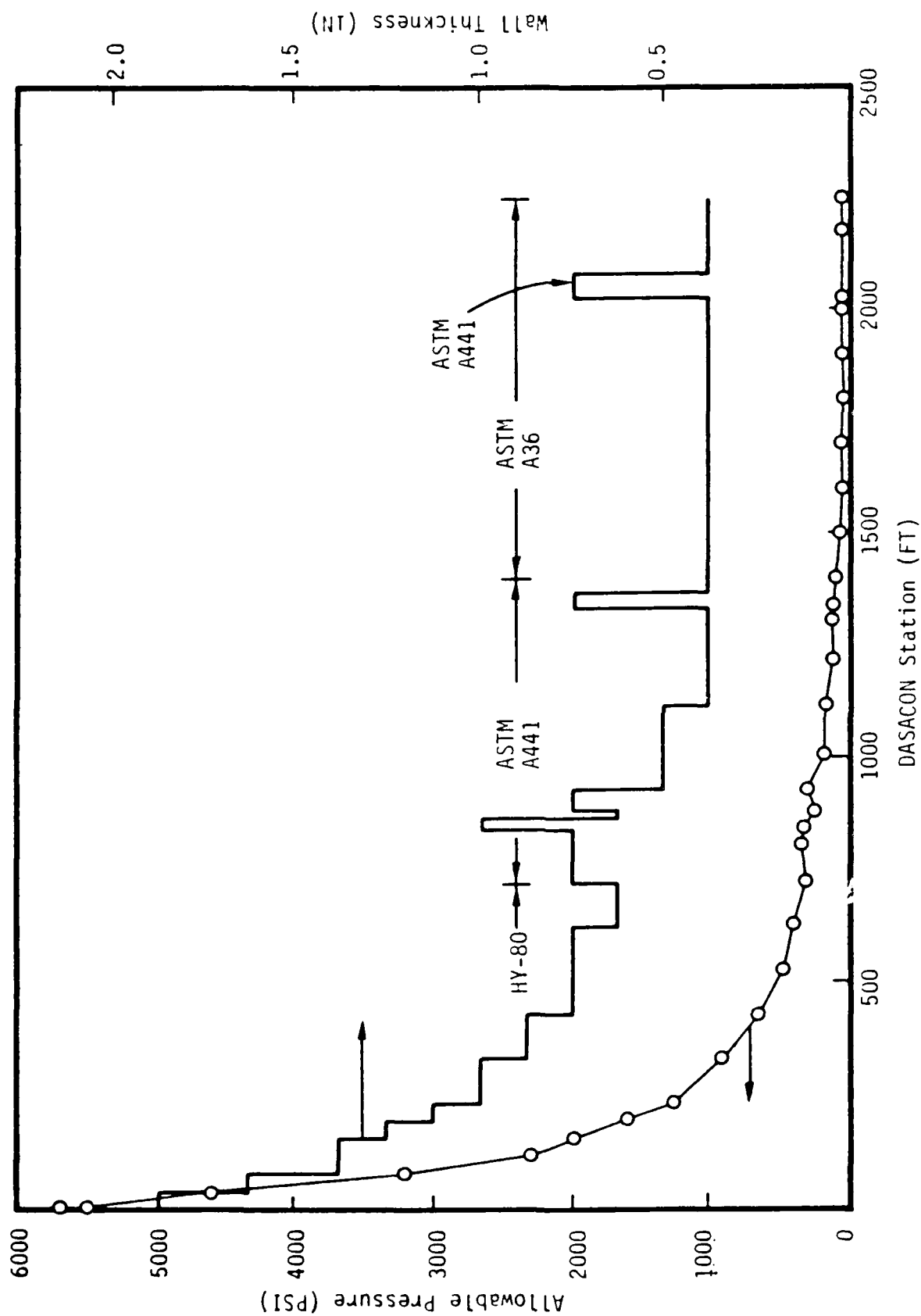
Figure 4.9. Wall thickness and material for the "as designed" DASACON. The allowable pressure is also presented. The station locations are measured from the end of the gun barrels 133 ft from the cone apex which is used as a reference in other parts of this report.

92

4.3.2 Detonation System

If a detonation driver is to be used in a simulation facility such as DASACON, a means must be installed to permit the detonable mixture to be prepared in isolation from the rest of the tube. This requires a method for mounting a diaphragm which would separate the tube into at least two independent chambers. Then, of course, techniques for filling, mixing, and igniting the gases must also be provided.

As mentioned above it is not necessary to provide vacuum capability in the driver region, nor is a significant overpressure contemplated in the injection and mixing process. Therefore, the diaphragm need not support a pressure difference. This dramatically simplifies many aspects of the operation. Probably the diaphragm could be a lightweight, coated fabric like tent or tarpaulin fabric, or perhaps construction grade plastic sheeting hooked over pins at the tube periphery and held in place by simple friction clips. An example of this system is sketched in Figure 4.10.

As an example of the fuel injection and mixing system, consider the case of propane and air. Stoichiometric mixture requires about 5 moles/0 fuel in air. It is contemplated that this fuel would be inserted at the small end of the tube while an equivalent volume of air was displaced from the vicinity of the diaphragm. On the other hand, if a fuel oxygen mixture were desired, oxygen would be first inserted at the small end as air is vented near the diaphragm. This process would be continued until an adequate oxygen purity had been obtained. Subsequently, fuel would be inserted as oxygen was vented. In no case would a significant pressure difference exist at the diaphragm. Incidently, about 100 lbs of propane would be needed for a 20 psi blast condition. It would cost approximately $20. (This assumes that LPG is mostly propane.)
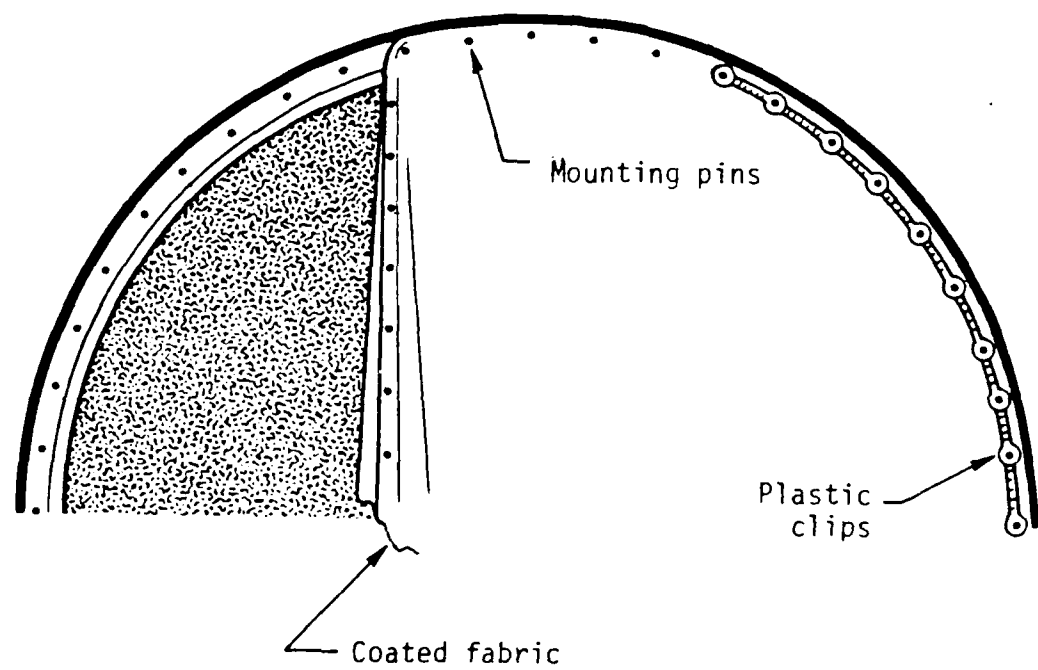
Figure 4.10. Sketch of one simple scheme for installing a diaphragm. It shows a partially installed diaphragm of light-weight coated fabric which is hooked on closely spaced pins and held in place by plastic clips.

END

FILMED

DTIC
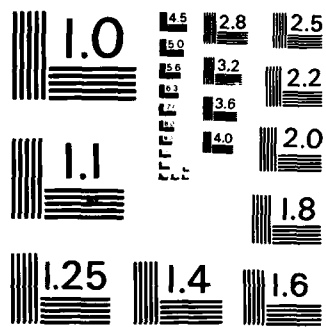
MICROCOPY RESOLUTION TEST CHART

NATIONAL BUREAU OF STANDARDS-1963-A

After the required gases are injected into the tube, they must be fully mixed in order to assure uniform and reliable detonation propagation. This can be accomplished by circulating the gas as indicated in Figure 4.11. It is imagined that a 16 to 18 in. pipe would connect to ports in the tube at appropriate locations. Large gate valves would isolate the mixing system from the tube proper. A limited investigation has shown that a Chicago Blower Company fan Model SQADD 16.5 running at 1750 rpm could deliver 2762 cu ft per minute against a 3 inch water static pressure differential. Such a fan would be driven by a 2 HP electric motor, and would cost approximately $1200 f.o.b. Chicago. That fan has the capability to circulate between 5 and 10 driver volumes of gas an hour through 16 inch lines. It is estimated that somewhere between 1 and 2 hours of circulation would be required to provide driver mixing for reliable simulator performance.

Of course, the explosive mixtures would not be inserted until the experiment objects had been installed and instrumentation was in place. This precaution is based on assuring personnel safety. Relatively inexpensive, commercially available, infrared analyzers exist which could be used to monitor the mixing process and assure that adequate driver gas uniformity had been obtained. It is anticipated that such instrumentation would be located in the 16 inch circulating pipe near the circulating fan.

After the gas driver is filled and mixed, it must be ignited. Propane and oxygen can be ignited in small volumes with a few tens of joules of energy in a bursting wire. The energy requirement is only about 1/6 of that needed for a methane-air mixture. Probably somewhat more energy would be required in a large volume propane-air mixture, but the requirements are modest and could be met easily by ordinary laboratory equipment. Alternatively, a small explosive charge could be used as an initiator. If more extreme conditions were desired involving acetylene, the detonation ignition requirements become trivial but the safety problems associated with handling this gas would be significant.
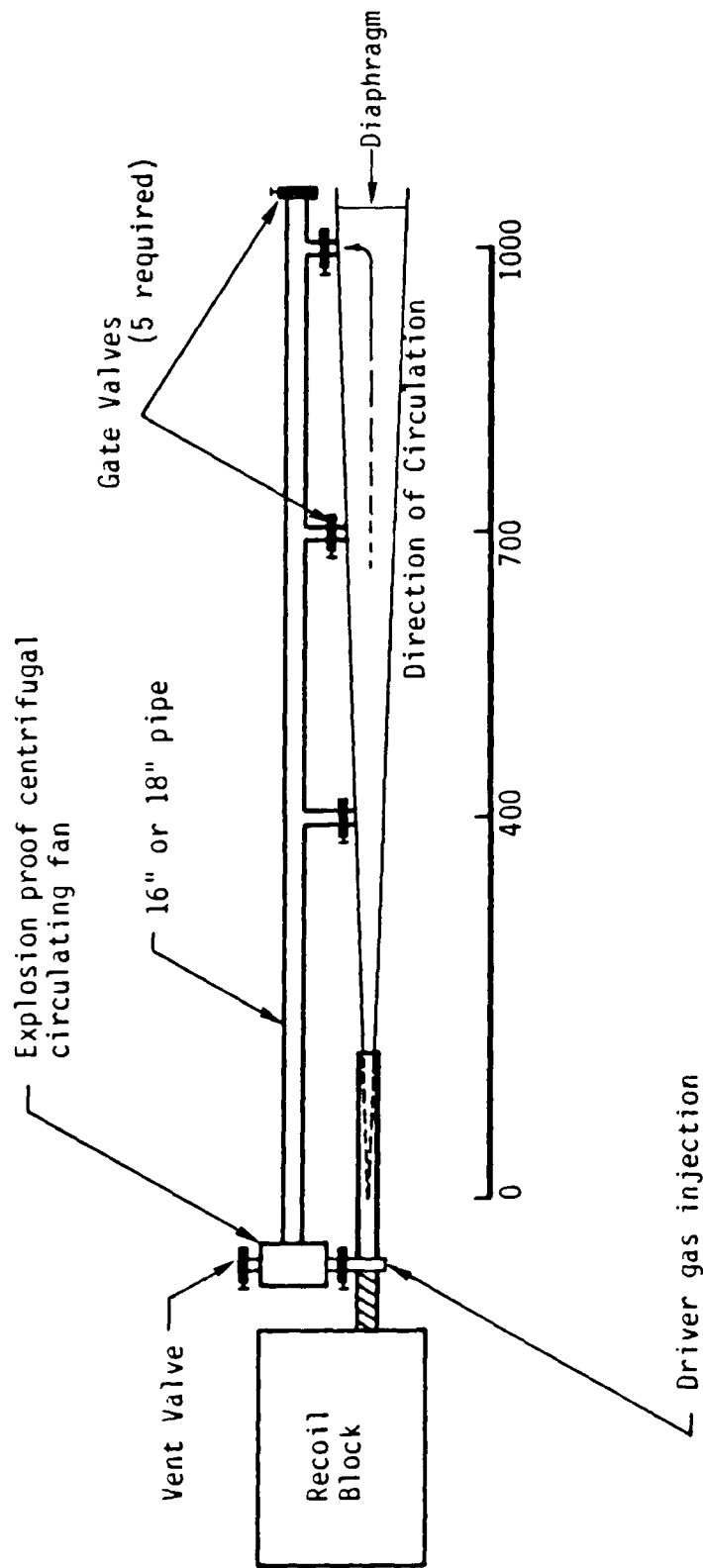
Figure 4.11. Suggested gas mixing system. The 400 and 700 ft connections are at the present vacuum pump ports, and the 1000 ft connection is through ports in the first test chamber.

The safety question has been considered to some extent. Since DASACON is a metal pipe and since the mixing system is expected to be metal also, the possibility of static electricity causing a preignition is quite small. It is anticipated that operating procedures will demand that no people be exposed to possible blast effects during the loading and mixing process. We believe DASACON can be operated safely using propane as a fuel. That would be more convenient than methane.

4.3.3   Instrumentation

In addition to the gas mixing monitor mentioned above, the only other instrumentation required is that which indicates detonation propagation and pressure levels reached at the appropriate test chambers. The detonation propagation can be indicated by simple ionization gauges which could be little more than automotive spark plugs screwed into existing threaded holes in the tube wall.

Pressures or blast conditions obtained at the test chambers could be monitored with wall mounted pressure gauges. It is anticipated that all performance and recording would be accomplished in the existing control building in which the required control panels could be installed in straightforward fashion.

4.3.4   Summary

Preliminary inspection of the DASACON facility indicates that it is in remarkably good shape after a decade of idleness. It appears that minimal structural modifications would be required to permit a propane-air gas detonation driver to be used with a diaphragm located near the 1000 ft station. Such a driver would produce 20 psi blast conditions at the 2200 ft test chamber and 45 psi conditions at the 1500 ft chamber. A simple diaphragm can be used to separate the driver from the driven sections in DASACON, and driver gas injection and mixing does not require tube evacuation or the generation of any significant pressure differential. Gases could be mixed through a exterior circulating loop in roughly 1 to 2 hours.

It presently appears that there are no significant engineering limitations to the reactivation of the DASACON facility with a gas detonation driver.

4.4   COMBUSTION DRIVER

An additional series of calculations was done in an effort to provide a quasicontinuous source to overcome the limitation on flow duration at low overpressure discussed in Section 4.2.4. The calculations were made with the FLIP code. They assumed mass injection at numerous points within the unit sphere, and the results were scaled to DASACON dimensions and nuclear yields as described above. This system was adopted because work done at S-CUBED over the last several years with a steam torch system (Reference 10) has shown that large mass fluxes could be provided under well-controlled conditions. Further, these calculations assumed that the torch combustion products were cooled by liquid N_2 to a temperature of 500 K. By assuming injection at a large number of stations over the desired interval it would not be necessary to significantly advance the state of the demonstrated art of burner development to obtain the desired conditions. The following discussion assumes each burner is immediately cooled with LN_2 and the total system mass flux is no larger than that used in the steam torch. Such assumptions are very conservative, and they lead to unreasonably large numbers of individual torches.

At each station the calculated mass injection rate was assumed to follow the profiles shown in Figure 4.12. For each case the total mass injected is shown in Table 4.2. Figure 4.13 shows an example of the pressure and dynamic pressure calculated for this system. Note that good approximations to ideal blast waves, both in static and dynamic pressure, are predicted at the 2200 ft test chamber.

A few additional comments about this system are in order. The mass injection rate required for 2 of the 3 cases summarized (Runs 6 and 6N) is about 1/2 tonne per second. The rise time of the source is
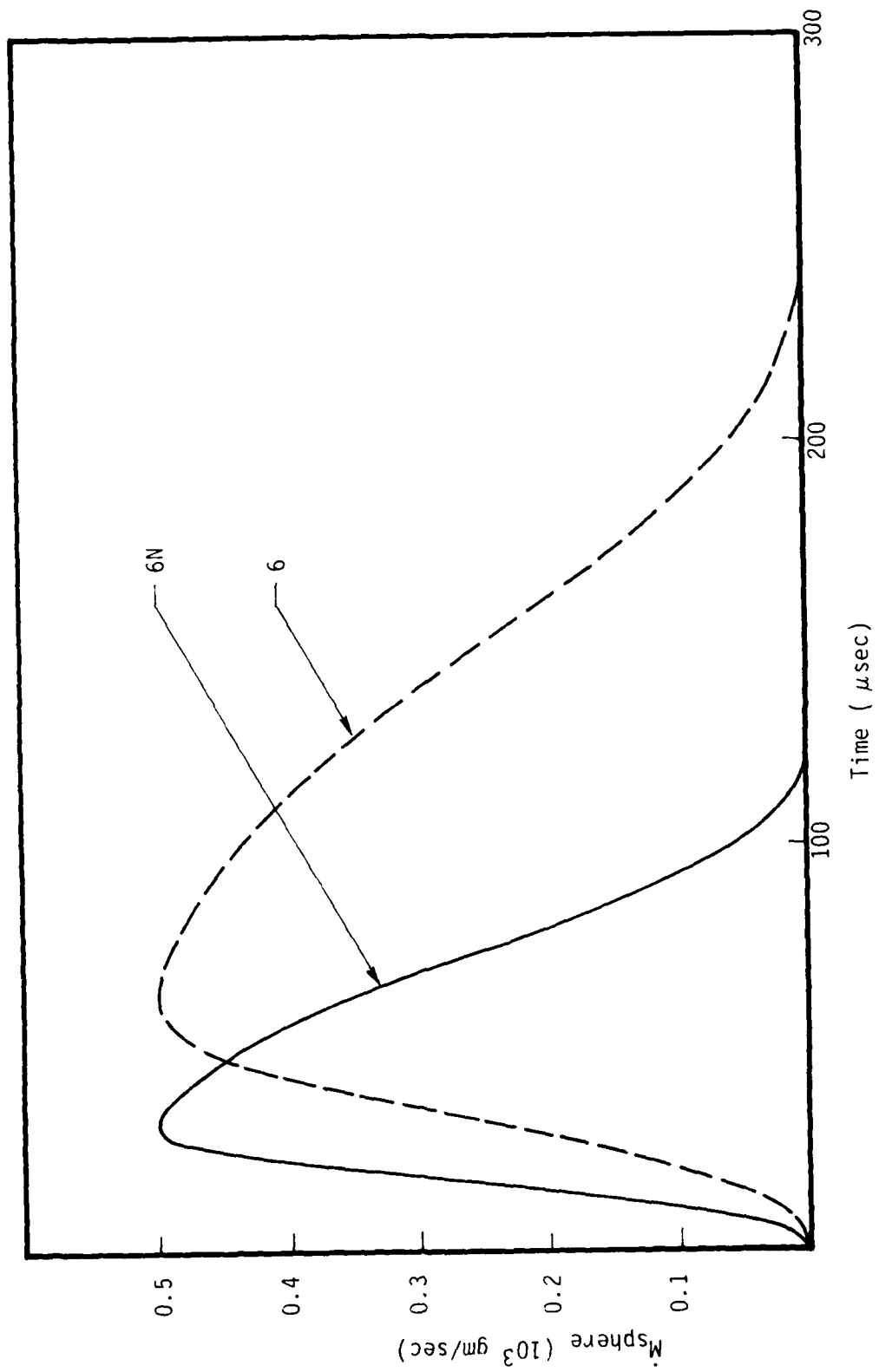
Figure 4.12. Mass injection rate into a 1 cm radius sphere for combustion driven blast simulation calculations. The rate for RUN-5 is 8 times larger than for RUN-6.
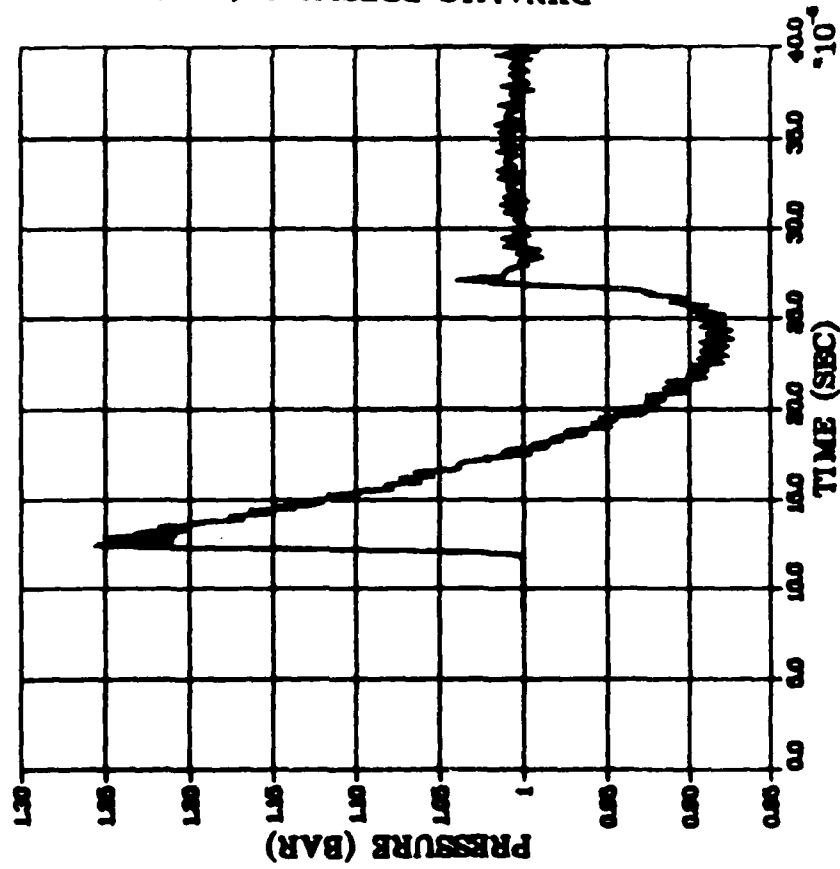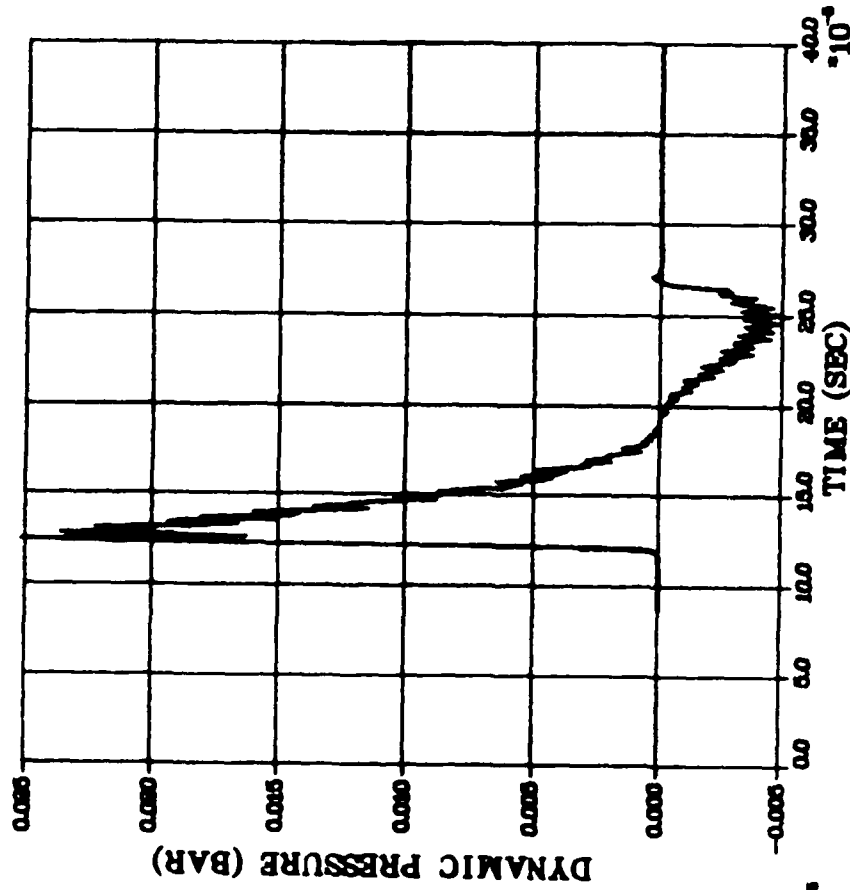
Figure 4.13. Representative static and dynamic pressure pulses generated at the 2200 ft. station in DASACON from a 440 ft. long combustion driven driver defined in RUN-6N in Figure 4.12. The negative sign on the late-time dynamic pressure signal means only that the flow is toward the apex, not away from it.

100

Table 4.2. Mass injection data for the combustion driver. In each case the combustion system was assumed uniformly distributed from the apex to the 440 ft station.

Run	$\dot{M}_{Max}$ (Tonnes/s)	Time to Peak $\dot{M}$ (s)	Total Mass (Tonnes)	Total Fuel Mass (kg)
6	0.56	0.8	0.90	10.8
6N	0.56	0.4	0.45	5.4
5	5.62	0.8	9.04	108

about 0.8 seconds. This should be doable without major difficulty. If mass flow capability per torch were restricted to levels demonstrated, about 500 individual burners would be required. The size of this number would be a powerful motivator to increase the output of each torch. An order of magnitude increase seems well within the realm of the possible. The major problem is to supply reactants and coolants at the required rate.

It is not the intent of this section to suggest that DASACON could be driven by a torch system as easily as it can be driven by a detonation. The truth is quite different. Probably the economic and engineering complications which would be encountered would be of the same magnitude as those involved in a compressed air driver system.

An alternate approach to long duration flows would involve the installation of baffles in the driver region to slowly vent the reaction products and thus get low blast pressures and long durations. That option was not considered here for two reasons. The baffles should be relatively ineffective in a conical tube because there is little volume available near the apex. Also, baffles would introduce very large axial forces into particular pipe sections. The DASACON structure was not designed to accept such loads.

4.4.1 Results

The several burn rate as a function of time profiles shown in Figure 4.12 lead to different overpressure equivalent yield relations as shown in Figure 4.6. It is clear that the performance envelope of a modified DASACON facility could be significantly expanded by including a multi-nozzle combustion driver.

A characteristic feature of this modification is the ability to change the equivalent pressure and yield at a given test chamber as shown by the results presented above. The essentially fixed relationships governing a spherical blast wave are relaxed in this configuration.

Calculated static and dynamic pressure records for a 5 psi blast at the 2200 ft test chamber are shown in Figure 4.13. The late-time return flow probably would not be seen if the finite lengths of the tube had been considered in the calculation. The interface between reaction products and shocked air does not quite reach the 1000 ft station.

4.4.2 Engineering Consequences

The engineering problems associated with the combusion driver are non-trivial. It is certainly a more complicated driver system than provided by the detonation option. The total mass, the mass rates and time to peak required are indicated in Table 4.2 for several of the cases illustrated above. This mass and mass rate could be obtained using already developed and demonstrated hardware if 500 torches were assumed distributed along the driver interval, assumed to be 440 ft long in this series of calculations. The total amount of fuel required is only about 11 kg, only 22 g per burner. Combustion air is 0.8 lbs per burner. This could be supplied by conventional compressed air bottles. The total LN_2 required varies between 0.36 and 7.1 tonnes. These numbers show that the main requirements is for cryogenic N_2. Since the fuel burned at each torch is so modest, large scale up should be easy, especially if the burners and LN_2 supply systems were separate.

4.5 IMPLICATIONS FOR ARMY REQUIREMENTS

The performance envelope desired to meet Army requirements in a blast simulator is shown in Figure 4.14 (Reference 11). The trend lines obtainable from detonation and combustion drivers in DASACON at the 2200 ft test chamber are shown on this requirements figure. In general, higher pressures and shorter durations could be obtained at the 1500 ft station. It is interesting to note that many of the desired flow conditions (but not the physical size) could be obtained

USA LARGE BLAST/THERMAL SIMULATOR

REGIONS OF INTEREST FOR SIMULATION
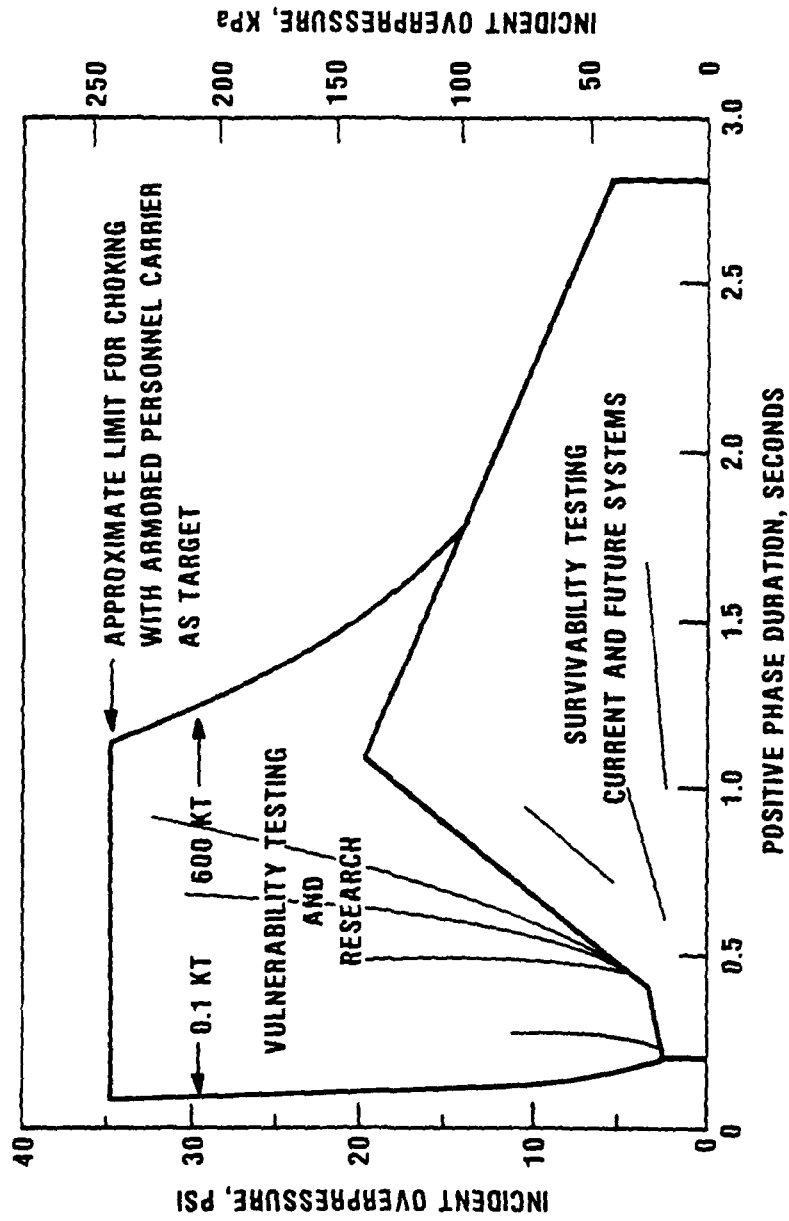
Figure 4.14. Simulation envelope required to meet Army requirements. Gas detonation or combustion driven DASACON performance at the 2200 ft test chamber has been overplotted (——lines). In general, higher pressures and shorter durations are obtained at the 1500 ft test chamber.

in DASACON or in a modified DASACON simulation facility. In particular, the "Vulnerability Testing and Research" domain is well covered by the detonation option, while the combustion system is needed for "Survivability Testing". Additional duration in this domain could be obtained by simply running the combustion system longer.

4.6   HARDENED MOBILE LAUNCHER CALCULATIONS

The hardened mobile launcher development program contemplates an approximately 1/5 scale test of launcher models during late 1984 and full scale launcher testing in 1986 or beyond. The following paragraphs will illustrate that DASACON with a detonation driver should be able to provide valuable simulation capability in support of this program.

Because of engineering constraints to be described more fully in the following sections, the driver options considered here consist only of propane-air detonation driver. If a diaphragm were located at 1000 ft, the blast conditions which are predicted at the 1500 and 2200 ft test chambers are summarized in Table 4.3. Since there is programmatic interest in blasts from 20 to 50 psi, certainly the DASACON can provide interesting flow conditions for a high equivalent yield within this pressure range.

In addition, DASACON equipped with a gas detonation driver could provide a large scale facility for the demonstration of non-ideal simulator concepts which will be essential in the later stages of the HML testing program. For instance, it might be decided that the non-ideal environment characteristic of a precursed nuclear blast could be best simulated by developing a precursor in a simulator through the use of a light gas layer along the test surface. Demonstration experiments of the efficacy of such a scheme could be conducted at large scale in the DASACON facility.

These possibilities have been more fully discussed in other communications to DNA.

Table 4.3. Predicted blast conditions expected at the several DASACON test chambers with the diaphragm located at X feet from the apex. In each case the driver is a stoichiometric C_2H_6 + air mixture.

Test Chamber Location

X = 1000	1000'	1500'	2200'
Δp (psi)		46.0	20.3
Y (kT)		111	94
X = 800			
Δp (psi)		27.0	13.2
Y (kT)		54	40
X = 500			
Δp (psi)	24	11.3	6.3
Y (kT)	12.7	9.5	8.0

The 30 psi condition could be obtained at the 1500' station using a diaphragm at 833 ft. The equivalent yield would be 61.2 kT.

106

4.7 COMPRESSED AIR DRIVER

A major objective of this contract is to investigate alternate
driver options for the DASACON simulator. Obviously our main effort
has been directed towards the exploration of gas detonation and gas
combustion drivers. As reported above, it appears that such systems
can produce interesting blast levels and wave shapes in DASACON.

An alternative approach involving a compressed nitrogen driver
was described by Osofsky at a recent Large Blast Thermal Simulator
Technical Interchange meeting (Reference 12). For completeness and in
order to get a better comparison of the two techniques, an air driver
example was calculated with the FLIP code using procedures identical
to those used for the detonation case. The results obtained are
presented below.

Calculations confirmed the general flow features produced by
this driver presented previously. The predicted pressure pulse at the
2200 ft station of DASACON driven by a 5 ft diameter, 165 ft long
pressure chamber filled to 200 atm at ambient temperature is shown in
Figure 4.15. The fast acting valve was assumed to open instantaneously.
Comparable, even higher pressure results were obtained if the opening
took 100 ms because less driver energy was wasted in producing a strong
shock close to a diaphragm.

Two features of the pressure pulse are noteworthy. The pulse is
concave downward rather than upward as in a blast wave, and the nega-
tive phase approaches a good vacuum. The first feature is related to
the fact that the flow is in transition from a flat topped shock to a
blast wave. It does not yet fully realize that it is a divergent
geometry.

A more serious limitation of this driver is apparent when one
examines the velocity field. The velocity is not approaching zero
within the time scale of the calculation. This means that the dynamic
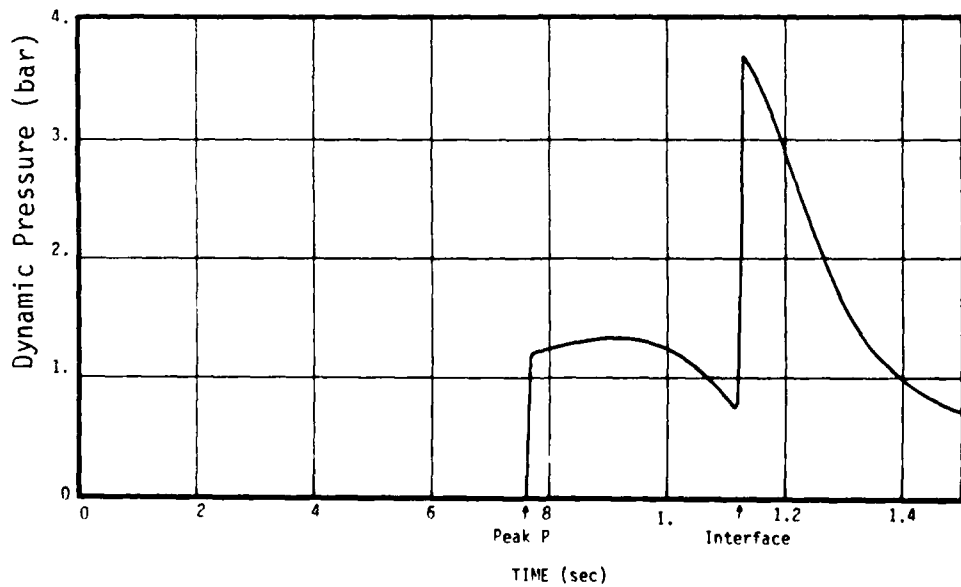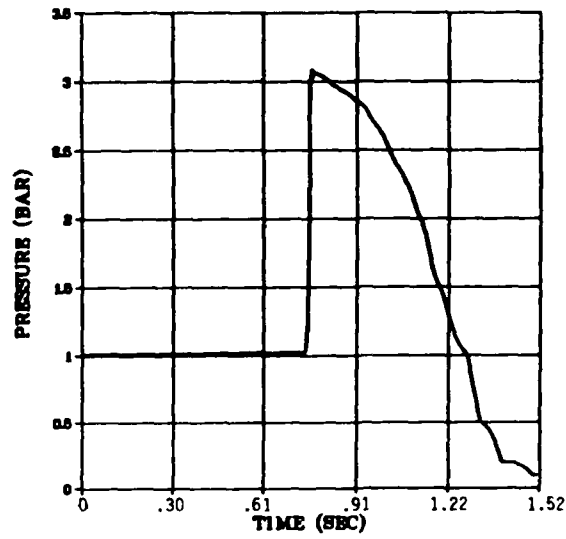
Figure 4.15. Static and dynamic pressure expected at the 2200 ft test chamber of DASACON from a compressed N_2 driver. The compression chamber is 5 ft in diameter and 165 ft long. The valve between the two chambers was assumed to open instantaneously. The initial driver pressure was 200 atm, and the temperature was ambient.

pressure pulse is much longer than it should be as also indicated in Figure 4.15. The early part of the pulse shows the transition towards a blast shape is far from complete. When the interface between driven and driver gas arrives, the dynamic pressure pulse increases by almost a factor of five. Such a profile is probably of limited interest if ideal blast conditions are desired. It may, however, be quite attractive if non-ideal conditions associated with precursed waves are of interest.

Raising the initial temperature of the driver gas by some preheat technique would reduce the density discontinuity at the interface, but probably it would not influence the early part of the pulse very much.

Concern was expressed that nitrogen gas condensation might occur in the driver section as the gas is cooled by the rarefaction process. This possibility has been investigated. It appears that for the conditions involved in this case the condensation phase line is not approached and condensation should not occur.

NOTE ADDED IN PROOF

After this report was completed, an error was discovered. An incorrect composition of air was assumed in the detonation conditions calculations. As a result, the driver conditions used in the DASACON performance were too modest. Simple linear scale up of performance estimates would increase the pressure values reported here by about 13%. The maximum C-J pressure for a C_3H_8 + air mixture is 19.3 atm, 284 psi. This occurs at a full mole fraction of 5% and a fuel weight fraction of 7.4%.

SECTION 5
RAREFACTION WAVE ELIMINATOR CONSIDERATIONS

Any practical blast simulator other than a free-field experiment
is of limited extent. As a result a reflected rarefaction will be
generated at the open end and will return to the test chamber at some
time unless successful efforts are made to eliminate the rarefaction.
Both active and passive rarefaction wave eliminator (RWE) systems have
been developed. The French tube at Grammat uses an active system in
which a set of hydraulically driven "venetian blinds" is closed after
shock passage in such a way as to counter the rarefaction with a
reflected shock from the blinds themselves. Passive systems such as a
fixed reflecting surface near the open end of a shock tube have been
used by the British at their Foulness facility and at DASACON. An
example of the influence of a passive RWE on DASACON performance is
shown in Figure 5.1 from Reference 6.

5.1 FLIP CALCULATIONS

The variable area, quasi-one-dimensional FLIP code can be used
to study wave reflection processes in both the active and passive
situations. An example of the geometric configuration used as an
approximation to the RWE problem is shown in Figure 5.2. The inlet
section to the throat was 1.7 tube diameter long for the 20 psi
results presented below. It was only .7 diameters long in the 5 psi
case. This probably explains the numerical noise (Figure 5.6) on the
profiles. This nozzle approach is similar to the one used by Mark at
BRL (Reference 13).

Wave profiles at the 2200 ft test chamber assuming infinitely
long and actual DASACON dimensions are shown in Figure 5.3 for a 20
psi case. In the actual case the calculation was made with a simple
expansion beyond the tube end. The angle of expansion was assumed to
be about 30°, and the influence of the ground plane which actually
exists at Dahlgren was ignored. The results were insensitive to

110
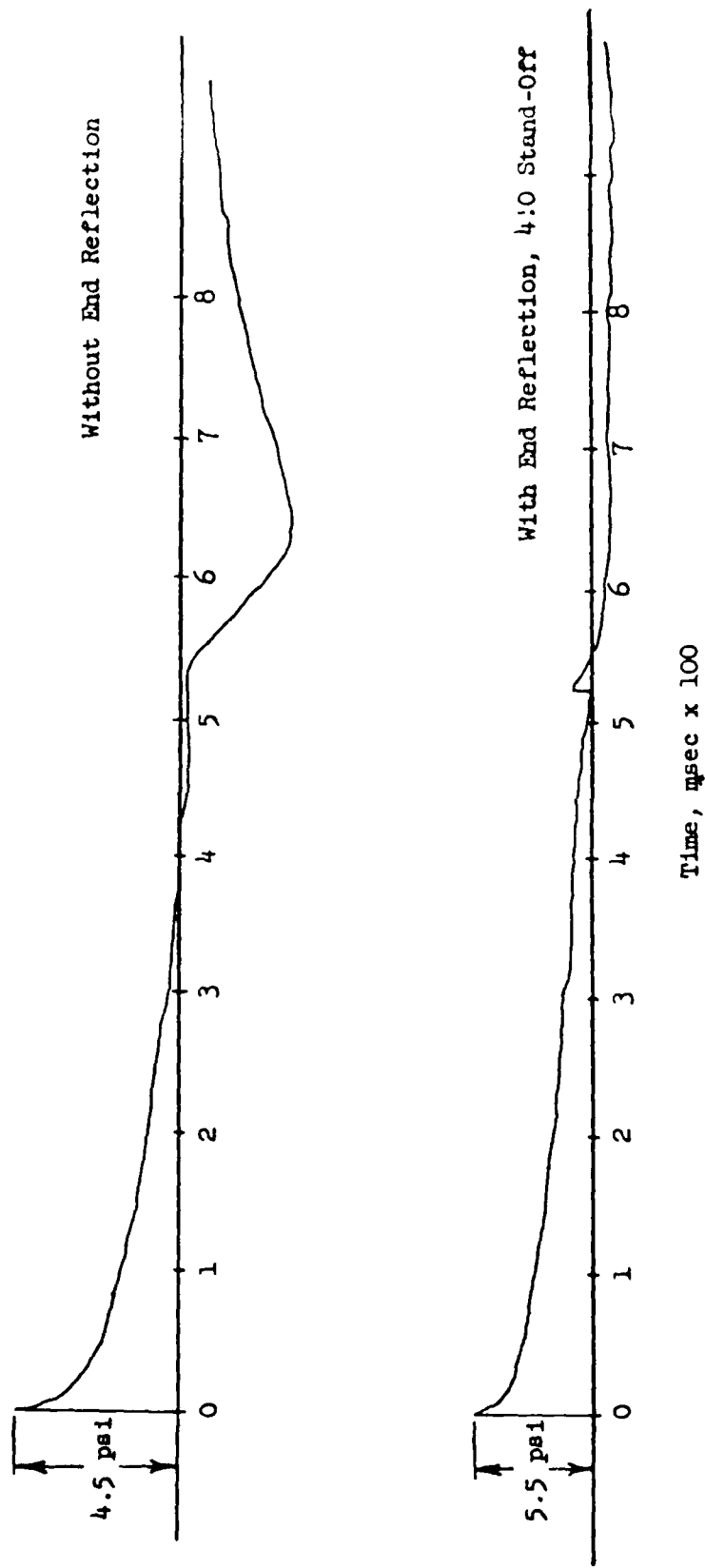
Figure 5.1. Pressure-time measurements made at the 2100 ft (21 ft dia.) station of DASACON. A large reflecting plate was mounted 4 ft from the open end of the tube.

111
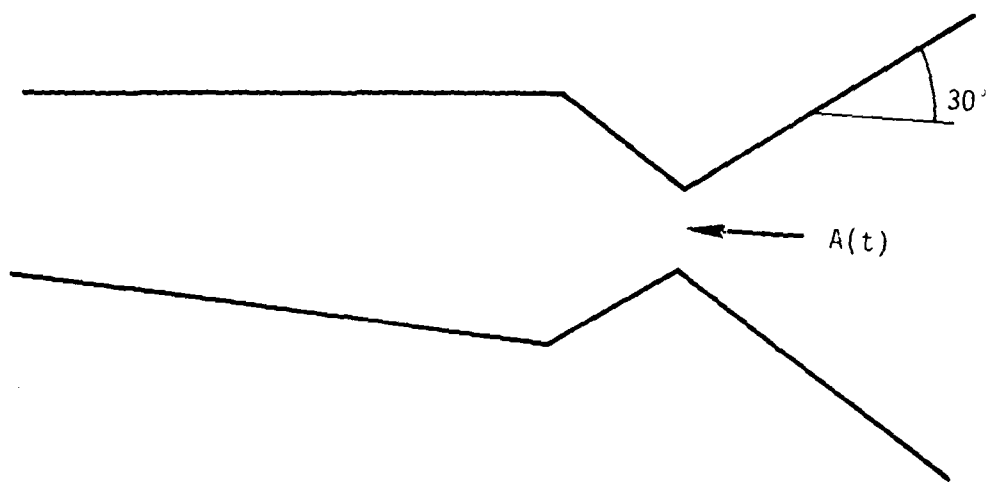
Figure 5.2. Sketch of the geometry assumed in FLIP calculational studies of rarefaction eliminators. The throat area was changed as a function of time in some cases.
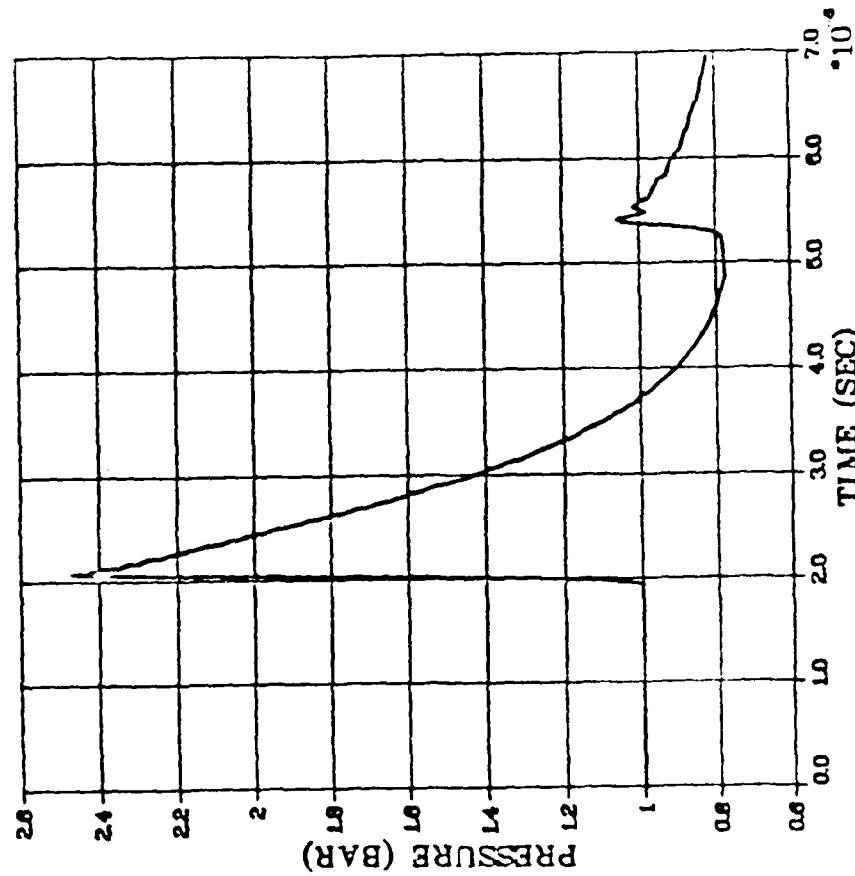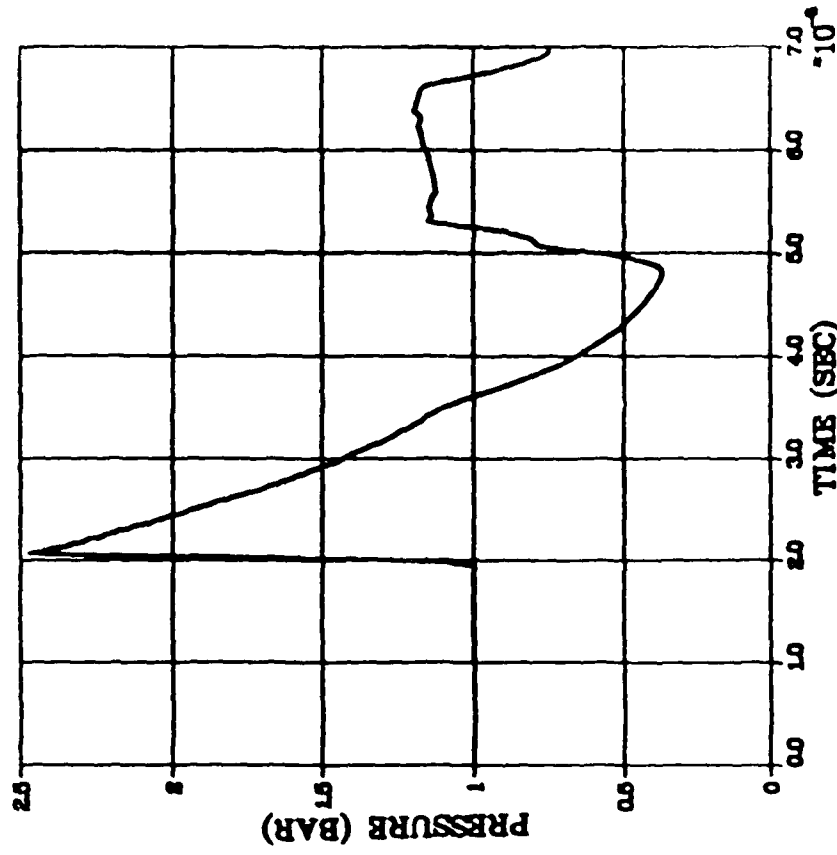
Figure 5.3. Calculated pressure profiles at the 2200 ft test chamber for an infinitely long tube and for the actual tube with no RWE. The shock was driven by C_2H_6 + air, and the diaphragm was located at 1000 ft.

the expansion angle. Note that for the nominal blast conditions considered the rarefaction does not return to the test chamber until very close to the end of the positive phase of the pressure pulse. By this time the dynamic pressure is quite low, so the reflected rarefaction would have little influence on the drag. This is one of the advantages of the DASACON. Approximately 200 ft of simulator has been constructed beyond the test chamber to delay the rarefaction significantly.*

A number of passive RWE calculations have been made by assuming the simulator to be terminated by a fixed nozzle which partially closes the outlet. The nozzle is followed by an expanded pipe assumed infinitely long and of constant expansion angle. Figure 5.4 shows the pressure as a function of time for two assumed RWE blockage values. When excessive blockage is assumed, a reflected shock is seen. When insufficient blockage is provided the rarefaction predominates. No set of blockage conditions was identified which truly eliminates the effect of the rarefaction. It is reduced but not eliminated, and this is consistent with the experimental results shown in Figure 5.1.

Many additional calculations have been made with assumed active RWE action. These calculations were made by assuming the RWE nozzle in the FLIP calculation to move as a prescribed function of time as sketched in Figure 5.5. These curves show blockage; note the ordinate scale. An initial closure is assumed. That aperture subsequently decreases with time as shown. At late time 10 % or less of the initial area was assumed open. The curves labeled "Sonic conditions" is the nozzle throat area ratio predicted to produce sonic flow if the instantaneous blast conditions at the end of the DASACON were assumed to be a steady state. Figure 5.6 shows the pressure profiles

*It is interesting to note that the DASACON length between the test chamber and the open end of approximately 200 ft is much longer than the 100 ft provided in the French Grammat facility. Therefore, the rarefaction problem is much more important to the French than it is to potential users of DASACON.

114
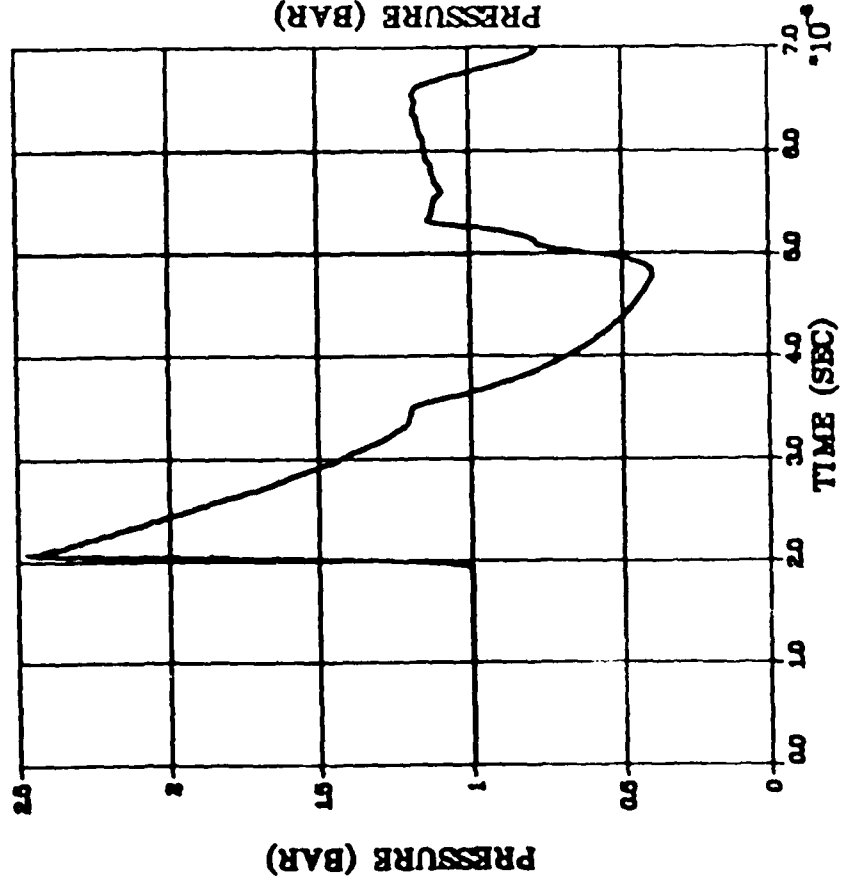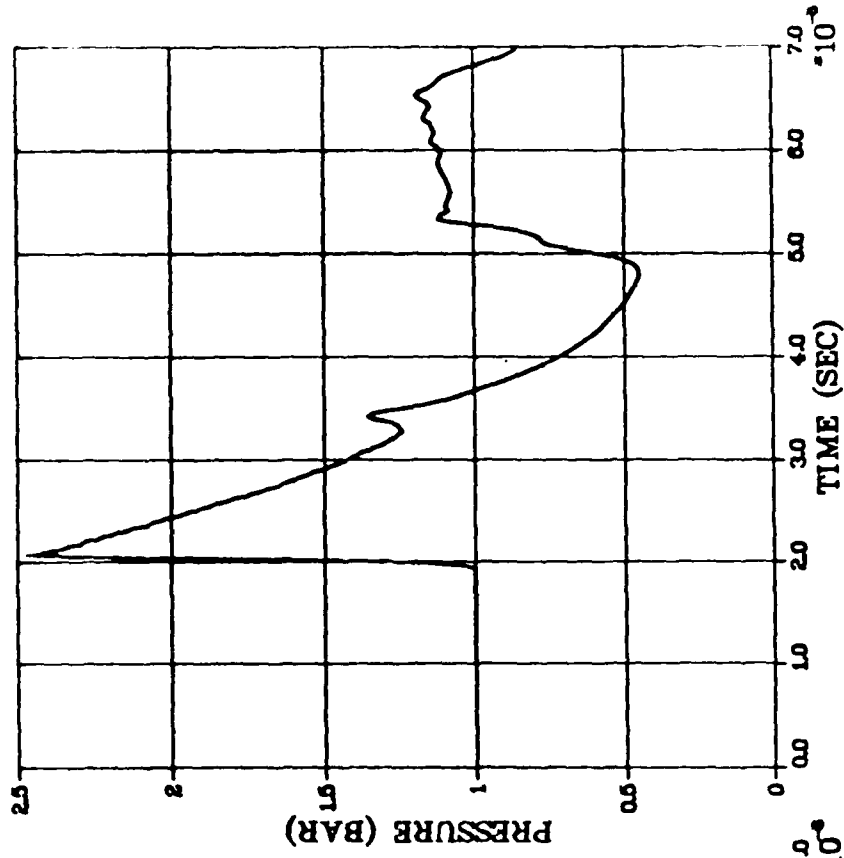
Figure 5.4. Pressure-time profiles at the 2200 ft test chamber for fixed blockage conditions of 12½ and 25%. A 20 psi blast exists at the test chamber.

115
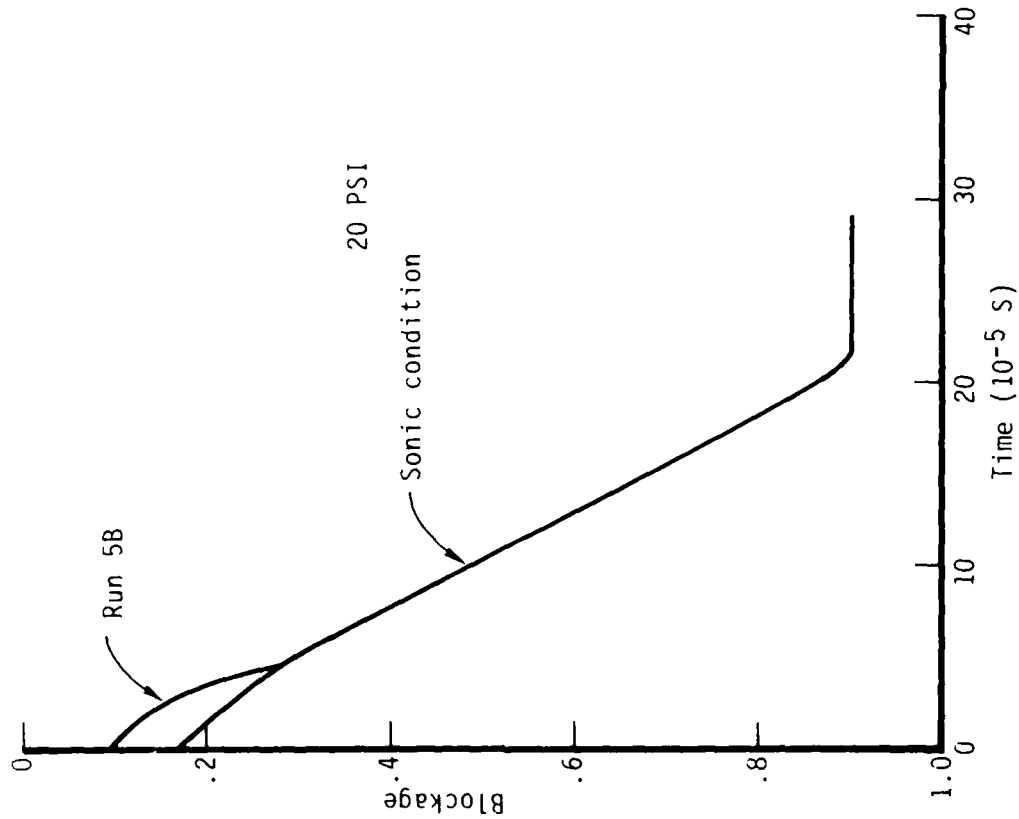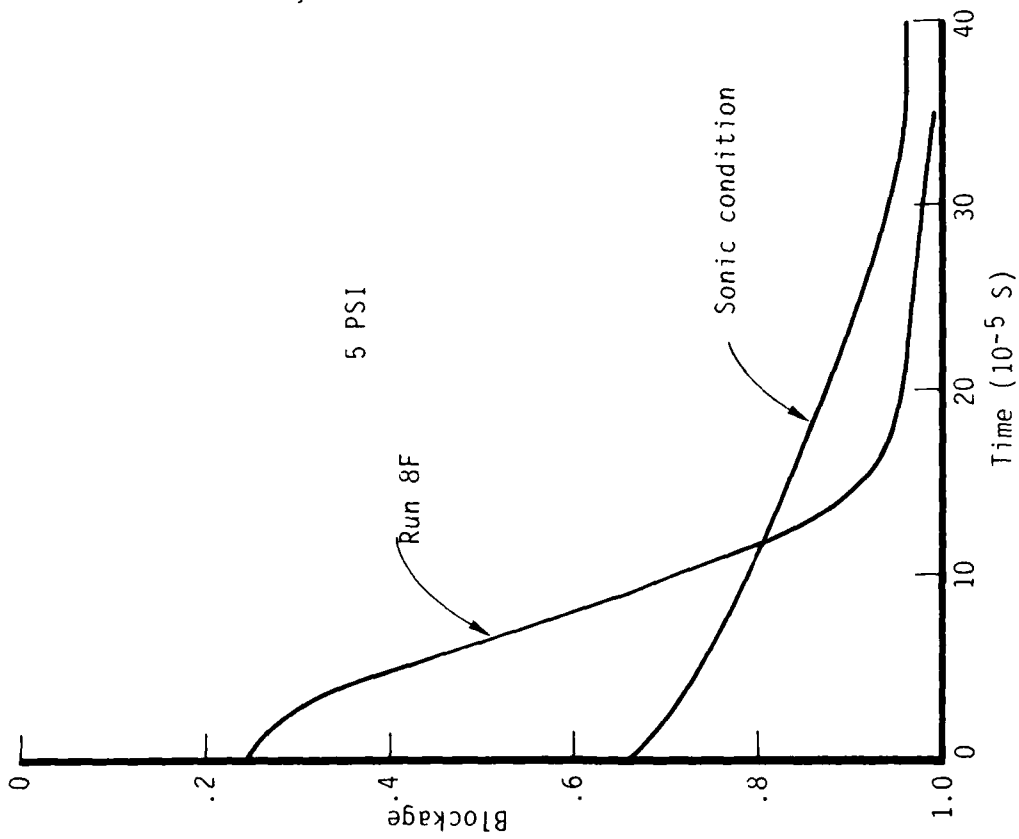
Figure 5.5. Blockage profiles as a function of time in RWE calculations which assumed the driver length to be 1 cm. The Run number designations refers to pressure profiles in Figure 5.6.

C2H6 + AIR FLIP RUN5A

R = 2.20 (CM)
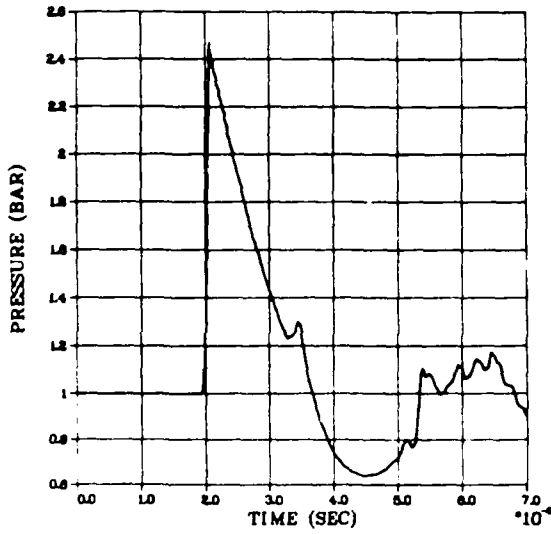
20 psi sonic

C2H6 + AIR FLIP RUN8

R = 5.50 (CM)
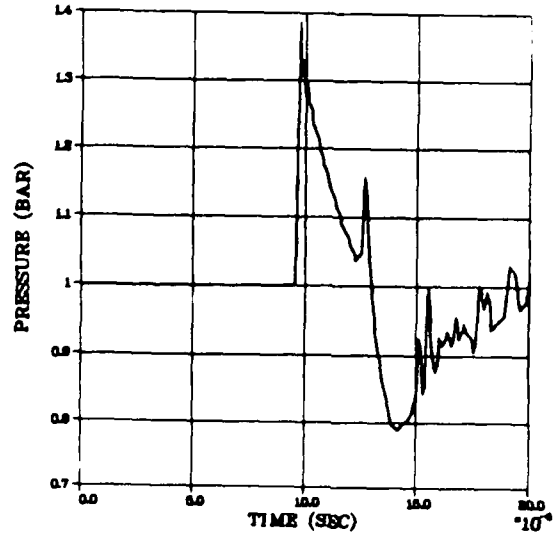
5 psi sonic

C2H6 + AIR FLIP RUN5B

R = 2.20 (CM)
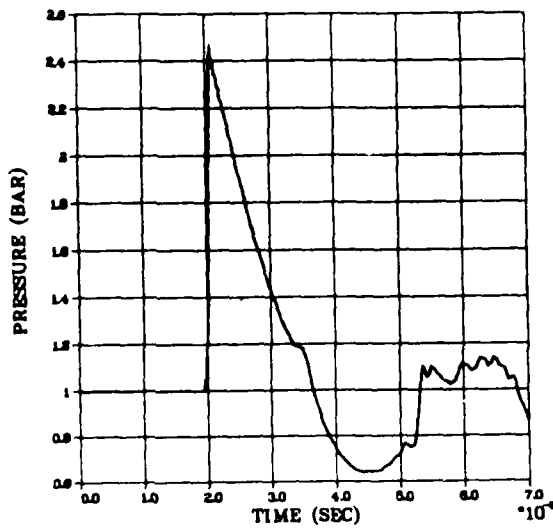
20 psi 10% initial blockage

C2H6 + AIR FLIP RUN8F

R = 5.50 (CM)
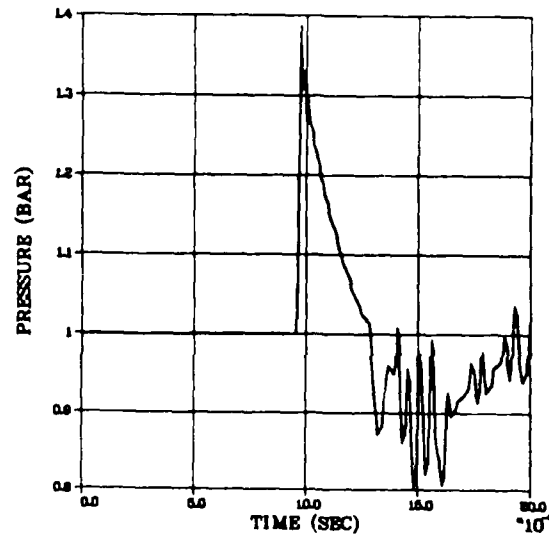
5 psi   Run 8F

Figure 5.6.   Pressure profiles at the 2200 ft test chamber for 20 and 5 psi
blast waves showing the effects of the RWE action shown in
Figure 5.5.

117

developed for the several active RWE trajectories illustrated earlier. None of them, particularly including the sonic case, provides a good suppression for the rarefaction. Many are superior to the simple passive RWE but none provides an ideal solution to the RWE problem. The 5 psi examples are more "noisy" than those for 20 psi. As mentioned above, this probably is related to the rather abrupt convergent section employed in those calculations.

5.2 A PASSIVE/ACTIVE RWE

The simple passive rarefaction wave eliminator is obviously of limited capability. On the other hand, a system as complex as the French is expensive and difficult to control for a large simulator. These two objections can be overcome by the passive/active RWE concept sketched in Figure 5.7. The idea is to occlude a fraction of the exit of the simulator with a vane. After the blast impinges on this vane, the vane will move, and if its initial position is as indicated the motion will tend to decrease the available exit area of the simulator as would an active RWE system. A simple vane can be augmented by linked vanes as shown in the figure such that as the effect of one reaches its maximum value it could be superceded by another. Such a system would be very easy to construct, and it could be adjusted by opening or closing panels in a vane or by increasing the radial extent of vane segments. In this way, a better approximation to desired RWE performance could be obtained in a completely passive, easily adjusted system.

The performance of this novel RWE system cannot be simply analyzed because the initial loading and angular acceleration experience a "diffraction phase" similar to that shown in Section 2. The open domain beyond the simulator also makes performance estimation difficult. Nevertheless, it appears obvious that this system would work as described and that convenient adjustments exist which should make it possible to generate almost any closure function desired.

118

DASACON End

Aerodynamic Flaps
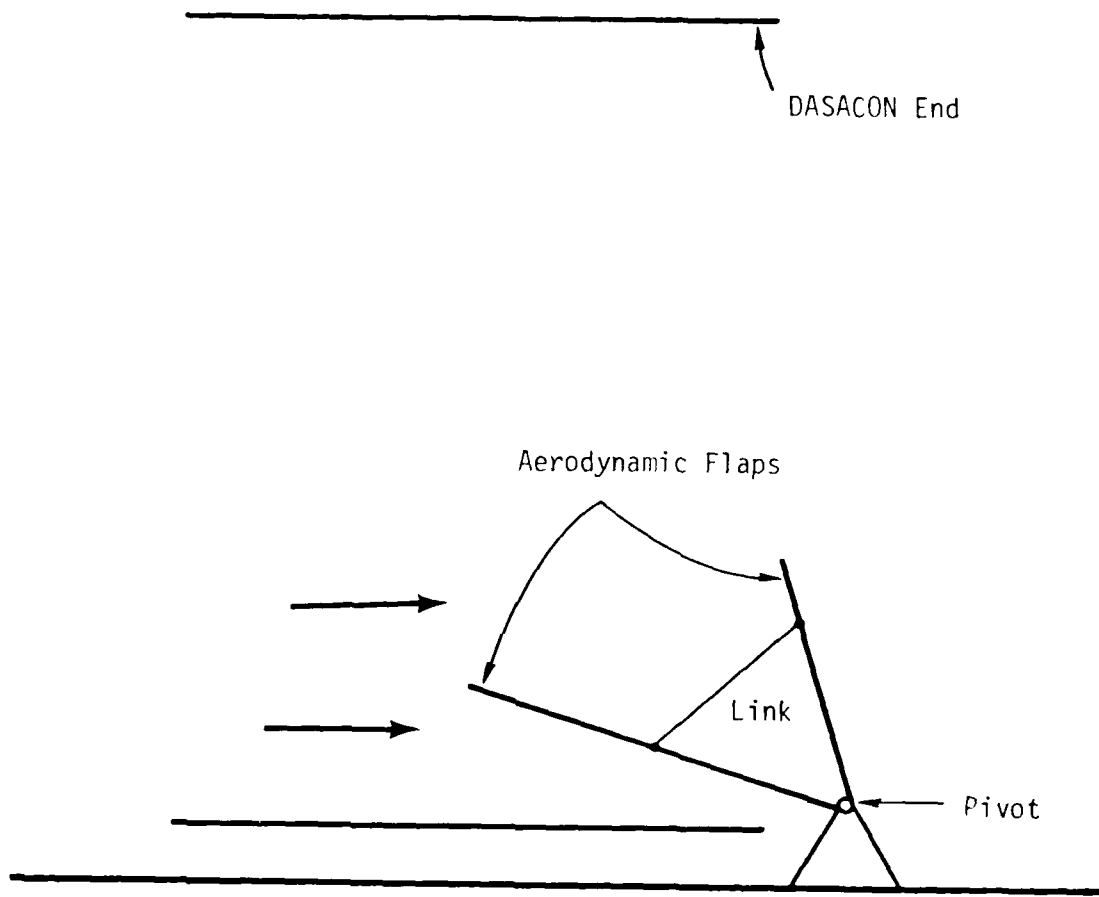
Link

Pivot

Figure 5.7. Simple sketch of a passive/active rarefaction wave eliminator driven by the flow itself. More than one pivot may be needed or desired, and the blockage function can be varied by changing flap area and density and linkage conditions.

119

SECTION 6.
DISTRIBUTED FUEL AIR EXPLOSIVES

A simple, solid high explosive driven blast simulator was developed and patented by one of the present authors approximately 20 years ago (Reference 14 and 15). This was subsequently extended to the DABS and Thunderpipe systems. A major shortcoming, however, was that a long facility was required if relatively modest blast conditions were desired. The work by Colton and associates, Reference 16, led to the development of the short DABS in which the initial explosive configuration was chosen to approximate the desired wave shape with the result that the length of the facility required to generate given blast conditions was significantly reduced.

It is an interesting question whether or not a similar application of a distributed explosive charge can be effectively made with fuel air explosives. This possibility was calculated in one-dimensional slab geometry using the SKIPPR code. The shock conditions generated by a given layer of detonable gas were compared with conditions to be expected from the same mass of gas distributed in several segments as sketched in Figure 6.1. The calculated results were not encouraging. As can be seen in Figure 6.2 the pressure-range relation is identical in the two cases after a range of 10, based on the dimensions of Figure 6.1. In addition, the wave profiles from the two explosive distributions are quite similar. It therefore appears that there is little to recommend a distributed charge FAE configuration for blast simulation applications.
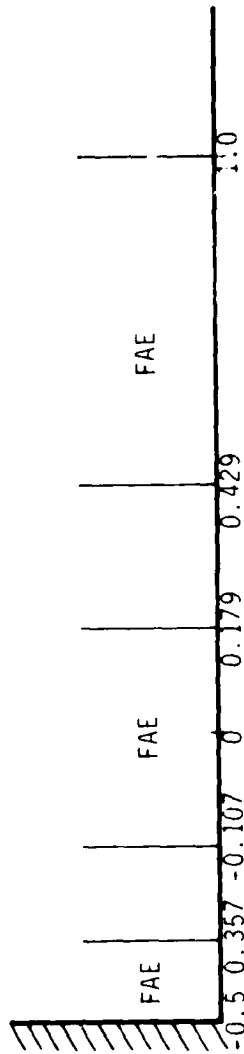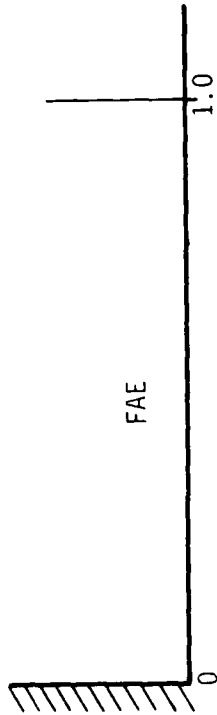
Figure 6.1. Comparison of conventional and distributed charge fuel-air explosive charges used in a study of the utility of distributed charge.... The charge mass is
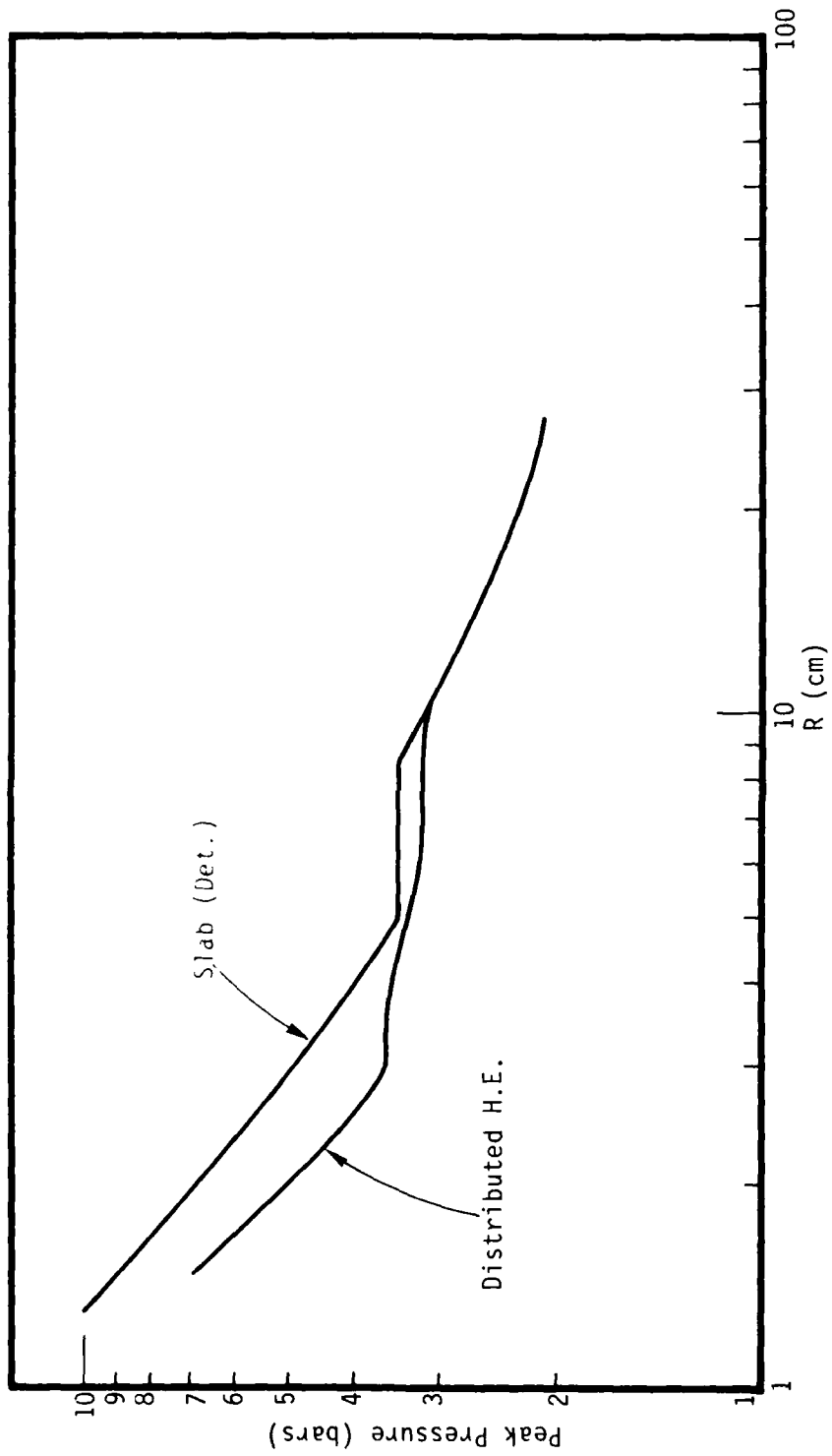
Figure 6.2. Pressure-range relationships for the uniform and distributed charge configurations shown in Figure 6.1.

REFERENCES

1. Ethridge, N.E., et al, "Flow Blockage and Its Effect on Minimum Incident Overpressures for Overturning Vehicles in a Large Blast Simulator," BRL contribution to the Seventh International Symposium on Military Applications of Blast Simulation, Medicine Hote, Alberta, Canada, July 1981.

2. Wortman, J. D. and Lottero, R.E., "Comparison of HULL Hydrocode Computational Shock Tube Blockage Effects on Target Loading for Step Shocks and Rapidly Decaying Shocks," BRL Memorandum Report ARBRL-MR-03232, December 1982.

3. Duff, R. E., Northrop, J., and Pierce, T., "Blast/Thermal Simulator Facility Review," DNA-TR-81-156, 1 June 1982.

4. Kitchens, C.W., Jr. et al, "Blast Wave Modification During Combined Thermal/Blast Simulation Testing," BRL Technical Report ARBRL-TR-02352, July 1981.

5. Filler, W.S. and Porcel, F.B., "Improved Driver Systems for the DASACON," Appendix I-K, Final Letter Report of Ad Hoc Panel on Large Shock Tubes for Defense Nuclear Agency, prepared by Naval Surface Weapons Center, 5 December 1974.

6. Culberson, W., Private Communication, Naval Surface Weapons Center, Dahlgren, VA. 1983.

7. Cowperwaite, M. and Zwisler, W.H., "Tiger Computer Program Documentation," SRI Report AD/A-002 791 prepared for Naval Ordnance Lab, Picatinney Arsenal, March 1974.

8. Barthel, J., Private Communication

9. Speicher, S.J., Brode, H.L., "Airblast Overpressure Analytic Expression for Burst Height, Range and Time - Over an Ideal Surface," Pacific Sierra Research, PSR Note 385, November 1981.

10. Lagus, P.L, Peterson, E.W., and Wu, H.E., "In Situ Steam Fracture Experiments," S-CUBED Report SSS-R-83-6288, August 1983.

11. Balicki, J. W., Private Communication, 1983.

12. Osofsky, I., Presentation at Large Blast/Thermal Simulator Technical Interchange Meeting, May 1983.

13. Mark, A., "Computational Design of Large-Scale Blast Simulators," AIAA Paper 81-0159, January 12, 1981.

14. Duff, R.E. and Blackwell, A.N., U. S. Patent 3318144, "A Supersonic Test Facility", May 9, 1967.

REFERENCES (continued)

15. Duff, R.E. and Blackwell, A.N., "Explosive Driven Shock Tubes,"
     Rev. Sci. Inst., 37, 579 (1966). Also Fifth International Shock
     Tube Symposium Proceedings, 28-30 April 1965, p. 259.

16. Sanai, M., Lindberg, H.E. and Colton, J.D., "Simulation of Blast
     Waves with Tailored Explosive Charges", SRI International
     Report, 1983.

DISTRIBUTION LIST

DEPARTMENT OF DEFENSE

Asst to the Secy of Defense, Atomic Energy
    ATTN: Executive Assistant

Defense Intelligence Agency
    ATTN: DB-4C
    ATTN: DB-4N
    ATTN: DT-1C
    ATTN: DT-2
    ATTN: RTS-2A, Tech Lib
    ATTN: RTS-2B

Defense Nuclear Agency
    2 cy ATTN: SPSS
    2 cy ATTN: SPTD
    4 cy ATTN: STTI-CA

Defense Technical Info Center
    12 cy ATTN: DD

Dept of Defense Explo Safety Bd
    ATTN: Chairman

Field Command, Defense Nuclear Agency
    ATTN: FCL
    ATTN: FCPR
    ATTN: FCT

Under Secy of Defense for Res & Eng
    ATTN: Strat & Space Sys (OS)
    ATTN: Strat & Theater Nuc For, B. Stephan

DEPARTMENT OF THE ARMY

Deputy Chief of Staff for Ops & Plans
    ATTN: DAMO-NC, Nuc Chem Dir

Harry Diamond Laboratories
    ATTN: DEKGD-DTSO
    ATTN: DELHD-NW-P, 20240
    ATTN: DELHD-NW-RA
    ATTN: DELHD-TA-L, 81100, Tech Lib

US Army Communications Command
    ATTN: Technical Reference Div

US Army Corp of Engineers
    ATTN: DAEN-ECE-T
    ATTN: DAEN-RDL

US Army Material Command
    ATTN: DRXAM-TL, Tech Lib

USA Ballistic Research Lab
    ATTN: DRDAR-BLT
    2 cy ATTN: AMXBR-TBD
    2 cy ATTN: DRDAR-BLA-S, Tech Lib

USA Concepts Analysis Agency
    ATTN: CSSA-ADL, Tech Lib

USA Eng Waterways Exper Station
    ATTN: J. Strange
    ATTN: J. Zelasko
    ATTN: Library
    ATTN: WESSD, J. Jackson
    ATTN: WESSE

DEPARTMENT OF THE ARMY (Continued)

USA Foreign Science & Tech Ctr
    ATTN: DRXST-SD

USA Material & Mechanics Res Ctr
    ATTN: DRXMR, J. Mescall
    ATTN: Technical Library

USA Nuclear & Chemical Agency
    ATTN: Library

USA White Sands Missile Range
    ATTN: STEWS-FE-P
    ATTN: STEWS-TE-N, K. Cummings

DEPARTMENT OF THE NAVY

David Taylor Naval Ship R&D Ctr
    ATTN: Tech Info Ctr Code 522.1

Naval Civil Engineering Lab
    ATTN: Code L51, J. Crawford

Naval Facilities Eng Command
    ATTN: Code 04B

Naval Material Command
    ATTN: MAT 08T-22

Naval Postgraduate School
    ATTN: Code 1424 Library

Naval Research Laboratory
    ATTN: Code 2627, Tech Lib
    ATTN: Code 4040, D. Book
    ATTN: Code 4040, J. Boris

Naval Surface Weapons Center
    ATTN: Code F31

Naval Surface Weapons Center
    ATTN: Tech Library & Info Svcs Br

Naval Weapons Center
    ATTN: Code 266, C. Austin
    ATTN: Code 343, FKA6A2, Tech Svcs

Ofc of the Deputy Chief of Naval Ops
    ATTN: NOP 03EG
    ATTN: NOP 981

Office of Naval Research
    ATTN: Code 474, N. Perrone

Strategic Systems Project Office
    ATTN: NSP-272
    ATTN: NSP-43, Tech Lib

DEPARTMENT OF THE AIR FORCE

Air Force Inst of Technology
    ATTN: ENA
    ATTN: Library

Deputy Chief of Staff, Rsch, Dev & Acq
    ATTN: AF/RDQI

DEPARTMENT OF THE AIR FORCE (Continued)

[illegible] Weapons Lab
    ATTN: SUL
    ATTN: NTES, M. Plamondon
    ATTN: NTES, R. Matalucci
    ATTN: NTES, R. Henny
    ATTN: [illegible]

[illegible] Command
    ATTN: [illegible]
    ATTN: [illegible]
    ATTN: [illegible]
    ATTN: [illegible]

DEPARTMENT OF ENERGY

[illegible]
[illegible] ATTN
    ATTN: [illegible]

OTHER GOVERNMENT AGENCIES

[illegible] Defense [illegible] Agency
    ATTN: [illegible]

[illegible]
    ATTN: [illegible]

Federal Emergency Management Agency
    ATTN: [illegible] for Rsch, D. Kerr
    ATTN: [illegible] Kumar, NP-CP

DEPARTMENT OF ENERGY CONTRACTORS

University of California
Lawrence Livermore National Lab
    ATTN: L-[illegible], R. [illegible]
    ATTN: L-[illegible], T. Butkovich
    ATTN: P. [illegible]
    ATTN: Technical Info Dept Library

Los Alamos National Laboratory
    ATTN: MS P364, Report Library
    ATTN: MS [illegible], [illegible] Spillman
    ATTN: R. Whitaker

Oak Ridge National Laboratory
    ATTN: Central Rsch Library
    ATTN: [illegible]

Sandia National Laboratories
    ATTN: Div 7111, B. [illegible]
    ATTN: [illegible] Carpenter
    ATTN: Div 7111, [illegible]
    ATTN: Tech Lib 3141
    ATTN: [illegible]

Sandia National Laboratories
    ATTN: Library & Security Clas Div

DEPARTMENT OF DEFENSE CONTRACTORS

[illegible] Corp
    ATTN: [illegible]
    ATTN: Library, Acquisition M[illegible]

[illegible] Associates
    ATTN: M. [illegible]

DEPARTMENT OF DEFENSE CONTRACTORS (Continued)

Analytic Services, Inc (ANSER)
    ATTN: G. Hesselbacher

Applied Res Assocs, Inc
    ATTN: J. Bratton

Applied Res Assocs, Inc
    ATTN: D. Piepenburg

Applied Res Assocs, Inc
    ATTN: R. Frank

Applied Theory, Inc
  2 cy ATTN: J. Trulio

ARTEC Associates, Inc
    ATTN: S. Gill

AVCO Systems Division
    ATTN: Library A830

BDM Corp
    ATTN: A. Lavagnino
    ATTN: Corporate Lib
    ATTN: T. Neighbors

BDM Corp
    ATTN: F. Leech
    ATTN: R. Hensley

Boeing Co
    ATTN: Aerospace Library
    ATTN: M/S 42/37, P. Carlson

Boeing Co
    ATTN: MS-8S-2U, D. Choate

California Res & Technology Inc
    ATTN: K. Kreyenhagen
    ATTN: Library

California Research & Technology, Inc
    ATTN: F. Sauer

California Research & Technology, Inc
    ATTN: Technical Library

Calspan Corp
    ATTN: Library

Carpenter Research Corp
    ATTN: H. Carpenter

University of Denver
    ATTN: Sec Officer for J. Wisotski

EG&G Wash Analytical Svcs Ctr
    ATTN: Library

Electro-Mech Systems, Inc
    ATTN: R. Shunk

General Research Corp
    ATTN: Technical Information Office

H-Tech Labs, Inc
    ATTN: B. Hartenbaum

DEPARTMENT OF DEFENSE CONTRACTORS (Continued)

Horizons Technology, Inc
        ATTN: R. Kruger

IIT Research Institute
        ATTN: Documents Library
        ATTN: M. Johnson
        ATTN: R. Welch

Information Science, Inc
        ATTN: W. Dudziak

Institute for Defense Analyses
        ATTN: Classified Library

Kaman Sciences Corp
        ATTN: Library
        ATTN: N. Hobbs
        ATTN: R. Ruetenik
        ATTN: S. Criscione

Kaman Sciences Corp
        ATTN: F. Shelton
        ATTN: Library

Kaman Sciences Corp
        ATTN: E. Conrad

Kaman Tempo
        ATTN: DASIAC
        ATTN: W. Chan

Kaman Tempo
        ATTN: DASIAC

Lockheed Missiles & Space Co, Inc
        ATTN: J. Weisner
        ATTN: Tech Info Ctr D/COLL, D/90-11, B/106

Martin Marietta Corp
        ATTN: G. Fotieo

McDonnell Douglas Corp
        ATTN: R. Halprin

McDonnell Douglas Corp
        ATTN: M. Potter

Merritt CASES, Inc
        ATTN: J. Merritt
        ATTN: Library

University of New Mexico
        ATTN: N. Baum

Nichols Research Corp, Inc
        ATTN: N. Byrn

Pacific-Sierra Research Corp
        ATTN: H. Brode, Chairman SAGE

Pacifica Technology
        ATTN: R. Allen
        ATTN: R. Bjork

Patel Enterprises, Inc
        ATTN: M. Patel

Physical Research, Inc
        ATTN: W. Mendes

DEPARTMENT OF DEFENSE CONTRACTORS (Continued)

Physics International Co
        ATTN: E. Moore
        ATTN: L. Behrmann

R & D Associates
        ATTN: A. Kuhl
        ATTN: D. Simons
        ATTN: J. Lewis
        ATTN: Technical Info Ctr
        ATTN: W. Wright

R & D Associates
        ATTN: G. Ganong

Rand Corp
        ATTN: P. Davis

Rand Corp
        ATTN: B. Bennett

S-CUBED
        ATTN: D. Grine
        ATTN: Library
        ATTN: T. Riney
 2 cy ATTN: K. Lie
 2 cy ATTN: L. Kennedy
 2 cy ATTN: R. Duff

Science & Eng Assocs, Inc
        ATTN: B. Chambers III

Science Applications Intl Corp
        ATTN: G. Binninger

Science Applications Intl Corp
        ATTN: Technical Library

Science Applications Intl Corp
        ATTN: J. Cockayne
        ATTN: M. Knasel
        ATTN: R. Sievers
        ATTN: W. Layson

Science Applicaitons, Inc
        ATTN: D. Maxwell

Southwest Research Institute
        ATTN: A. Wenzel
        ATTN: W. Baker

SRI International
        ATTN: G. Abrahamson

Structural Mechanics Assocs, Inc
        ATTN: R. Kennedy

Teledyne Brown Engineering
        ATTN: D. Ormond
        ATTN: F. Leopard
        ATTN: J. Ravenscraft

Terra Tek, Inc
        ATTN: A. Jones
        ATTN: Library
        ATTN: S. Green

Tetra Tech, Inc
        ATTN: L. Hwang

TRW Electronics & Defense Sector
      ATTN: Technical Information Center
 2 cy ATTN: N. Lipner

TRW Electronics & Defense Sector
      ATTN: E. Wong
      ATTN: G. Hulcher
      ATTN: P. Dai

Universal Analytics, Inc
      ATTN: E. Field

Weidlinger Assoc Consulting Eng
      ATTN: I. Sandler
      ATTN: M. Baron

Weidlinger Assoc Consulting Eng
      ATTN: T. Deevy

Weidlinger Assoc Consulting Engrg
      ATTN: J. Isenberg

END

FILMED

1-86

DTIC